

Control of the interaction of a gantry robot end effector with the environment by the adaptive behaviour of its joint drive actuators

PARIKSHIT KASHIKAR

A thesis submitted in partial fulfilment of the
requirements of the University of the West of England, Bristol
for the degree of Master of Philosophy

in the

Faculty of Environment and Technology
University of the West of England, Bristol

October 2014

Abstract

The thesis examines a way in which the performance of the robot electric actuators can be precisely and accurately force controlled where there is a need for maintaining a stable specified contact force with an external environment. It describes the advantages of the proposed research, which eliminates the need for any external sensors and solely depends on the precise torque control of electric motors. The aim of the research is thus the development of a software based control system and then a proposal for possible inclusion of this control philosophy in existing range of automated manufacturing techniques.

The primary aim of the research is to introduce force controlled behaviour in the electric actuators when the robot interacts with the environment, by measuring and controlling the contact forces between them. A software control system is developed and implemented on a robot gantry manipulator to follow two dimensional contours without the explicit geometrical knowledge of those contours. The torque signatures from the electric actuators are monitored and maintained within a desired force band.

The secondary aim is the optimal design of the software controller structure. Experiments are performed and the mathematical model is validated against conventional Proportional Integral Derivative (PID) control. Fuzzy control is introduced in the software architecture to incorporate a sophisticated control. Investigation is carried out with the combination of PID and Fuzzy logic which depend on the geometrical complexity of the external environment to achieve the expected results.

Acknowledgement

Thanks to the University of West of England (UWE), Bristol for giving me the opportunity to carry out the research work. My debt of gratitude to Mr. Farid Dailami for being of constant help and support to me, for guiding perfectly my work on this thesis from the very beginning – with his precious ideas, advice and remarks, his words of encouragement and motivation, when I needed them the most.

I like to express my sincere gratitude to my Director of Studies, Dr. Anthony Pipe, and Dr. Quan Zhu for all their efforts, encouragement and support during the entire thesis work. Thanks to all of the supervisory team –each of them for having a desk with knowledge, experience and vision -without which it would not have been possible.

Thanks to Mr. Terrence Blake, Mr. David Worgan, and Mr. Gary Slocombe for the experimental aspect of the research work, and their guidance and unstinting help. Thanks to all my past and present colleagues and friends at UWE, Bristol, where I studied and worked for more than six years, in a wonderful atmosphere of team spirit, union and friendship. All of you that I have probably forgotten to thank here.

Most importantly I would like to dedicate the thesis to my parents for their endless and tireless support, encouragement and blessings. I would also like to thank J. Hierl for his strong support and encouragement.

Parikshit Kashikar.

Contents

Abstract	1
Acknowledgement	2
List of figures:.....	6
Terminology and Nomenclature used in the presented work:	8
Thesis Structure and Summary	11
1. Introduction	14
1.1 Introduction and Motivation of the Research	14
1.2 Research Objectives	16
1.3 Adopted Research Strategy	17
2. Literature Survey	20
2.1 Introduction	20
2.2 Literature review	21
2.3 Introduction and Justification of the research undertaken.....	27
2.4 Application Areas.....	31
3. Mathematical modelling of the electric actuator (PMSM) for the controlled interaction with environment	36
3.1 Mathematical representation of a PMSM.....	37
3.2 Introduction to spring like behaviour in electric actuators.....	43
4. Development of the experimental setup for robot interaction with the environment and initial tests	45
4.1 Introduction of the system	45
4.2 Description of the control system architecture, electrical actuator and controller ..	46

4.3 Data acquisition, interpretation and utilisation in the controller	50
4.4 Calibration of motor current to force experiment	55
4.5 Development of the system and initial robot interaction experiments	57
4.6 Approach to development of contour following system	59
4.7 Software development flow charts	60
5. PID control modelling and implementation on the experimental system	67
5.1 Background and Introduction	67
5.2 Introduction	69
5.3 Approach to the development of the PID controller	74
5.4 Modelling and validation of the controller	75
5.5 Results and Conclusion	79
5.6 Further Development with PID Controller	80
6. Development and Implementation of Fuzzy Logic Controller on the experimental system	82
6.1 Introduction and Justification for the need of fuzzy controller.	82
6.2 Approach adopted in designing the fuzzy controller	84
6.3 Implementation and Tests	89
6.4 Comparison between the performance of PID and fuzzy controllers	92
6.5 Proposed modified controller structure for PID+Fuzzy Controller	96
7. Main Contributions and Conclusions of the research	99
8. Recommendations for future work	103
References and Bibliography	106
Appendices:	114
I. DSP TMS320F2812 Introduction-	114

II. Infranor Amplifier:	Error! Bookmark not defined.
III. Introduction and operation of PWM in the amplifier of the motor	116
IV. PID Control Appendix	117
V. Vector Control Summary	119
VI. Description of coordinate transforms.....	121
VII. Mathematical derivations for torque control in PMSM.....	123
VIII. DSP Software code-	126
a. Program for the X axis controller for conventional PID controller	127
b. Program for the Y axis controller for conventional PID controller	137
c. Program for the X axis controller for fuzzy controller	145

List of figures:

Figure 1: Permanent magnet synchronous motor (PMSM).....	37
Figure 2: A Generic gantry manipulator layout.....	45
Figure 3: Control system architecture employed in the research.....	46
Figure 4: Block diagram of Vector control of an AC motor	47
Figure 5: Block diagram of the control system architecture implemented for a single robot axis.....	52
Figure 6: Robot manipulator.....	53
Figure 7: Two arms of InFACT.....	66
Figure 8: robot electric actuator and manipulator.....	53
Figure 9: robot interaction with environment	55
Figure 10: Calibration of the motor current to force	55
Figure 11: Calibration of the electric motor current to force with two linear regions..	57
Figure 12: Graph showing torque/current limiting values over 10 seconds interval.	57
Figure 13: The force vector components f_x and f_y and the resultant force vector..	58
Figure 14: Different geometric surfaces used for 2 dimensional contour following with the knowledge of starting (A) and finish (B) points.....	59
Figure 15: Flowchart describing robot electric actuator with the environment....	61
Figure 16: Flowchart describing robot electric actuator with the environment for two dimensional surfaces.....	63
Figure 17: Flowchart describing robot electric actuator with the environment for two dimensional surfaces.....	65
Figure 18: Block representation of a process with input output variables	67
Figure 19 - A Traditional PID Controller.....	72
Figure 20: Different values of ζ calculated from the step inputs to the plant.....	76
Figure 21: Different values of ω calculated from step inputs to the plant.....	76
Figure 22– Simulink model for the PID controller implementation and comparison with plant open loop response. ($K_p=1.4$, $K_i=2.8$, $K_d=0.18$).....	76
Figure 23 - Graph showing the Simulink plant output with and without PID control...	78
Figure 24 – Practical implementation of the PID controller on the Experimental setup($K_p=0.001$, $K_i=0.002$, $K_d=0.01$).....	79

Figure 25: Force profile while following a straight surface.....	79
Figure 26: Force profile following an inclined surface.....	80
Figure 27: Example of membership functions.....	84
Figure 28: Fuzzy logic membership functions example.....	84
Figure 30: Design of the Fuzzy Controller for 2D surface following.....	89
Figure 31: Design of Tagaki Sugeno fuzzy logic controller and specifying inputs and outputs.....	90
Figure 32: Force signature while following an inclined surface using fuzzy logic...	91
Figure 33: Comparison between the PID and Fuzzy Controller for geometrical profiles	93
Figure 34: Comparison between the PID and Fuzzy Controller for geometrical profiles	94
Table 35: Performance comparison between PID and Fuzzy Controller on the experimental rig	95
Figure 36: Modified Controller structure for PID+Fuzzy controllers.....	97
Figure 37: Profile of the surface following using the modified control strategy...	97
Figure 38: Top View of the ezdsp F2812 Board.....	115
Figure 39: Force profile following a curved surface.....	121
Figure 40: Stator and rotor flux linkages in different reference frames.....	128

Terminology and Nomenclature used in the research work:

V_q : q axis stator voltage

λ : flux linkage

λ_q : q axis flux linkage

u_i : Integral term

T_i : integral time

K_p : proportional gain

λ_s : amplitude of stator flux linkage

K_{conv} : constant used for force to torque conversion

λ_d : the d axis flux linkage

I_d : d axis stator current

V_d : d axis stator voltage

T_e : electromagnetic Torque

I_q : q axis stator current

λ_f : rotor flux linkage

R_s : stator resistance

L : stator self inductance and with the d and q subscripts represents inductances for those axes

e : control error

F : force exerted by the robot on the environment.

u_d : derivative term

T_d : derivative time

u_0 : nominal value of control variable

u_p : Proportional term

P : number of poles

p : differentiation operator d/dt

u : control variable

δ : angle between stator and flux linkage

ω : electrical angular velocity of the rotor

$i_{ds}^{r*}, i_{qs}^{r*}, \theta_r$: inputs to the inverse Park transform as described in Chapter 4

i_u^*, i_v^*, i_w^* : outputs to the inverse Clarke transform as described in Chapter 4

i_{ds}^*, i_{qs}^* : inputs to the inverse Clarke transform as described in Chapter 4

i_{ds}^r, i_{qs}^r : outputs to the Park transform as described in Chapter 4

i_{qs}, i_{ds} : inputs to the Park transform as described in Chapter 4

i_{ds}, i_{qs} : outputs to the Clarke transform as described in Chapter 4

i_u, i_v : inputs to the Clarke transform as described in Chapter 4

Abbreviations:

AC motor : Alternating Current Motor
ADC :Analog to Digital Converter
BIT: Bristol Institute of Technology
B : Damping of the mechanical spring
CAN: Controller Area Network
CCS :Code Composer Studio Software environment
CFRP : Carbon Fibre Reinforced Plastic
CMM : Coordinate Measurement Machine
CNC : Computer Numeric Control
DAC :Digital to Analog Converter
DC: Direct Current motor
DSP : Digital Signal Processing
FL: Fuzzy Logic
FSV :Full Scale Value
GPIO: General Purpose Input Output
InFACT: Integrated Flexible Assembly Cell Technology
IO: Input/Output port
K : mechanical spring constant
MIMO: Multi Input Multi Output
P : Proportional controller
PC: Personal Computer
PI: Proportional Integral controller
PID: Proportional Integral Derivative Controller
PMSM: Permanent Magnet Synchronous Motor
PWM: Pulse Width Modulation
RCC: Remote Centre Compliance
SISO: Single Input Single Output system
SPI: Serial Peripheral Interface bus
TI: Texas Instruments

Thesis Structure and Summary

- **Chapter 1:** Introduction:

In this chapter, introduction of the research is described. Afterwards the motivations, research objectives of the presented work are explained to aid the reader.

- **Chapter 2:** Literature Survey:

This chapter explains the specific field of research to which this work relates to. It explains the justification and the inspiration of the work undertaken. The detailed explanation is carried out of the potential application areas of the proposed control philosophy.

- **Chapter 3:** Mathematical representation of the PMSM:

The mathematical representation of the PMSM is described in this chapter which forms the basis of the proposed control philosophy for the electric actuators. The chapter also describes the introduction of the force controlled behaviour in the robot joint drive actuators.

- **Chapter 4:** Development of the experimental setup:

The chapter begins with the description of the experimental setup used in the research. It describes the data acquisition and interpretation of the controller signals. The calibration experiments related to force exerted on the environment and the motor current is described in this chapter. The initial basic development is explained with the aid of software flow charts for contour following experiments.

- **Chapter 5:** Development of PID Controller:

This chapter gives an introduction and justification for the PID controller. The chapter then explains the modelling and implementation of the PID controller on the robot gantry experimental setup. The tests are conducted on the experimental setup for contour following applications.

- **Chapter 6:** Development of Fuzzy logic controller:

This chapter presents the justification for the introduction of Fuzzy controller in the software for torque control on the present experimental rig. The chapter describes the approach adopted in the design of the fuzzy controller. The fuzzy controller is designed and implemented on the experimental setup for torque control. The tests and results are presented and compared with PID controller. The research work is then focussed on the design of controller using both the PID and the fuzzy controller for interaction with complex geometrical contours.

- **Chapter 7:** Main Contributions and Conclusions:

This chapter presents the main contributions of the most salient points made throughout the thesis, along with the examination of how the work undertaken has addressed the issues raised in the research questions.

- **Chapter 8:** Future Work:

Fruitful ideas for future work are identified and are discussed further in this chapter. Some new areas are depicted- some are future-work while the rest are modifications of the existing research work.

- **Appendices:**

The appendices provide an abundance of ancillary information for the project. Whilst the main chapters explore the theoretical background and results of practical tests, the appendices provide more practical aspects of the research such as the controller introduction and its operation and the entire software code for the undertaken research work.

Chapter 1

1. Introduction

1.1 Introduction and Motivation of the Research

Automation (ancient Greek: self dictated) or industrial automation or numerical control is the use of control systems such as computers, to control industrial machinery and processes, reducing the need for human intervention [Dictionary Reference, 2008]. Robot automation plays an increasingly important role in industrial applications and global economy. Engineers strive to combine automated devices with mathematical and control tools to create complex systems for a rapidly expanding range of industrial applications. Robot automation improves quality, speed, production and cost. It has found numerous applications in material handling applications such as pick and place, packaging, and robotic assembly and manufacturing applications such as polishing, deburring, spot welding and grinding.

Robotics has matured as a system integration engineering field defined by M. Bradley as *“the intelligent connection of the perception to action”*. Programmable robot manipulators provide the *“action”* component. A variety of sensors and sensing techniques are available to provide the *“perception”* of the interaction with the environment [Petriu et al, 2008]. The industrial robot applications such as cranking a wheel, twisting a screw or deburring a machined part require the robot end effector to physically interact with an external surface

or object. This interaction is aided with elastic pads or springs inserted in the robot end effector or sensors such as position sensors, vision sensors, force sensors, proximity sensors. The insertion of springs or elastic pads aids to limit the interaction forces between the robot end effector in order to avoid damage to the surface or object in deburring, polishing applications. The position, vision, force sensors are used to give feedback to the robot controller and therefore the controller can take appropriate actions to bring about the required motion in the electric actuators of the robot arm, and thereby in the robot structure, to attain the desired outcomes.

There is an inherent disadvantage in the inclusion of the sensors in the robot controller structure. The acquisition, interpretation and utilization of the sensory information in the controller can affect the responsiveness of the robot to external changes. Another disadvantage is the cost and unsuitability to adapt to different working conditions. The different working environments also demand compliance in the traditionally stiff robot structures. This is important so that the interaction of the robot end effector with the environment can be controlled precisely and accurately. Compliance can be introduced in an active or a passive manner in the robot structure. The use of mechanical springs or elastic pads is termed as a passive manner of introducing compliance. This method has limited performance and lack of adaptability to different applications. The amalgamation of pneumatic system in the robot end effector introduces active compliance in the system but the cost, difficulty of control remains the main drawbacks.

Robot applications such as grinding, surface finishing operation like deburring require the robot position control as well as force control and it becomes a complex Multi Input Multi

Output (MIMO) system. The research focuses on the inherent architecture of the robot without any additional or subordinate sensors connected to the robot. The aim is the precise and accurate control of the robot joint electric motors and introduction of active compliance in the system. The performance of the electric motor is varied in accordance with the environmental constraints. The motor current is used as an indicator for torque and shaft encoder data provides the necessary feedback information to enable motor control to be exercised. Thus the robot interaction with external object or surface is made programmable in real-time applications. The advantages are less cost, less acquisition and the utilization for the interpretation of force information and the varied performance based on external conditions or desired applications.

The outcome of the research can be applied to processes such as assembly, grinding, deburring and potentially coordinate measurement systems. The experimental work is carried out on a permanent magnet synchronous motor. The experimental work can also be extended to both permanent magnet and brushless DC motors.

1.2 Research Objectives

- To develop a software based controlled behaviour in the joint electric actuator so that the interaction of the actuator, and thereby the robot, is made programmable in real time applications and to exhibit this behaviour when the robot interacts with the environment.
- To develop and implement software architecture for a two dimensional contour following force control strategy based on the accurate torque control of the electric actuators of the robotic system.

- To engineer the robot force control system that will traverse two dimensional artefacts without previous geometrical knowledge and within a configurable force deviation tolerance range.
- To design and validate control strategies such as the conventional PID control and fuzzy control to obtain a stable, accurate and reliable system; controller selection being based upon the optimum performance under various operating conditions.
- To provide a survey of various research and manufacturing areas where this innovative control strategy can be applied.

1.3 Adopted Research Strategy

The experimental studies of the research are carried out on a robot gantry manipulator at the University of the West of England (UWE), Bristol. A generalised study and inspection is carried out on the rig. The electric actuator used in the research is a Permanent Magnet Synchronous Motor (PMSM) but the control philosophy demonstrated is applicable to other electric actuators. The research is focused on automation of manual deburring although it can be extended to other applications. A broad literature survey is performed.

An experimental study is also carried out with a force sensor connected to a robot arm and to compare its results with the proposed control philosophy.

Design and implementation of the controller and data acquisition boards is carried out and introductory experiments are conducted on the test rig for two dimensional contour following. Calibration experiments are performed on the experimental setup for torque-force relationship.

A two dimensional contour following robotic system based on torque control of the electric actuator is designed and implemented for surfaces with unknown geometry.

The data acquisition, which included, current feedback is employed on practical experimental setup. Contour following experiments were carried out on different surfaces with unknown geometry.

Mathematical representation of the electric actuator is carried out and is validated on the rig to demonstrate force control behaviour in the real actuator. The force control of the actuator is made programmable so it exhibits active compliance.

PID controller design and implementation is carried out to give a stable, reliable and repeatable robotic system. Simulation studies are performed and validated on the experimental setup.

With an aim to incorporate control strategies for complex environments for automation applications like deburring, fuzzy control is considered and tested. A switching mechanism is developed between the conventional PID and fuzzy controller and, depending on the environment conditions; a combination of both the controllers can be used.

The research carried out is focussed on automation of robotic deburring but this research can be extended to various other robotic applications. Therefore, a detailed research survey was performed, to identify the possible application areas of the control philosophy.

Chapter 2

2. Literature Survey

2.1 Introduction

A robot is defined in many ways: "A reprogrammable, multifunctional manipulator designed to move material, parts, tools, or specialized devices through various programmed motions for the performance of a variety of tasks" [Robot Institute of America definition, 1979]. "An automatic device that performs functions normally ascribed to humans or a machine in the form of a human." [Webster Dictionary]. The first definition is restricted to what a robot manipulator is doing in a mechanical sense. The second definition is more general but still limited to what robots are supposed to do.

The basic idea of a practical robot is to replace humans in repetitive, dangerous, or tiring tasks. As these repetitive, tiring jobs were found on production lines in industries, Industrial robots were the first real beings to enter our world as operating machines. Cars, electronic devices to consumer home appliances today are manufactured by automated machines or "industrial robot" that replace the common worker in the production line.

An industrial robot manipulator is constituted of:

1. A *mechanical structure* or manipulator that consists of a sequence of rigid bodies (links) connected by means of articulations (joints); a manipulator is normally characterized by an arm that ensures mobility, a wrist that confers dexterity, and an end effector that performs the task required of the robot.
2. *Actuators* that set the manipulator in motion through actuation of the joints, the motors employed are typically electric or hydraulic, and occasionally pneumatic. Actuators are needed to perform motion or manipulation in the external world.
3. *Sensors* that measure the status of the manipulator and, if necessary, the status of the environment.
4. A *control system* (normally a computer) that enables control and supervision of manipulator motion.[Sciavicco et al, 2000].

2.2 Literature review

Traditional/Conventional industrial robotic tasks, which are generally related to manipulation or assembly, require only control of the position of the robot arm. The managing of the robot interaction with the environment by adopting a purely motion or position control strategy turns out to be inadequate for tasks like grinding, deburring or composite layouts. Implementation of all these tasks intrinsically necessitates that a robot, besides realizing the predisposed position, provides the necessary force to either overcome the resistance from the environment or to comply with the environment. Also, the unavoidable modelling errors and uncertainties in these applications may cause a rise of the contact forces ultimately leading to an unstable behaviour of the robot arm during the interaction [Zeng, 1997].

During the early work on telemanipulation, the use of force feedback was introduced to assist the human operator in the remote handling of objects with a slave manipulator. More recent research has been conducted on cooperative robotic tasks have been implemented such as fingers of a dexterous robot hand where the robot force control is of crucial importance as it has to limit the exchanged forces and avoid squeezing of a commonly held object. Robot force control is used widely because autonomous field robots for heavy industry must be rugged and reliable. Force control in industrial robotics has been a key research area to increase robot performance and to introduce new functionalities for the last 30 years and has been documented in research articles. Also, in robot force feedback for deburring and grinding tasks and automated solutions have been proposed and implemented. [Raibert and Craig, 1981, Siciliano and Villani, 2001, Brogardh, 2007 Lu et al, 1992 Aertbelien et al, 1999]

Precise position and force control is required for applications such as assembly of precision-component systems, grinding and deburring. A classification of robot force control algorithms based on application of the relationship between position and applied force or between velocity and applied force, or the application of direct force feedback, or their combinations includes:

- methods involving the relation between position and applied force;
- methods applying the relation between velocity and applied force;
- methods applying directly position and applied force: hybrid position / force control, and hybrid impedance control;
- methods applying directly applied force feedback: explicit force control.

[Salisbury, 1980, 1982, Borrel, 1979, Whitney, 1977, 1987, Colbaugh, 1992, Mason, 1981, Raibert, 1981]

The two basic approaches to force control are *Hybrid* and *Impedance* control [Hogan, 1985]. Hybrid control [Raibert, 1981] is based on the decomposition of the workspace into purely motion controlled directions and force controlled directions. In *Hybrid control*, both a motion controller and a force controller are implemented but the force controller is given precedence. The insertion of a peg in a hole can be achieved using hybrid force decomposition. The position error is changed proportionally to the equivalent force error in the working space first. This is transformed to joint torque error and then fed to the controller. The controller also compensates for the friction force. The force can be applied to a direction orthogonal to the position control [Raibert, 1981]. *Impedance control* is similar to pure position control where a desired velocity is commanded, except that the impedance of the robot is regulated to avoid excessive force build-up. Impedance control [Hogan, 1985] does not regulate motion or force directly but regulates the ratio of force to motion which is the mechanical impedance.

Impedance control is robust while making contact with unknown surfaces. Hybrid control has to be divided into two modules: one for free space motion and the other for impact transition for dealing with unknown surfaces. The advantage of a hybrid controller over Impedance control is that the contact force can be regulated accurately [Hogan, 1985 Schutter, 1997 Raibert, 1981 and Sung-Hyun Han, 1999]. In the presented work, Hybrid force controller has been used and the force and motion control strategies are separate in the control system architecture.

To achieve robot force control, the adoption of sensors is of crucial importance to achieve high-performance robotic systems. These are divided into two classes: *proprioceptive* sensors and *heteroceptive* sensors. The former are joint position, joint velocity and joint torque sensors which measure the internal state of the manipulator while the latter are force sensors, proximity sensors, range sensors and vision sensors that provide the robot with knowledge of the surrounding environment. The goal of these sensors is to extract features characterizing the interaction with environment, thus enhancing the degree of autonomy of the system. Sensing is particularly difficult because industrial environments are often dirty, dusty and noisy, both acoustically and electromagnetically. For these conditions, force sensing is one of the most appropriate technologies, because it is relatively insensitive to these factors, is well developed and economical. This force information is used for path modifications in the robot controller to achieve the desired operation [Sciavicco et al, 2000].

Robot interaction with the environment can be controlled by the inclusion of sensors which feedback the force data. The force signals are used in a path trajectory controller to make the required changes in the robot path. It is crucial to adhere to the required forces on the environment, otherwise too much force could damage the surface/environment or too little force could not give the desired results perhaps even losing contact with environment. One solution is to have a mechanical device (remote centre of compliance) interposed between the manipulator end effector and the environment which has high stiffness in one direction and high compliance in the other directions, which can avoid excessive force build-up. This is termed passive compliance. The disadvantages of this

method are rigidity of the device, cost, and failure to adapt to different environments. Therefore, another solution is preferred where the force acting on the environment can be monitored in real time and the robot can comply with either the desired trajectories or set force bands. This is active compliance [Siciliano & Villani, 2001].

Force sensors usually consist of an array of strain gauges which delineate the linear and/or rotational components of the vector force along the three/six axes of the sensor coordinate frames [Sponge, 1989]. Measurement of force and/or torque is usually reduced to measurement of the strain induced by the force (torque) applied to an extensible element of suitable features. Therefore, an indirect measure of force is obtained by means of measurements of small displacement. The basic component of a force sensor is the strain gauge which uses the change of electric resistance of a wire under strain. The strain gauge is constituted by a wire of low temperature coefficient. The wire is disposed on an insulated support which is glued to the element subject to strain under the action of stress. As dimensions of the wire change, they cause a change of electric resistance. Design parameters are chosen in such a way that the resistance changes linearly in the range of admissible strain for the extensible element. To transform changes of resistance into an electric signal, the strain gauge is inserted in one arm of a Wheatstone bridge which is balanced in the absence of stress on the strain gauge itself.

The sensor type which has gained a lot of industrial and academic attention is the six axis force/torque sensor. The sensor is used widely in industrial applications with increased product quality and reliability. However, the force sensors, in general, have some drawbacks. The programming and tuning methods need further development [Brogardh,

2007]. The speed of response; in particular can have a significant effect on the efficacy of this approach. Also, force sensors are expensive, can be damaged whilst in operation. The force data from the sensor needs to be acquired, modified and then utilised in the controller structure which is difficult. Therefore, the precise utilisation of the force signal becomes a crucial issue in these applications; otherwise it may lead to robot actuator saturation or damaging the object/ work-piece.

Some research in robot force control focuses on using the position feedback and relating the velocity with the force exerted on the environment. Thus, the position feedback is calibrated to force values exerted on the environment and, in real time applications, knowledge of the environment can be obtained by monitoring the robot position [Siciliano & Villani, 2001]. In [H. Kawasaki et al, 2006], research has also been carried out without using a force sensor but by observing the joint position and velocities of the robot arm. Thus, research has been conducted on force feedback without a force sensor.

But in these researches, the inherent stiffness of the robot arm is not changed or altered. This makes sense in traditional position controlled robot systems where high stiffness reduces instability. But lower interface stiffness has advantages such as more accurate and stable force control and less damage during inadvertent contact. This alteration in the stiffness aids in the controlled interaction with the environment and improvement in the compliant interaction [Schutter et al, 1986].

2.3 Introduction and Justification of the research undertaken

Automation of manufacturing tasks like deburring and polishing require introduction of science into traditionally art based processes. The aim is to design and implement complex behaviour in the control structure. This is introduced in a robotic system or a Computer Numerical Control (CNC) machines by force control strategies. The force control methods can be broadly implemented as rigid structures and compliant structures. With conventional rigid structures/tools it is very difficult to control the interaction with an object/surface.

Compliance is the ability of an object to yield elastically or in a spring like manner when subjected to a force. Compliance control is very important and it is normally introduced in the system with the addition of external sensors such as mechanical springs and pneumatic actuators which are unadaptable to different geometrically varying surfaces and difficult to control respectively.

Adaptive force control is crucial during this interaction as the operation demands the alteration of the performance during the process execution. An example is the need for the increased grip force when pressing against a spring as more force is required as the spring is compressed. Another example of adaptive control is the application of more power to a motor to maintain a constant speed, as when a robot moves from a level ground to an incline or when it tries to move a heavy object.

This research aims to provide this type of adaptive compliant behaviour in an electric actuator attached to a mechanical system without the above mentioned external sensors. The goal of the research is the control of the electric actuator wherein a stable and specified contact force with the environment is to be maintained. The research work aims to develop this innovative approach by the control of electric actuators. Instead of generating this force data through a mechanical and rigid force sensor, force information can be obtained from the electric actuators (PMSM) driving the robot arm.

Brushless AC servo drives are increasingly used in high performance positioning systems such as robots and manipulators because of their excellent parameters compared to conventional DC motors or induction motors. The power density of a PMSM is higher than the induction motor due to the fact that there is no stator power dedicated to magnetic field production. These motors are controlled by techniques such as Vector control. In this method, the position feedback from the motor rotor is required to transform the three phase variable into two phase axes frame in the synchronously rotating reference frame aligned with the rotor flux linkage vector. This is done to maximise the torque supplied by the motor. Research on the control and performance of PMSM has been carried out and documented in articles. [Schutter et al, 1986, Kaewjinda, 2007 and Pillay et al, 1988, 1989, Vector control, NEC application notes, 2002]. Research has been done on the precise modelling and method of operation of PMSM [Pillay et al, 1988, 1989]. In [Hyunbin et al], the dynamic behaviors of a BLDC motor are analyzed, when the motor undergoes mechanical and electromagnetic interaction due to an air gap variation between the stator and rotor and thereby controlling the torque.

The motor current reflects the torque of the actuator and thereby the force of the system [Sponge et al, 1989]. The torque of the motor can be altered depending on the load on the system and hence the force exerted by the system. Thus, the motor current can be calibrated to reflect the force exerted by the manipulator on the environment. By achieving this, we are able to introduce active compliance in the system. The robot interaction with the environment can be made programmable and the force exerted can be changed. Thus, the electric actuator behaves as a programmable spring. The contact force depends on the robot joint actuator stiffness. The stiffness can be varied to yield elasticity or a spring like behaviour when a force is applied, thereby introducing compliance in the system. Therefore, the need for an external force sensor is avoided.

Using an adaptive controller for real time applications like grinding and deburring requires a powerful processor. Nowadays, the development of new materials, the improvement in the mechanical design of robot manipulators and faster microprocessors have highlighted the necessity of applying more sophisticated control algorithms in the new generation of industrial robotics [Siciliano and Villani, 2001]. An adaptive controller continuously tracks plant parameters and constantly, or periodically, modifies the parameters of the control system to provide optimum performance. To achieve this, a Digital Signal Processor (DSP) is required.

Significant research in intelligent and Adaptive control has been performed based upon the PID control, fuzzy control and neural network approaches. PID controllers are extensively used because of the advantageous properties they exhibit such as robustness, simplicity and accuracy. However, due to non-linearities whilst dealing with the

environment, sometimes the preferred solution is fuzzy control or neural networks, which aim to incorporate more complex behaviour and reasoning skills in the automation of robot operations to handle non-linearities. Fuzzy control has become a popular approach for performing the task of controller design because the human reasoning skills can be incorporated in the controller structure. Therefore, fuzzy control is often applied to some ill-defined systems. This explains the current trend in the theoretical development to combine fuzzy control techniques with conventional PID control techniques to obtain adaptive fuzzy control.

For example, in [Ahn et al, 2011] an online smart tuning fuzzy PID approach based on a robust extended Kalman filter for the development of high force control precision is presented, where force or position control with high accuracy is exceedingly necessary. In [Hamit] a neurofuzzy controller has been used to linearize the highly nonlinear sensor and motor output signals.

In some cases, industrial robot operation demands high accuracy performance that is not achievable by using a conventional PID control. In [Kaitwanidvilai, 2004], the concept of switching between a PID controller and a neurofuzzy controller has been implemented on a pneumatic system. The experimental results have confirmed that the concept of multimode switching yields better results than classical control or the neurofuzzy controller acting alone. Research has been documented in articles. [Trusca, 2003, Burn, 2003 Chang, 1999, Hassan, 2002].

2.4 Application Areas

Robot force control can be used for various robot automated operations like polishing, assembly and deburring. The automation of the preceding mentioned applications is often restricted because of the complexities associated with the applications. Therefore, in some cases, manual work option is still given precedence to automated operations. The research can be applied to these applications because the performance of the robot electric actuator can be varied in real time in accordance with the environmental constraints. This proposed control philosophy aims to include these complexities and non linearities in the adaptive control structure.

Automated Deburring applications-

A burr is a sharp and raised edge that is formed in several manufacturing processes such as milling, drilling, turning and other machining operations. These burrs have to be removed for ergonomic, aesthetic, and/or functional reasons. A small series of large components pose a problem and are most often manually cleaned with a grinding tool. Manual deburring techniques have disadvantages such as poor working conditions, production delays and inconsistent work quality. The robot should have a stable force control throughout the entire machining process. Automation normally requires the detailed knowledge of the environment beforehand. Automated robot deburring systems are becoming crucial as the cost of manual deburring can be around 30-35% of overall production costs [Murphy, 1990 Hsu, 2000]. Several problems prevent a breakthrough in this area which includes variations in the work piece position which are unavoidable without expensive clamping and fixtures systems. These specially designed clamping

systems cannot be used on small series of components. Due to the nature of the processes such as casting and forgings, work pieces commonly have high geometrical inaccuracies. These factors limit the use of traditional position controlled robots. Other sensors can be used to solve these problems. Force feedback is a good candidate, but its use necessitates specific control strategies that depend on the type and size of the burrs, the materials of the work-piece and grinding tool, and the task goals.

The presented work has been researched and implemented and can be applied to robotic deburring. To achieve this goal, a cutting tool with a fixed spindle speed has to chamfer the part edges while undergoing contour-following motion. While driving the cutting tool to perform a deburring process, the deburring robot must implement two major motions. One motion applies a suitable chamfering force to the part's edges to remove the burrs while avoiding damage to the part. The other motion performs contour following. This ensures the cutting tool remains in contact with all the burrs over the chamfer by appropriate torque control. A heuristic deburring control policy can attain the desired chamfering force by controlling the feed-rate of the cutting tool. The heuristic policy simply consists of slowing down the feed-rate of the cutting tool when the encountered burr is large, and speeding it up if otherwise [Kazerooni, 1987, Lu et al, 1992 Hsu Feng-Yi et al, 2000].

Most industrial robots rely on teach programming, a process that is tedious and time consuming. An alternative method uses Computer-Aided Design (CAD) data and a representation of the robot's environment to compute manipulator coordinates off-line. Unfortunately, robots usually have insufficient accuracy to use off-line programming

alone, and it is ineffectual without on-line modification. Finally, for a work piece with partially unknown contours, planning a trajectory may be infeasible. An alternative approach could be to use accurate on-line trajectory teaching via the work piece's surface geometry; a roller bearing, or a properly designed jig, is mounted on the robot end-effector. However, these machines are very expensive and frequently cost too much to justify their use in a deburring applications. Also, the mechanism is more complex [Seng Chi-Chen et al, 1999, 2000].

Researchers have worked on automation of deburring and polishing on unknown geometrical contours. Research has been done in these industrial operations but a majority of them rely on the force signature from the additional mounted sensors on the end effector [Garcia et al, 2008, Seng Chi-Chen, 1999, 2000].

Coordinate measurement machines-

Another application is coordinate measuring machines. Coordinate measurement machines (CMM) also demand a precise and accurate force and position control of the component. The overall measurement time of the component can be reduced if the actuators are introducing the compliance rather than at the probe used on the end of the arm in CMM. The compliance behaviour in the electric actuators will allow a certain specified position error to develop between the probe and the component to be measured. This control philosophy can also been implemented in biomedical engineering research involving automation of surgical procedures.

Composite layout force control-

The new Boeing B787 and Airbus A380 are seen as an indication of a step change in the use of composites in commercial aviation. The aircraft industry is undergoing a rapid shift to composite materials in the development programmes for new aircraft and is facing what it calls a ‘historic expansion of demand for such materials’. The use of reinforced plastic in aircraft has grown enormously since the early 1970. The challenge now is increasing the use of this composite material throughout the aircraft in order to increase durability, decrease weight (thus increasing fuel efficiency) [Airbus, 2007].

The composite material used in aircraft in layers, with adhesive applied in-between each layer. The aerospace industry is producing composite material called Carbon Fibre Reinforced Plastic (CFRP) and a significant proportion of its manufacturing involves high precision work performed by skilled labourers. Segments of the fuselage and the other large artefacts are manufactured by existing robotic systems, but the more intricate, complex geometrical shapes (aerodynamics) are considered to be outside the robot capabilities. This is because the workers who perform these tasks possess skill, knowledge and experience that arise from the intimate involvement with the environment and involves very accurate force and position control. This is a complex non-linear, multivariate control environment [Airbus, 2007].

The current research can be applied to these applications where compliance and stiffness of the system are real time programmable and aims to include complex behaviour in these automated robot operations. Thus, the presented research work focuses on the torque control in the electric actuators which is then applied to follow unknown geometrical

contours with desired force values. Therefore, this novel control philosophy which eliminates external sensors and also introduces spring-like behaviour in the electric actuator of a robot is very beneficial to these above mentioned applications.

Chapter 3

3. Mathematical modelling of the electric actuator (PMSM) for the controlled interaction with environment

Introduction

There is a vital interface between electrical and mechanical engineering. Wherever mechanical motion is controlled by electronics, it is commonly referred to as a part of “*Mechatronics*” [Miller, 1989]. Mechatronics involves control of mechanical motion control systems in industrial, manufacturing and technological processes. The motion control systems aim to achieve the specified performance demanded by users and industrial standards in electric actuators [Lyshevski, 1999]. The electric actuator used in the research work is a PMSM which requires a sophisticated electronic control, called Vector Control.

Motion control in Robotics is a long established and well understood field and forms the basis of most modern manufacturing technology. The demand for high accuracy and repeatability is traditionally achieved by employing high stiffness mechanisms with high-fidelity sensors and control systems [Bigge et al, 2007].

3.1 Mathematical representation of a PMSM

The PMSM used in servo-mechanical systems is generally called “a brushless servomotor” or “brushless AC servomotor” [Kaewjinda et al, 2007]. As results of the progress in power electronics, software engineering, and materials, the PMSM, based on modern rare earth magnet variety, has become a serious competitor to the induction motor and conventional wound rotor synchronous motor. PMSM drives are used in many applications. They are receiving increased attention because of their high efficiency, and small size. The PMSM is preferred, in industrial servo applications, to the DC motor due to considerations of the cost, size, low maintenance, maximum speed, capability, and simplicity of design. The power density of a PMSM is higher than that of an induction motor with the same ratings, due to no stator power dedicated to the magnetic field production. For this reason, they have evolved into the preferred solution for speed and position control drives on machine tools and robots. They are used in applications which require rapid torque control and high speed operation [Zhong et al, 1997].

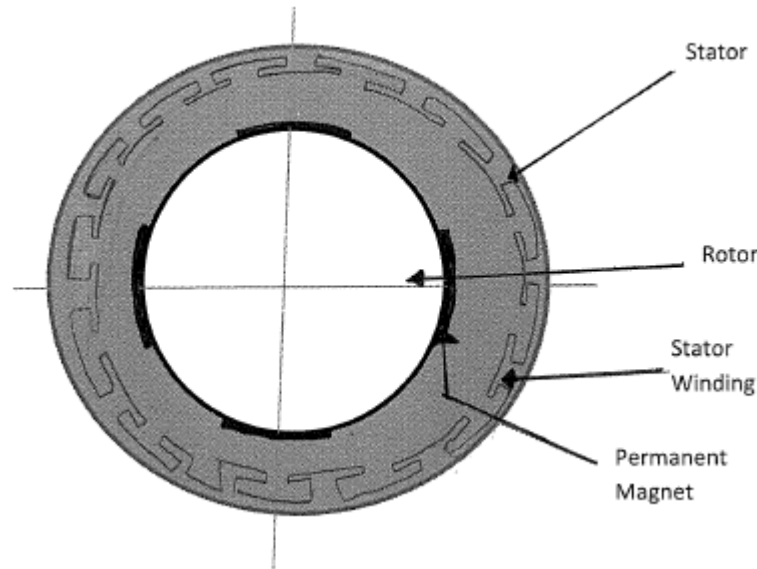


Figure 1: Permanent magnet synchronous motor (PMSM)

The PMSM, as shown in Figure 1, is a rotating electric machine where the stator is a classic three phase stator, like that of an induction motor, and the rotor has surface-mounted permanent magnets. In this respect, the PMSM is equivalent to an induction motor where the air gap magnetic field is produced by a permanent magnet. The use of a permanent magnet to generate a substantial air gap magnetic flux makes it possible to design highly efficient PM motors.

For a common 3-phase PMSM, a standard 3-phase power stage is used. The same power stage is used for AC induction motors. The power stage utilizes six power transistors with independent switching. The power transistors are switched in the complementary mode. The sine wave output is generated using a Pulse Width Modulation (PWM) technique.

A PMSM is driven by a sine wave voltage coupled with the given rotor position. The generated stator flux, together with the rotor flux, which is generated by a rotor magnet, defines the torque, and thus the speed of the motor. The sine wave voltage outputs have to be applied to the 3-phase winding system in such a way that the angle between the stator flux and the rotor flux is kept close to 90° to get the maximum generated torque. To meet this criterion, the motor requires electronic control for proper operation, called Vector Control. This is facilitated by the use of modern DSP and microcontrollers to attain the functionality, flexibility and reliability required for the accurate torque control in electric actuators.

Vector control is easily understood by forming a mental image of the coordinate reference transformation process. If an AC motor operation is visualised from the perspective of the stator, a sinusoidal input current applied to the stator is observed. This time-variant signal generates a rotating magnetic flux. The speed of the rotor is a function of the rotating flux vector. From a stationary perspective, the stator currents and the rotating flux vector look like AC quantities.

The picture is visualised being inside the motor and running alongside the spinning rotor at the same speed as the rotating flux vector generated by the stator currents. If the motor is observed from this perspective during steady state conditions, the stator currents look like constant values, and the rotating flux vector is stationary.

Ultimately, the aim is to control the stator currents to obtain the desired rotor currents (which cannot be measured directly). With coordinate reference transformation, the stator currents can be controlled like DC values using standard control loops.

In vector control drives, the highly accurate position, derived from a position sensor, is required to transform the three variables of the three phases (abc) to the two variables (dq) in the synchronously rotating reference frame aligned with the rotor flux linkage vector. The stator flux linkages, voltage and electromagnetic torque equations in the dq reference frame are as follows:

$$V_d = R_s I_d - \omega \lambda_q + p \lambda_d \dots\dots\dots (1)$$

$$V_q = R_s I_q - \omega \lambda_d + p \lambda_q \dots\dots\dots (2)$$

$$\lambda_d = L_d I_d + \lambda \dots\dots\dots (3)$$

$$\lambda_q = L_q I_q \dots\dots\dots (4)$$

The electromagnetic torque is given by the following equation for synchronous machines

$$T_e = \left(\frac{3}{2}\right) \left(\frac{P}{2}\right) (\lambda_d I_q - \lambda_q I_d) \dots\dots\dots (5)$$

Substituting Equations (3), (4) in (5), we have

$$T_e = \left(\frac{3}{2}\right) \left(\frac{P}{2}\right) \left((L_d I_d + \lambda) I_q - L_q I_d I_q \right)$$

$$T_e = \left(\frac{3}{2}\right) \left(\frac{P}{2}\right) \left(L_d I_d I_q + \lambda I_q - L_q I_d I_q \right)$$

$$T_e = \left(\frac{3}{2}\right) \left(\frac{P}{2}\right) \left(\lambda I_q + (L_d - L_q) I_d I_q \right) \dots\dots\dots (6)$$

In the above equation, the first term (λI_q) is called as the ‘magnet alignment torque’; and

L_d and L_q have the same value and equal to L, the equation is reduced to,

$$T_e = \left(\frac{3}{2}\right) \left(\frac{P}{2}\right) (\lambda I_q) \dots\dots\dots (7)$$

The d axis current is kept near zero to maximise the torque of the motor and the angle between the stator, rotor flux linkages is kept 90° in order to maximise the torque output from the motor. The mathematical proofs for the angle between the stator and rotor flux is given in Appendix.

From equation (7),

$$T_e \propto I_q \dots\dots\dots (8)$$

The torque is directly proportional to the q axis current.

The torque in equation (8) is calibrated to the force exerted by the robot on the environment. The following equation (9) is obtained, where K_{conv} constant is used for torque to force conversion.

$$F = K_{conv} * T_e \dots\dots\dots (9)$$

Substituting the value of T_e in equation (9),

$$\therefore F = K_{conv} \left(\frac{3}{2} \right) \left(\frac{P}{2} \right) (\lambda I_q) \dots\dots\dots (10)$$

$$\therefore F \propto I_q \dots\dots\dots (11)$$

The force of the electric actuator is directly proportional to the q component of the current. The current is maintained within a predetermined force band and is made programmable in the software. Therefore, the force exerted by the electric actuator on the environment can be controlled in accordance with the expected results.

3.2 Introduction to spring like behaviour in electric actuators

The aim of the research is to look into the introduction of a spring like behaviour in the robot electric actuator and thereby controlling the interaction of the robot with any object or surface. When a mechanical spring is considered, the damping (B) and the stiffness (K) are considered as the two main attributes. The same mechanical attributes are compared with the electrical analogies.

In a PMSM, the rotating frequencies of the rotor and the stator flux are the same, i.e., no slip. However, if the rotor speed departs from the steady synchronous value, there is a time difference before which the stator and rotor flux come into synchronisation. This characteristic of the PMSM is compared with the damping characteristic (B) of a mechanical spring. When the motor is given a step speed change it oscillates around the desired value before settling. This factor gives the damping of the system.

Compliance can be termed as the ability of an object to yield elastically, giving a spring like behaviour when a force is applied. The torque provided by the motor is directly proportional to the angle between the stator and rotor flux linkages and the torque is maximum at an angle of 90 degrees. In the presented work, the amplifier of the motor always tries to keep the angle at 90 degrees. However, with sophisticated control techniques, the angle can be reduced and thereby affecting the torque. The torque is also directly proportional to the magnitude of the stator flux linkage. These two entities affect the torque and thereby the stiffness of the electric motor. This is analogous to the stiffness

(K) of a mechanical spring. This control philosophy will guarantee adaptive stiffness and compliance can be introduced into the system.

The manipulation of the angle between the stator and rotor flux linkages is not employed in the research carried out due to the operational limitations of the drive amplifier for the electric actuator. Thus the electric actuator, with appropriate control strategies, can be designed to behave as a programmable spring and the interaction with the environment or the surface can be controlled as desired. The performance of the motor and the stiffness is altered in accordance with the environmental constraints.

Chapter 4

4. Development of the experimental setup for robot interaction with the environment and initial tests

4.1 Introduction of the system

The proposed research was carried out on a robot gantry manipulator at the University of the West of England (U.W.E.), Bristol. The following section provides an introduction to the experimental setup and describes the control system architecture employed in the research.

Background and Introduction-

The gantry robot machine was built for the InFACT (Integrated Flexible Assembly Cell Technology) Project, U.W.E. (then Bristol Polytechnic) was the project leader. The aim of the InFACT project was to build a flexible assembly machine that could assemble a large range of small consumer products. For this work, only one manipulator is being used. Each manipulator has three axes or modules (X, Y, & Z).

The structure is similar to nearly all commercial robots. The difference is that the entire gantry has been designed and built at UWE, so it can be modified far more easily than commercial machines, as there is access to the controller. This machine is aimed at research tasks so the configuration will change with time. To accommodate the changes, InFACT is made re-configurable. The basic diagram for one arm with three axis of the manipulator is as shown in Figure 2.

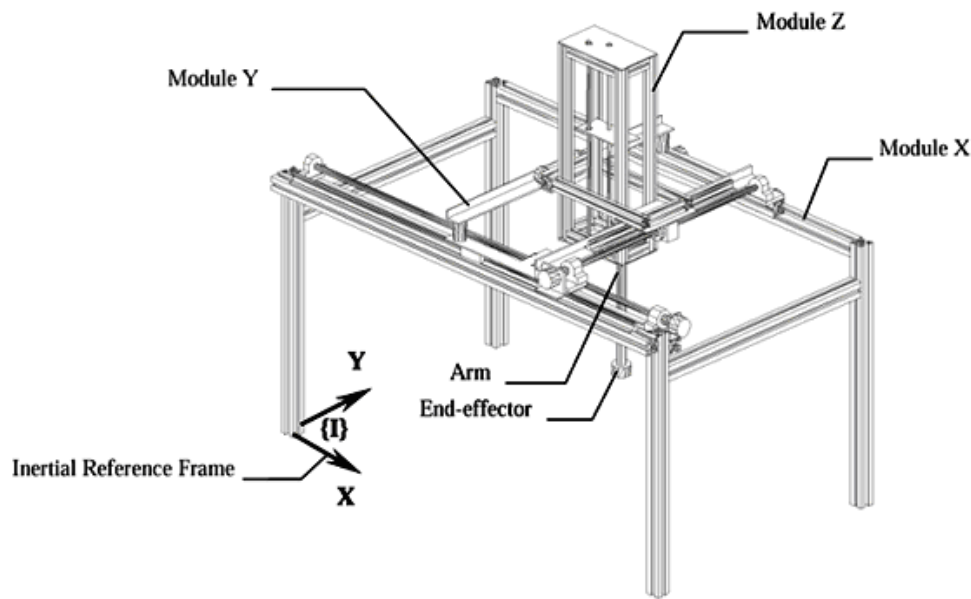


Figure 2: A Generic gantry manipulator layout

4.2 Description of the control system architecture, electrical actuator and controller

A typical control system has to supervise the activities of the robotic system and is aided with a number of tools providing the following functions:

1. Capability of moving physical objects in the working environment, i.e., *manipulation capability* related to the actuators.

2. Capability of obtaining information on the state of the system and the working environment, i.e., *sensory ability*;
3. Capability of exploiting information to modify system behaviour in a pre programmed manner, i.e., *intelligent and adaptive behaviour ability*;
4. Capability of storing, elaborating and providing data on system activity, i.e., *data processing ability*. [Sciavicco et al, 2000]

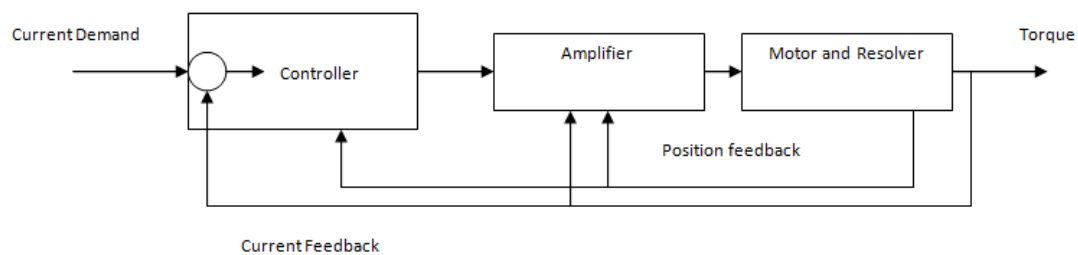


Figure 3: Control system architecture employed in the research

The control system architecture is implemented as shown in Figure 3. The used controller is the TMS320F2812, a mid-range DSP. DSPs are special purpose microprocessors that are particularly suitable for intensive numerical computations. Digital versions of most advanced control algorithms can be defined as sums and product of measured variables thus can be naturally implemented by DSPs (Z. Ma, 1995). The DSP generates the control signal which goes to the drive (Infranor amplifier SMTDB) of the motor which, in turn, provides current to the motor (MA-30 Mavilor). PMSM actuate individual robot gantry axes. All the electric actuators are installed with a resolver for providing position feedback. The resolver is an electromechanical position transducer. Its operating principle is based on the mutual

induction between two electric circuits which allow continuous transmission of angular position without mechanical limits.

Each motor is connected with two cables. One cable carries electric power to the motor. The second cable (resolver cable) tells the amplifier cabinet how far the motor has moved in a positive or negative direction. The motor and amplifier form a separate unit. There is a current feedback path from the motor and a position feedback path from the resolver on the motor, as shown in Figure 3. *The data sheets for the electric actuator, amplifier and controller can be found in the appendix I, II and III.*

As the research work is performed on a two dimensional gantry manipulator, there are two DSP boards used in the architecture. The two DSP boards communicate with each other via a CAN bus interface with a maximum speed of 1Mbps. The experimental setup has been designed for X-Y two dimensional tasks at present, but it has also a facility for a Z direction.

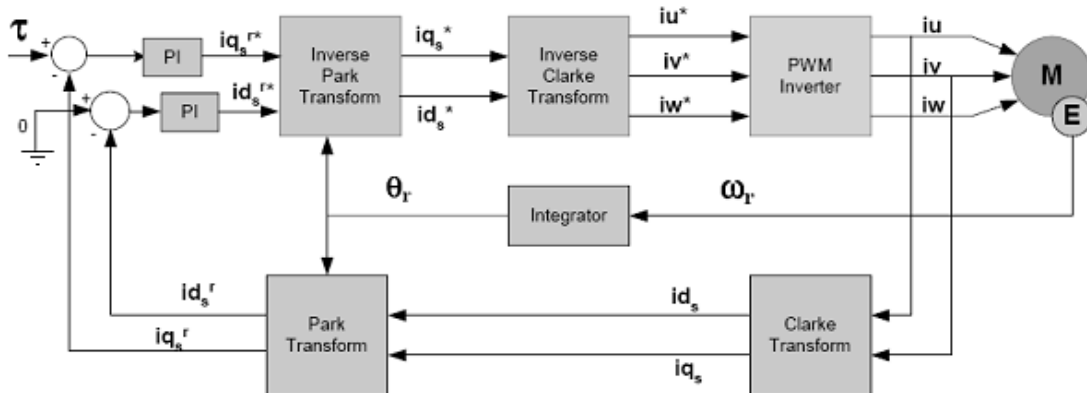


Figure 4: Block diagram of Vector control of an AC motor

(Detailed Description of Vector Control is given in the Appendix section-05)

The electric actuators on the robot are operated by Vector control. It is an elegant method of controlling the PMSM which is used to control space vectors of magnetic flux, current, and voltage. It is possible to set up the co-ordinate system to decompose the vectors into an electro-magnetic field generating and torque generating parts. Thus, the structure of the motor controller (vector control controller) is almost the same as for a separately excited DC motor, which simplifies the control of PMSM. This vector control technique was developed in the past especially to achieve similar excellent dynamic performance of PMSM.

The performance of three phase ac machines is described by voltage equations and inductances. AC machine inductances are functions of rotor speed. The coefficients of the differential equations which describe the behaviour of these machines is time varying. A change of variable can reduce the complexity of these differential equations. Therefore, Clarke and Park Transforms were introduced. The transformation of rotational circuits to a stationary circuit was developed by E. Clarke. The Park Transform was developed by R. H. Park. The Park Transform has the feature of eliminating all time varying inductances from the voltage equations [Toliyat, 2004]. Using these transforms, many properties of the electrical machines can be studied without the complexities of the voltage equations.

Vector control seeks to recreate the orthogonal components in the AC machine (i_d and i_q) in order to control the torque producing current separately from the magnetic flux producing current [Vector Control, NEC, 2002]. The i_q and i_d components of the (fictitious) stator current vector are referenced to the so-called rotor reference frame. This

reference frame is referenced to the rotor flux, and is synchronous to the rotor. There may be a phase difference, but this is usually assumed to be zero for our discussion. The axis along the rotor flux is the d (or direct) axis, and the axis 90 degrees (electrical) away from it is the quadrature (q) axis. Theta is the rotor flux position.

In a PMSM the flux component is produced by the permanent magnets (the fixed field winding is replaced with a rotating permanent magnet). The rotor flux produced by the PM rotates at the same speed as the rotor field i.e. there is no slip. So for a PMSM the ordered I_d component is set to zero and the rotor angle is obtained by integrating the rotor speed. The system configuration for vector control of a PMSM. For all the following transform equations, refer to Figure 4.

Vector control requires computationally intensive algorithms, this coupled with closed loop control and precise Pulse Width Modulation (PWM), requires a relatively powerful microprocessor along with the relevant peripherals to make vector control a practical proposition. This Vector control is implemented inside the amplifier. Although this can also be implemented in software, as the DSP controller has a very high sampling frequency.

4.3 Data acquisition, interpretation and utilisation in the controller

Signal conditioning means manipulating an analogue signal in such a way that it meets the requirements of the next stage for further processing. More generally, signal conditioning can include amplification, filtering, converting, and any other processes required to make sensor output suitable for conversion to digital format. It is primarily used for data acquisition, in which sensor signals must be interpreted and filtered to levels suitable for

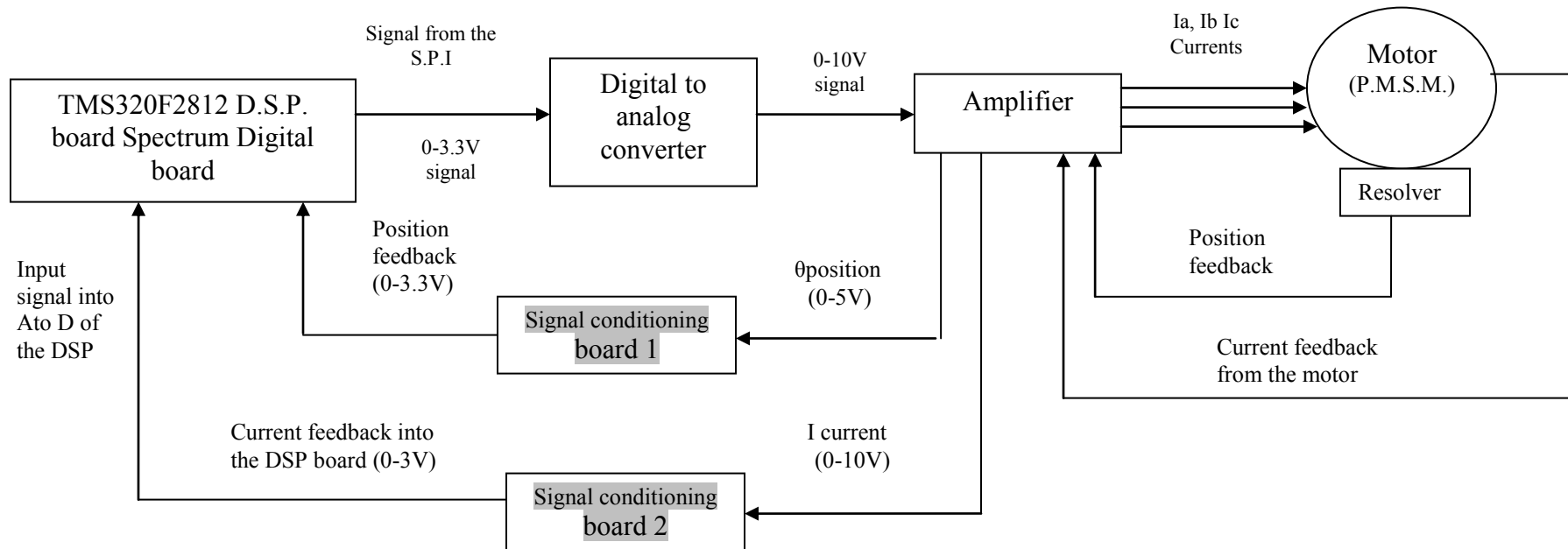
Analogue-to-Digital Conversion (ADC) or Digital-to-Analog Conversion (DAC) so they can be read by computerized devices.

The F2812DSP accepts analogue signals which are 0-3.3V. All the feedback signals from the amplifier are 0-10V. So, signal conditioning boards were manufactured to level shift these to input them into the DSP. The current signal from the amplifier is an analogue signal and has to be digitised which is done by the 12 bit ADC on board of the F2812 DSP with a fast conversion rate of 80ns at 25 MHz clock. Also, the output speed command from the DSP has to be in the range of 0-10V as the amplifier accepts 0-10V analogue signal at its input. There is also a DAC to convert it into an analogue signal. The other DSP functionalities used is the Serial Peripheral Interface (SPI), which is used for communications between the DSP and external peripherals or controllers. The SPI is a high-speed synchronous serial input/output (I/O) port that allows a serial bit stream of programmed length (one to sixteen bits) to be shifted into and out of the device at a programmed bit-transfer rate. *The circuit diagrams for the signal conditioning boards are included in the appendix of this thesis.*

The following block diagram, Figure 6, indicates the signal acquisition and utilisation in the controller. It is shown for a single axis actuator and the same structure is replicated while dealing with two dimensional environments. The Amplifier depicted in the Figure 5 has an internal position feedback loop and a current feedback loop from the electric motor. These mentioned feedback loops are hardwired in the amplifier.

The 2812 DSP position feedback loop and current feedback loop are depicted in grey boxes are designed in the software. These 2812 DSP feedback loops are separate to the amplifier feedback loops. Due to the hardwired feedback loops in the amplifier, the research work is focused only on the feedback loops in the 2812 DSP.

The Figures 6, 7 and 8 show the experimental setup used in the research.



(Same architecture is employed when used for 2 dimensional environments)

Figure 5: Block diagram of the control system architecture implemented for a single robot axis

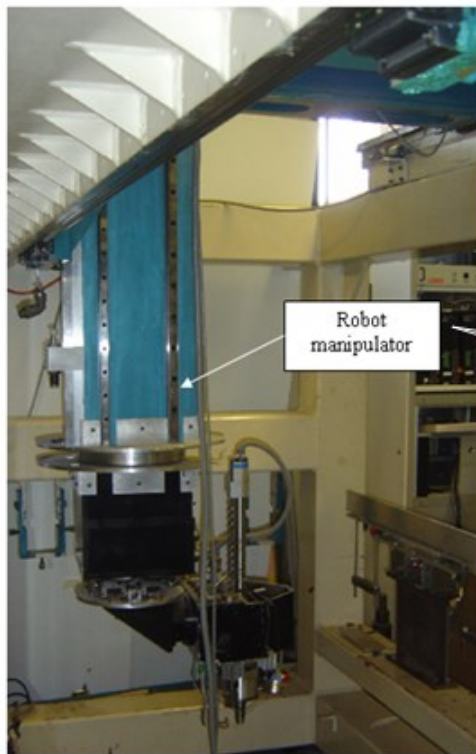


Figure 6: Robot manipulator

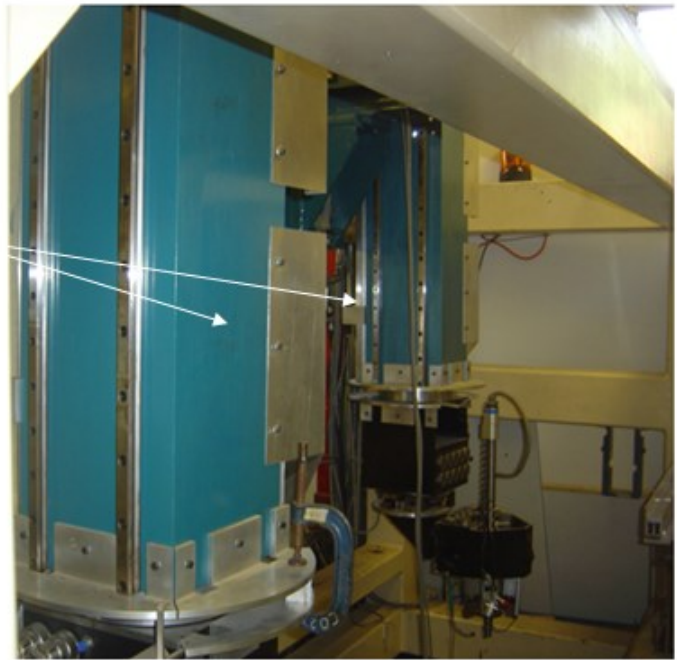


Figure 7: Two arms of InFACT

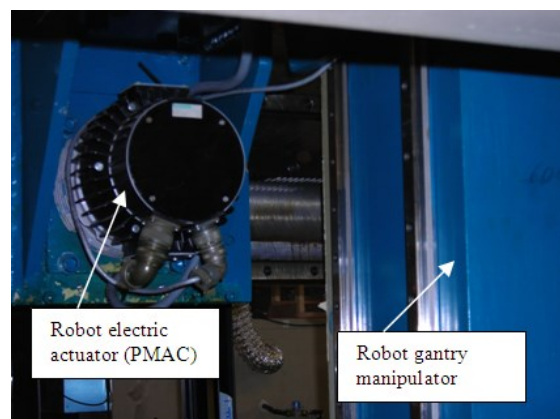


Figure 8: robot electric actuator and manipulator

4.4 Calibration of motor current to force experiment

When the robot interacts with an environment there is a change in the level of current in the electric actuator because the load torque increases. The motor current which reflects the torque, is calibrated to reflect the force exerted on the environment. The robot manipulator is made to interact with the environment, as shown in Figure 9, and the current from the electric actuator is monitored. As shown in the Figure 9, the end effector is in contact with the metal surface. The torque command is then increased which results in the level of current. Therefore, the force exerted by the robot manipulator increased. This force exerted by the manipulator is recorded using a spring balance connected between at the tip of the end effector.

The experiment was conducted for different commanded torque values and the corresponding force is observed in the spring balance. In Figure 10, the calibration experiment is conducted to obtain a relationship between the electric motor current to force. As shown in Figure 10, the force and current graph is plotted. It is found out that the force exerted bears a two-part linear relationship to the current of the motor, shown in Figure 10. This relationship is used in the software for control structure purposes. The two linear regions can be seen in the Figure 11 and this characteristic is incorporated in the software. The experimental work in the Thesis was carried out in the first linear region of the graph as shown in Figure 11.

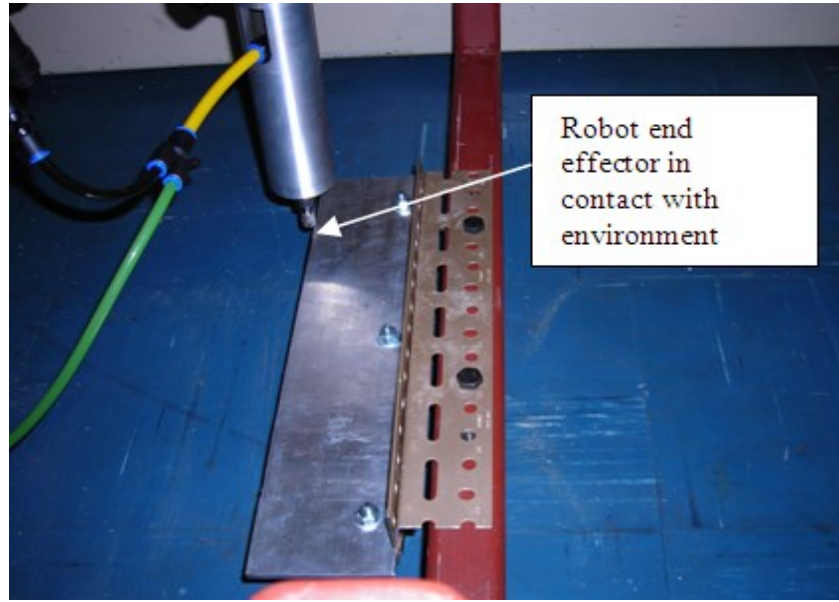


Figure 9: robot interaction with environment (a metal artefact)

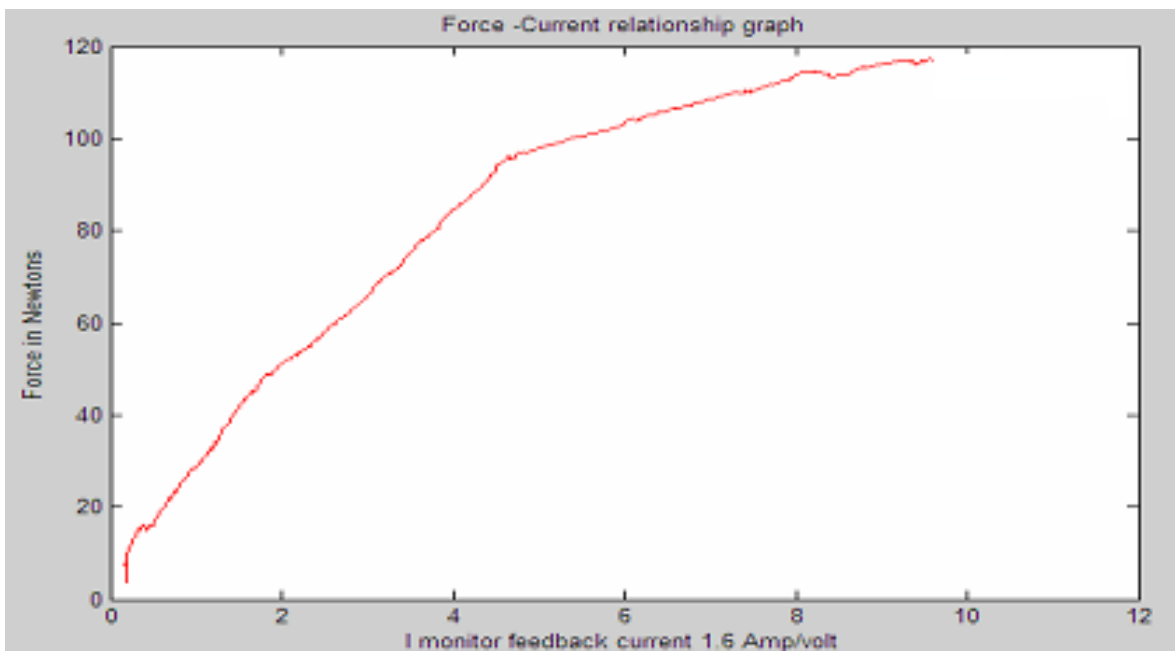


Figure 10: Calibration of the motor current to force

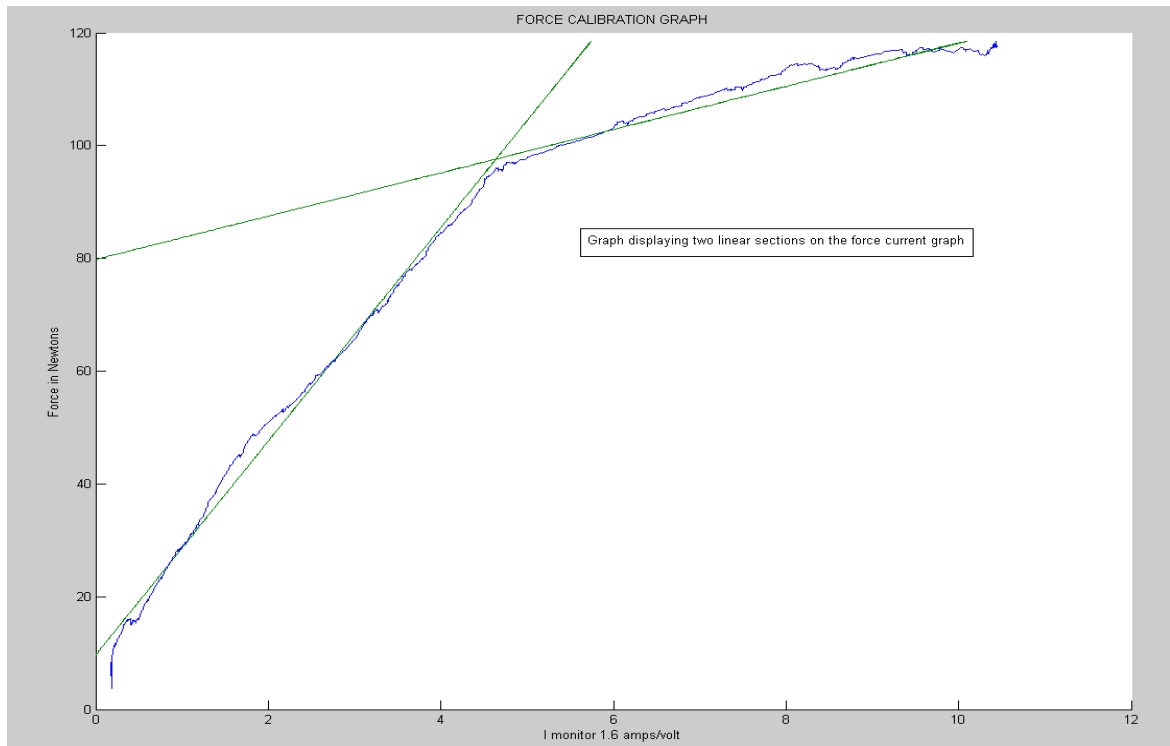


Figure 11: Calibration of the electric motor current to force with two linear regions

4.5 Development of the system and initial robot interaction experiments

After the force-current calibration experiment on the robot manipulator was conducted, the robot was made to interact with the environment with different torque limiting values.

As seen from the Figure 13, the robot interaction was controlled with pre-specified values.

This shows that the torque from the electric actuator can be made programmable in real time and the interaction can be controlled accurately and precisely in the software.

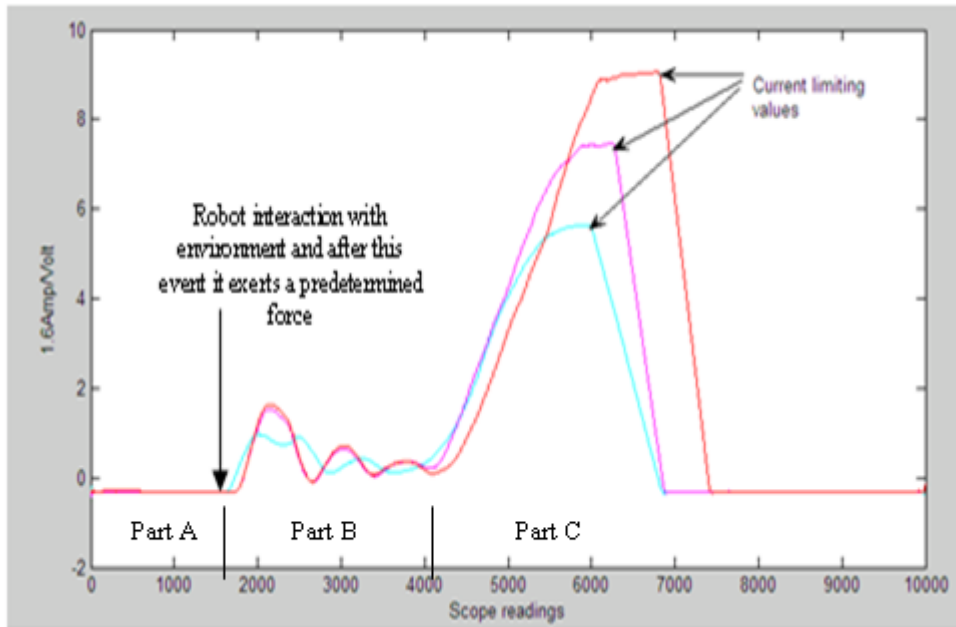


Figure 12: Graph showing torque/current limiting values over 10 seconds interval.

The Y axis is the scope readings from 0 to 10 seconds. The Figure 12 shows the three stages of the robot interaction with the environment. The Part A is the robot approach towards the environment. The Part B is the actual interaction with the environment and afterwards it settles down after the step change. The Part C is the increase of the force level on the environment to predetermined values which is termed as the current limiting values. The entire event is monitored on an oscilloscope.

4.6 Approach to development of contour following system

The research is based on the electric actuator force control on unknown geometrical environments. Therefore, a 2D contour following system was created. The contour following task is one of the most common control problems encountered by servomechanisms such as X-Y tables, robot manipulators and CNC machine tools [Cheng, 2005, Chen, 2000]. In this research work, two processors are used for each individual axis. In the following equations, f_n is the normal force while f_t is the tangential force applied on the surface. The resultant force is f as shown in Figure 13. While following two dimensional contours, the resultant force f is kept within the tolerance band set by the controller. This resultant force can be altered depending on the geometrical surfaces encountered during a control following system.

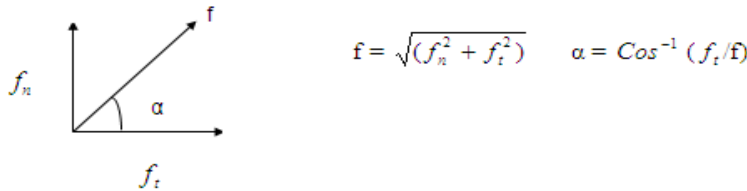


Figure 13: The force vector components f_n & f_t and the resultant force vector f

Experiments were planned on the robot manipulator for following surfaces with unknown geometry. The Figure 14 shows the various surfaces used in the experiments. In these

experiments only the start and the end points of the surface where input into the controller. The tests and results from these surfaces are in the next chapter.

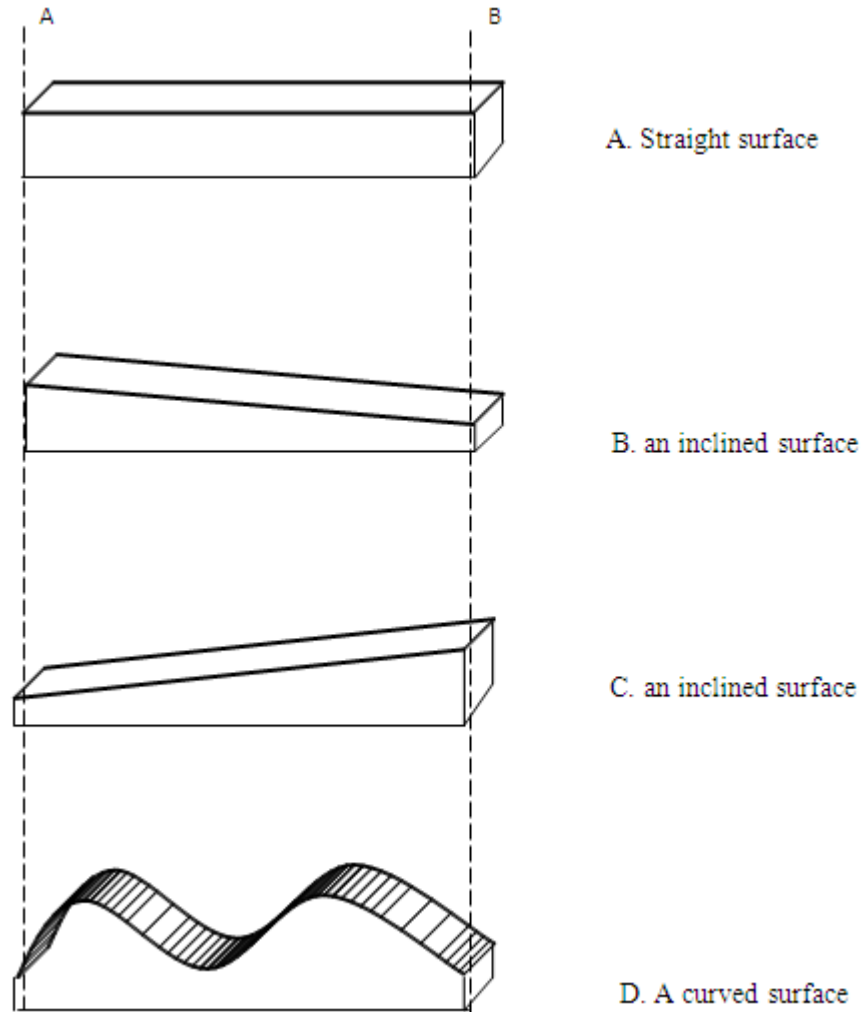


Figure 14: Different geometric surfaces used for 2 dimensional contour following with the knowledge of starting (A) and finish (B) points

4.7 Software development flow charts

A real time system is defined, according to Oxford dictionary, as “*any system in which the time at which the output is produced is significant*”. This is because the input corresponds

to some movement in the physical world, and the output has to relate to that same movement. Another way of thinking about real time systems is any information processing activity or system which has to respond to externally generated input stimuli within a finite and specific period.

Algorithm development is very crucial phase during software concept and specification phase of a real-time system. This section shows the software development of a basic two dimensional system which was used for robot contour-following with unknown geometry. It describes the development of the software rationale with the aid of flow charts. The software architecture was designed on a single axis and then both the axes were incorporated. Further investigations led to the inclusion of PID control and Fuzzy control in the software and that has been described in the subsequent chapters of this thesis. The software was written in the C language on the F2812DSP (Texas Instruments Code Composer Studio®). *The entire software code is included in the appendix of this thesis.*

The following flowcharts describe the basic development of the software in three stages:

1. Single axis robot interaction with the environment with force control loops, Figure 15.
2. Two axis robot interaction with the environment with one axis performing force loop while the other position loop operation, Figure 16.
3. Two axis robot interaction with the environment with the inclusion of both force control and position control loops, Figure 17.

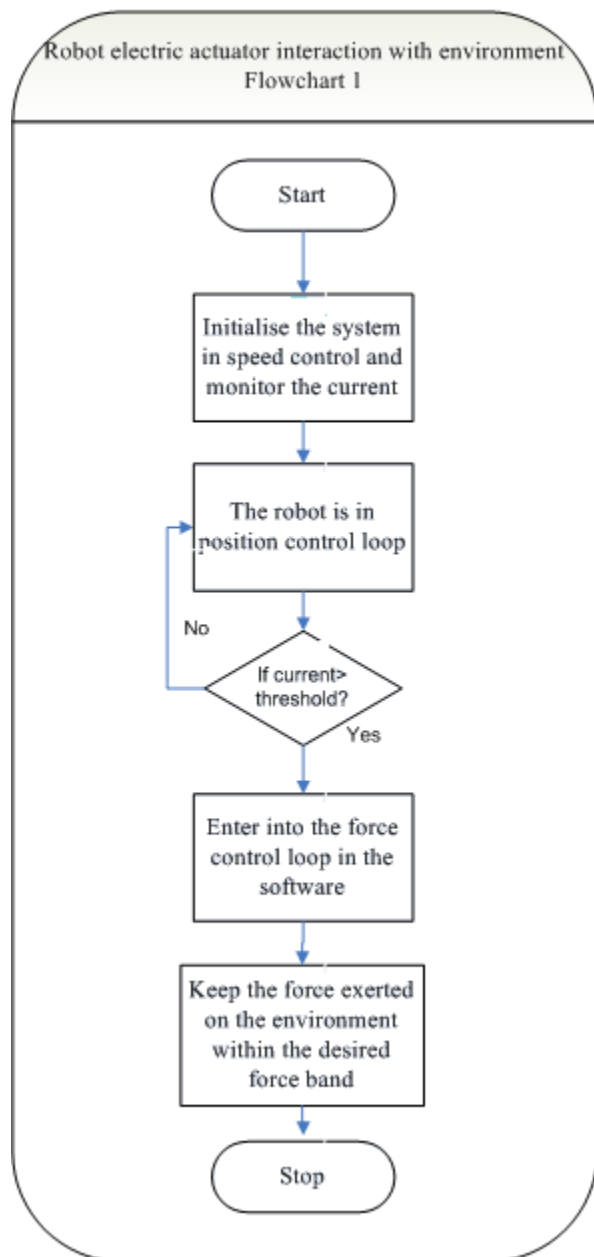


Figure 15: Flowchart describing robot electric actuator with the environment

The flow chart describes the algorithm for a single axis electric actuator. The robot initializes itself in a speed/position loop until it detects any external environment. If it does not encounter any external environment it remains in speed loop. However, on

encountering the environment it enters into a force control loop and exerts the desired force, which is real time programmable and is within certain predetermined tolerance limits.

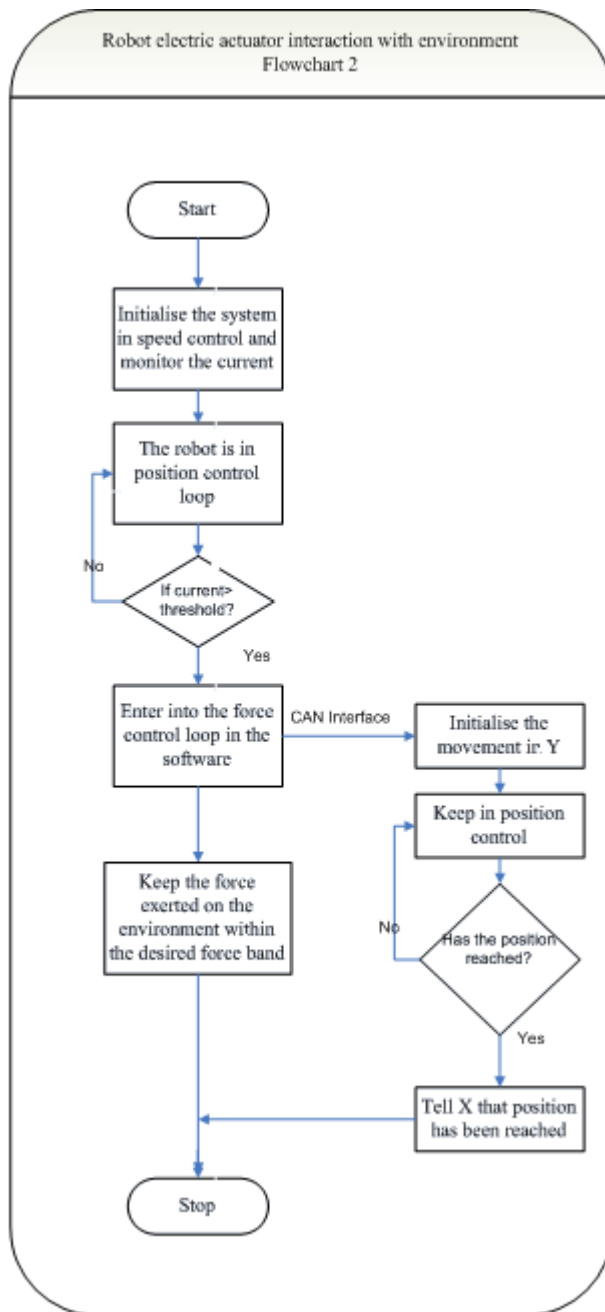


Figure 16: Flowchart describing robot electric actuator with the environment for two dimensional surfaces

The first flowchart has been modified to include a two dimensional environment. The communication between the controllers is achieved through a Controller Area Network (CAN). The controllers are termed as X and Y representing the 2D environments. The X controller is initialized in the speed/position control loop until an environment is detected. When the X controller enters the force control loop, it initializes the Y controller through the CAN to start traversing the environment. So the robot manipulator can be used to deal with 2D environments. In this software structure, the Y controller always stays in the position loop whilst the X controller stays in force controlled loop. The control algorithm can perform for a basic 2D contour following environment whilst exerting a constant desired force.

The third development is as shown in Figure 18. The X axis starts first in speed control until it interacts with the environment. As soon as the X controller detects any external environment, it switches to current control and thereby force/ torque control. As it exerts the desired force on the environment, a CAN signal is issued to the Y controller to start motion across the traverse of the environment. The Y axis controller now detects any increase in the feedback current. If there is an increase in the current, it asks the X controller through the CAN to switch into speed control and reverse back, while the Y controller exerts force on the environment. This is done according to the resultant force

vector between the X and Y axes force individual components. The X and Y axes controllers have position and force loops intertwined together and are switched depending on the circumstances. The Y axis controller always checks for a desired position signal. It issues a stop signal as soon as it encounters the desired position and forwards this information to X controller, which also stops. Otherwise, both the controllers stay in their respective loops. As the DSP controllers are very fast, the software has to be slowed down to match with the amplifier of the motor. Otherwise, the DSP issues commands which the amplifier cannot execute and results in an unsteady, jerky behaviour of the manipulator.

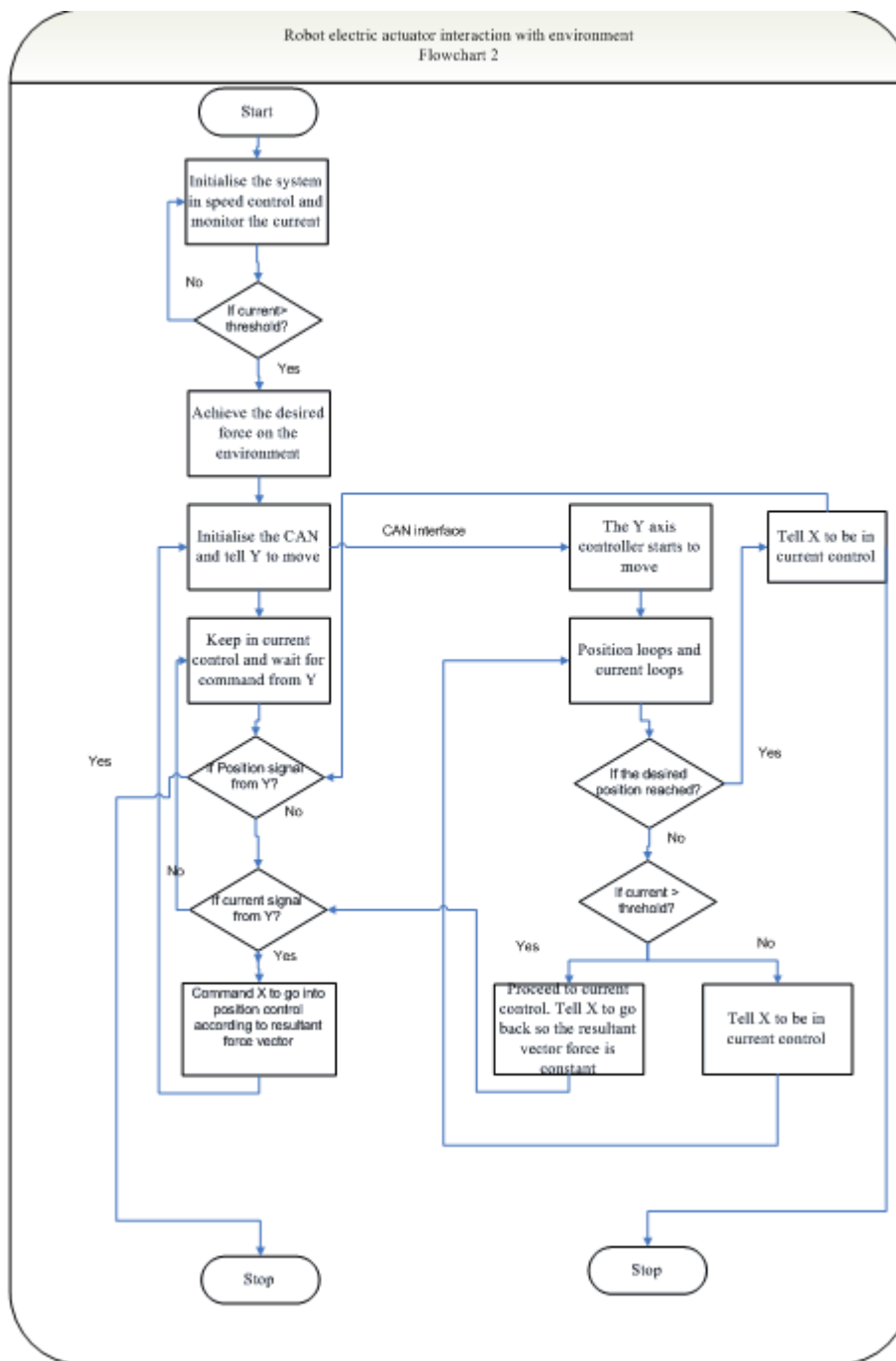


Figure 17: Flowchart describing robot electric actuator with the environment for two dimensional surfaces

Chapter 5

5. PID control modelling and implementation on the experimental system

5.1 Background and Introduction

Control systems engineering is a fascinating and important field. A control system is a device or set of devices to manage, command, direct or regulate the behavior of other devices or systems. It encompasses the methods and techniques for a continuous monitoring of the operating state of the system without operator intervention. These are referred as closed loop control systems which have the ability of automatically correcting its own behaviour so the desired results/outcomes are reached. Control engineers often utilize system/plant feedback to design control systems. For example, in an automobile with cruise control the vehicle's speed is continuously monitored and fed back to the system which adjusts the motor's torque accordingly.

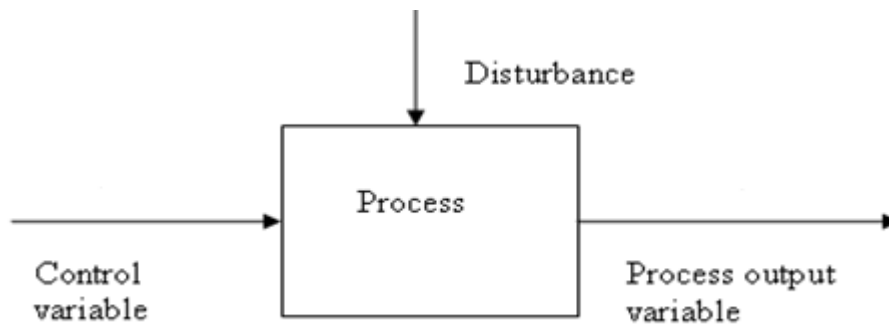


Figure 18: Block representation of a process with input output variables

As an example, as shown in Figure 18, the *process* is a physical system to be controlled. The *control variable* or the manipulating variable is the parameter which the controller uses to control or manipulate the process. The *process output variable* is the variable to be controlled so that it becomes sufficiently close to the set point. The *disturbance* is a non-controlled input variable to the process which affects the process output variable. The aim of the control algorithm is to adjust the control variable so that the control error (difference between the set point and the process output variable) is within acceptable/desired limits [Haugen, 2004].

As an example, in 1788, James Watt constructed a speed control system for a steam engine. Watt's speed control was based on feedback from measured rotational speed to the opening of the steam valve via a centrifugal controller which was based on a simple principle. The larger the speed, the smaller the valve opening (and steam supply), and vice versa acting proportional to the error. In this way the speed was held at or near a constant set-point value, despite the disturbances as variations in the steam pressure and changing

load torques acting on engine shaft. Watt's speed control system is regarded as the first industrial application of control engineering. It was based on experiments and trial and error. In 1868, James C. Maxwell made a mathematical analysis of the speed control system, and this analysis may be regarded as the starting point of the theoretical methods for analysis and design of control systems. [Haugen, 2004]

5.2 Introduction

Motion control deals with the use of high performance electric motors and is a very important part of industrial control systems. Motion control includes applications for speed and torque or position control in practically all branches of industry. Sophisticated motion control systems bring greater accuracy, flexibility and parameter sensitivity to the applications [Lorenz, 1994, Kiel et al, 1995, Bose, 1994]. As a consequence of this progress, more and more applications that have used simple electric drives for economic reasons are being replaced by motion control systems [Texas Instruments website, 2008].

The motion controller of the electric actuator (PMSM), used in the research, requires position feedback for electronic commutation. As the aim of the research is to perform torque control in the electric motor for controlled interaction with the environment, the controller also uses the current feedback from the motor. The current (calibrated to force) is compared with the desired force required and the controller takes appropriate action to equalise the current and desired force values. The research is focussed on the interaction

of the robot end effector with an unknown environment. Therefore, due to these process nonlinearities, closed loop control is required for the interaction forces to be regulated within the desired force tolerances.

This is commonly applied by a PID controller. It has enjoyed popularity as a purely mechanical device and as an electronic device. [Wescott, 2008]. A PID controller is a generic control loop feedback mechanism widely used in industrial control systems for over 50 years. A PID controller attempts to correct the error between a measured process variable and a desired set point by calculating and then outputting a corrective action that can adjust the process accordingly. It is a robust easily understood algorithm that can provide excellent control performance [Willis, 2008, PID website, 2008, Bhattacharya, 2004]. The PID algorithm consists of three basic modes, the Proportional mode, the Integral and the Derivative modes. When utilising this algorithm it is necessary to decide which modes are to be used and then specify the parameters (or settings) for each mode used. Generally, three basic algorithms are used P, PI or PID. The controllers are mainly used to reduce the fluctuations and also to minimize the error.

The ideal PID controller is in the following form:

$$u = u_0 + K_p e + \frac{K_p}{T_i} \int_0^t e d\tau + K_p T_d \frac{de}{dt} \dots\dots\dots (21)$$

In equation (21), there are three parameters. K_p is the Proportional gain, T_d is the Derivative time, e is the control error, u is the control variable and u_o is the nominal control variable.

P-Controller

The P controller calculates the control variable according to $u = u_o + u_p$ as follows:

$$u = u_o + K_p e \dots\dots\dots (22)$$

$$\text{and } u_p = K_p e$$

where u_p is the P-term [6]. The operation of the P-controller is to adjust the signal control accordingly or proportional to the error. By increasing the K_p value the static control error can be minimised in the controller as it gives more control to the variable adjustment $K_p e$, when the K_p value is increased for a give error e . This produces a small error. The limitation of this controller is that while the value of K_p is increased there is a *reduced stability* for the control loop and also when this value is increased by a large magnitude, the control loop becomes unstable [Haugen, 2004].

PI-Controller

In the PI controller (proportional + integral) the control variable is calculated as

$$u = u_0 + K_p e + \frac{K_p}{T_i} \int_0^t e d\tau \dots\dots\dots (23)$$

$$\text{and } u_i = \frac{K_p}{T_i} \int_0^t e d\tau$$

Here, u_i is the integral term, K_p is the proportional gain. T_i (s) is the integral time. K_i is the integral gain. The integral term is very essential and is calculated continuously from the initial time when $t=0$ to the present point of time. This is known as the integral of the control error. The contribution from the integral term is proportional to both the magnitude of the error and the duration of the error. Summing the instantaneous error over time (integrating the error) gives the accumulated offset that should have been corrected previously. The accumulated error is then multiplied by the integral gain and added to the controller output. The integral term (when added to the proportional term) accelerates the movement of the process towards set-point and eliminates the residual steady-state error that occurs with a proportional only controller. However, since the integral term is responding to accumulated errors from the past, it can cause the present value to overshoot the set-point value (cross over the set-point and then create a deviation in the other direction).

PID-Controller

This is a faster controller than the PI controller due to the addition of a control variable which is proportional to the time derivative or the rate of change of error e .

$$u = u_0 + K_p e + \frac{K_p}{T_i} \int_0^t e d\tau + K_p T_d \frac{de}{dt} \dots\dots\dots (24)$$

where $u_d = K_p T_d \frac{de}{dt}$ this is the derivative term.

In derivative controller, the rate of change of the process error is calculated by determining the slope of the error over time (i.e. its first derivative with respect to time) and multiplying this rate of change by the derivative gain. Thus, the PID controller can adjust process inputs based on the history and rate of change of the error signal, which gives more accurate and stable control. It can be shown mathematically that a PID loop will produce accurate stable control in cases where other control algorithms would either have a steady-state error or would cause the process to oscillate [PID website, 2008].

A conventional PID controller is depicted in Figure 19.

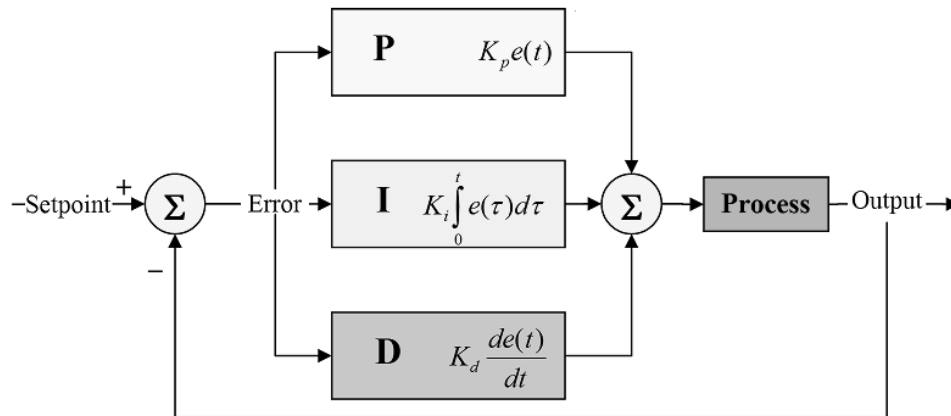


Figure 19 - A Traditional PID Controller

The controller sensor senses the signal, compares it with the setpoint value and determines the error. This error is then used to compute the change needed in input so as to eliminate the error from the output of the process. Thus in the PID loop, the function of the *Proportional* is to terminate the error present in the process at that point; the function of the *Integral* is to calculate the time for which the error has not become acceptable and the function of the *Derivative* is to estimate possible future error according to the rate of change of the past error.

5.3 Approach to the development of the PID controller

The gains of the PID controller need to be accurately tuned to achieve the desired results from the controller. The performance of the controller is often related to “*fast control but with satisfactory stability*” [Haugen, 2004]. There are various methods of tuning the actual PID gain parameters. They are based on trial and error methods, Zeigler Nichols method or the tuning software packages.

In this research work, the electric actuator is driven by an amplifier. As the electric motor is PMSM, it requires position feedback for commutation purposes. Therefore, the amplifier has a built in PID controller for the internal loop which facilitates the commutation. The PID controller designed and presented, in this chapter, is for the closed loop of the torque control in the system. The open loop response of the plant was observed and depending on that the PID controller is designed. PID controller is used in the

research work because of the intrinsic qualities simplicity in implementation and reliability in the motion control systems [Haugen, 2004].

5.4 Modelling and validation of the controller

The modelling of the PID controller is done in MATLAB/Simulink and then the PID controller is implemented on the experimental set-up for contour following experiments. The step input to the plant was a speed command and the current from the motor was observed for an open loop system. An overshoot in the response of the system was observed. From these tests on the experimental setup, the damping ratio and the natural frequency of the system were calculated and a second order transform function was obtained. It was modelled in MATLAB Simulink and a PID controller was developed using trial and error method as shown in Figure 22. This was then tested on the experimental setup by providing a step input to the system. As seen in Figure 24, the overshoot was reduced with the inclusion of the PID controller. The PID controller is designed based upon this criterion.

The calculation of the transfer function from the system/plant response to step inputs was carried out. The damping ratio and the natural frequency were observed for a number of trials as shown in Figures 20 and 21 . The damping ratio is calculated by measuring the amount of damping present in a system in the rate of decay of free oscillations. Logarithmic decrement can be defined as the natural logarithm of the ration of any two successive amplitudes. It is defined as follows:

$$\delta = \zeta \omega_n \tau \cong 2\pi\zeta$$

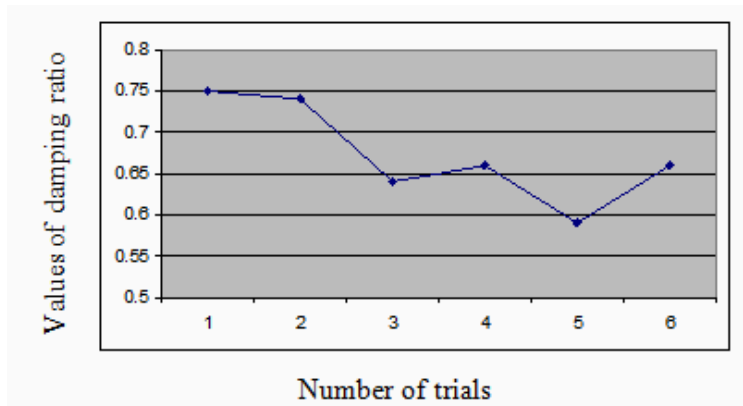


Figure 20: Different values of ζ calculated from the step inputs to the plant

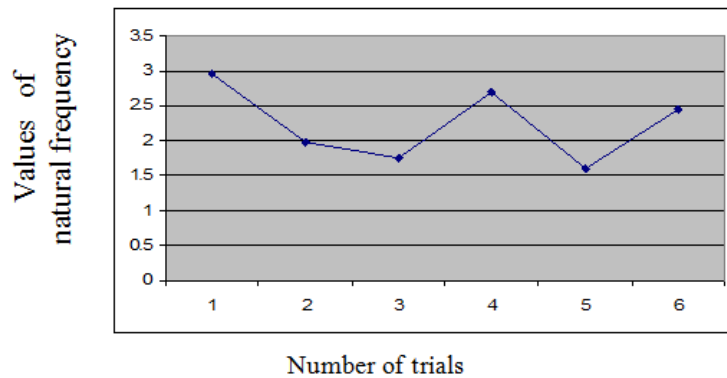


Figure 21: Different values of ω_n calculated from step inputs to the plant

The calculation of the transfer function is carried out by damping ratio and natural frequency of the system by observing the open loop response of the system.

$$\zeta = 0.75, 0.74, 0.64, 0.66, 0.59, 0.66$$

$$\omega_n = 2.96, 1.98, 1.75, 2.69, 1.6, 2.45$$

$$\text{Transfer function} = \frac{\omega_n^2}{s^2 + 2\zeta\omega_n s + \omega_n^2}$$

$$= 4.97/s^2 + 2.98s + 4.97$$

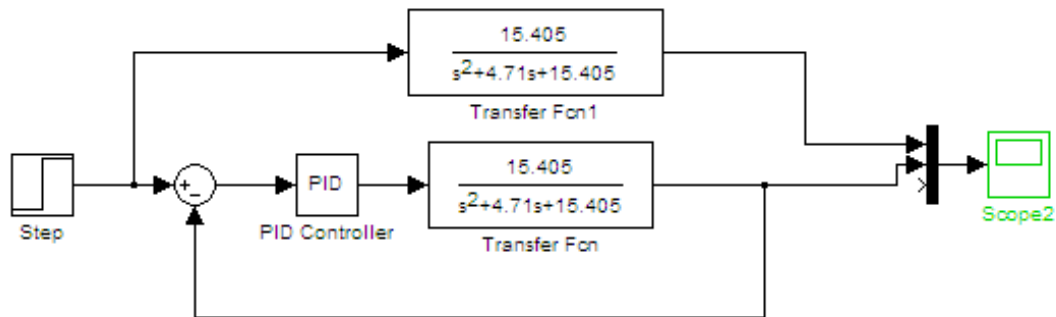


Figure 22– Simulink model for the PID controller implementation and comparison with plant open loop response. ($K_p=1.4$, $K_i=2.8$, $K_d=0.18$)

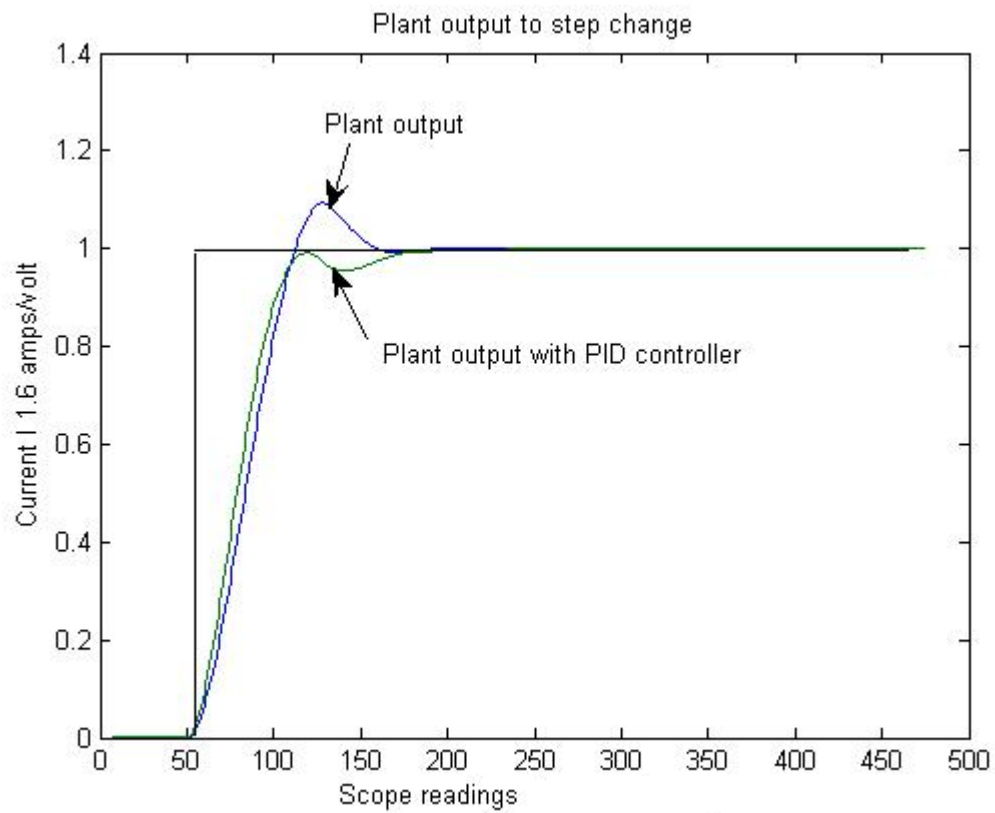


Figure 23 - Graph showing the Simulink plant output with and without PID control

The graph, in Figure 23, was obtained whilst following a straight surface. The first section is approaching the surface. As the robot interacts with the environment, there is a step change and it exerts a constant force as it follows the surface. An experimentally tuned PID controller is implemented in the software. In the open loop output response of the plant, there was a small overshoot which was eliminated with the PID controller. The values of PID are different in the model and the plant because the real plant has some amount of energy losses which are neglected in the simulation studies.

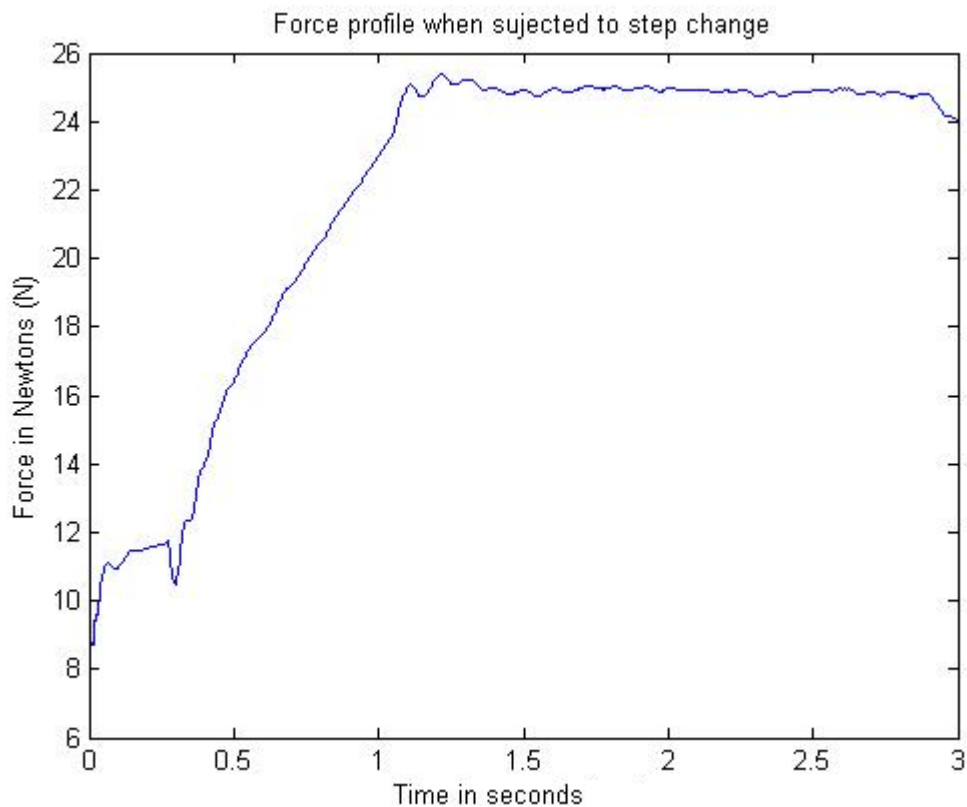


Figure 24 – Practical implementation of the PID controller on the Experimental setup($K_p=0.001$, $K_i=0.002$, $K_d=0.01$)

5.5 Results and Conclusion

Experiments are performed, using the PID controller, on the practical setup for contour following experiments with unknown geometry. The robot gantry manipulator was allowed to interact with different metal surfaces with varied geometries. The resultant force acting on the surfaces was monitored and the results are as shown in Figures 25 and 26. The feedback current values, calibrated to force (Newtons), are presented in the graphs. It is observed that the force values remain in the desired force band with an error of $\pm 2\text{N}$. A B

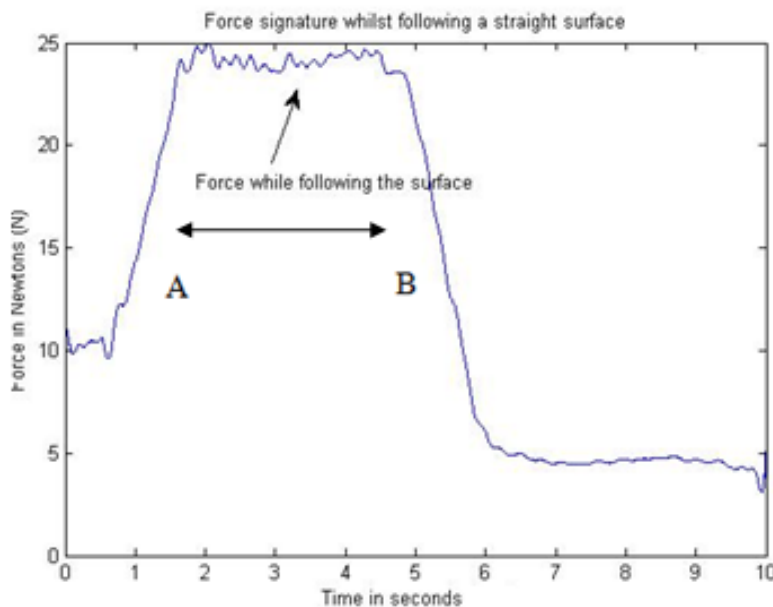


Figure 25: Force profile while following a straight surface

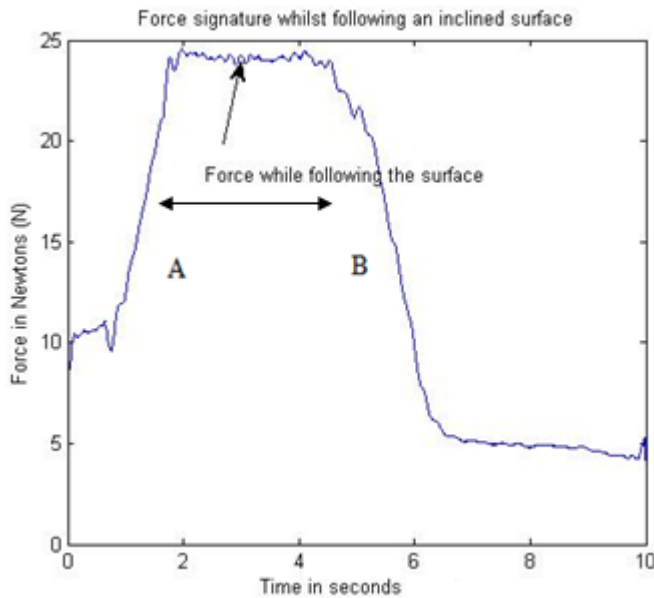


Figure 26: Force profile following an inclined surface

5.6 Further Development with PID Controller

The PID controller, employed in the research, has fixed gains. However, PID controller gains might need to be retuned whenever the processes are subjected to some kind of disturbance or when processes present complexities and nonlinearities. The controlled interaction of the robot force control with surfaces of different geometries suffers from the problem. Over the last few years, significant development has been established in the process control area to adjust the PID controller parameters in an automatic way, in order to ensure desired behaviour for a closed-loop plant. [Astrom &Wittenmark, 1989; Coelho et al., 1998; Coelho & Coelho, 1998; VanDoren, 1998]. This aspect can be further enhanced by using gain scheduling or the self-tuning of these gains which has been

demonstrated in these researches [Kazemian, 2001, Huang et al, 1996, Wang et al, 1998]. The self-tuning PID controllers can be designed using Fuzzy logic and neural networks in multivariate nonlinear environments. In [Malki et al, 1997], a fuzzy PID control is designed for flexible joint robot arm with uncertainties from time varying loads.

Chapter 6

6. Development and Implementation of Fuzzy Logic Controller on the experimental system

6.1 Introduction and Justification for the need of fuzzy controller.

The previous chapter was based on the torque control of the robot electric actuator using PID control. The work proved that the interaction of the robot interaction was experimentally force controlled for surface following applications, without previous geometrical knowledge. The results of the PID control algorithm are in the range of $\pm 2N$ based on the present experimental setup.

The application of PID controller is widely used in single loop controllers, distributed controllers and Programmable logic controllers and the performance is satisfactory in simple applications [Juang, 2008, Lyguoras, 2007]. The presented research work is focused on automation of manufacturing techniques such as deburring and polishing

which deal with complex, nonlinear and noisy environments. Therefore there is a need to have an adaptive controller which deals with these complexities. Fuzzy logic, which simulates human thinking using linguistic variables, can be applied as it takes into account the imprecision inherent in physical systems. Therefore, with the aim to accommodate complex environments and thereby the nonlinearities in them, fuzzy logic is introduced in the software to accommodate these conditions.

The concept of Fuzzy Logic (FL) was conceived by Lotfi A. Zadeh, professor at the University of California at Berkley. Professor Zadeh reasoned that people do not require precise, numerical information input, and yet they are capable of highly adaptive control. If feedback controllers could be programmed to accept noisy, imprecise input, they would be much more effective and perhaps easier to implement. Therefore, FL is a problem-solving control system methodology that lends itself to implementation in systems ranging from simple, small, embedded micro-controllers to large, networked, multi-channel PC or workstation-based data acquisition and control systems. It can be implemented in hardware, software, or a combination of both. FL provides a simple way to arrive at a definite conclusion based upon vague, ambiguous, imprecise, noisy, or missing input information [Seattle Robotics].

Conventional control systems use the physical models to deal with the process. That is time-consuming and needs a theoretical background of the designer. But many processes can be controlled by human being without any model, and these processes cannot be

controlled by conventional control systems. At first fuzzy control was treated with mistrust by the engineers who started with the conventional control theory. When fuzzy control systems were widely used in manufacture in Japan, people began to know fuzzy control system are cheap, easy to design, very robust, and better than the conventional control system.

6.2 Approach adopted in designing the fuzzy controller

Fuzzy controllers are special modern computer-controlled systems that use the rules to model process knowledge. The designer use rules to link the input variables with the control variables by linguistic variables. Human beings make decisions based on rules. Even though, we may not be aware of it, all the decisions we make are based on computer like if-then statements. Rules associate ideas and relate one event to another. Fuzzy machines, which always tend to mimic the behaviour of man, work the same way. Only this time the decision and the means of choosing that decision are replaced by fuzzy sets and the rules are replaced by fuzzy rules. Fuzzy rules also operate using a series of if-then statements. For instance,

if <conditions, and if satisfied>, then <action>

For example, if<force exerted on the environment is more than desired force>, then<reduce the current and thereby torque of the motor>

Linguistic rules describing the control system consist of two parts; an antecedent block (between the IF and THEN) and a consequent block (following THEN). Depending on the

system, it may not be necessary to evaluate every possible input combination since some may rarely or never occur. By making this type of evaluation, usually done by an experienced operator, fewer rules can be evaluated, thus simplifying the processing logic and perhaps even improving the FL system performance.

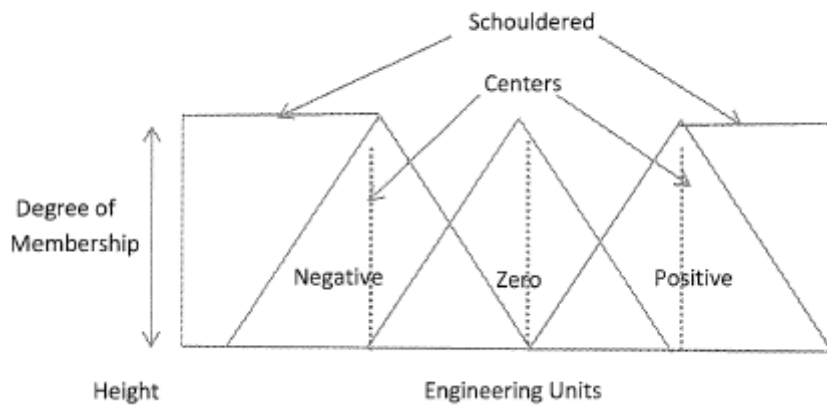


Figure 27: Example of membership functions[Mathworks website]

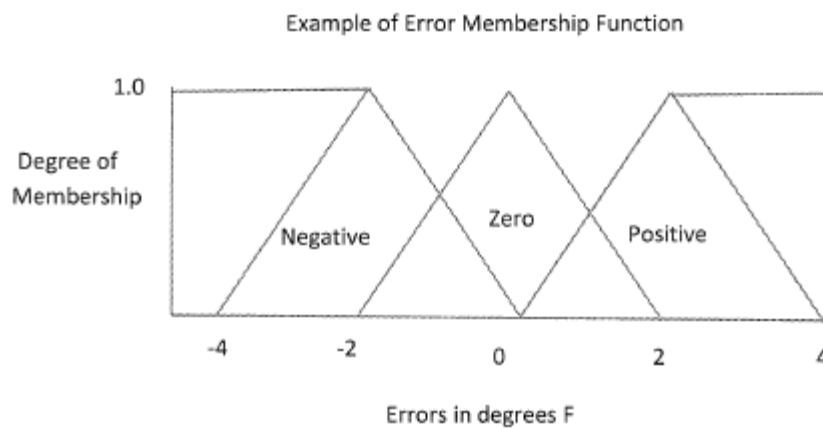


Figure 28: Fuzzy logic membership functions example[Mathworks website]

As shown in Figure 28, the membership function is a graphical representation of the magnitude of participation of each input. It associates a weighting with each of the inputs that are processed, define functional overlap between inputs, and ultimately determines an output response. The rules use the input membership values as weighting factors to determine their influence on the fuzzy output sets of the final output conclusion. The triangular shape is common, but bell, trapezoidal and, exponential have been used. More complex functions are possible but require greater computing overhead to implement. Once the functions are inferred, scaled, and combined, they are defuzzified into a crisp output which drives the system. There are different membership functions associated with each input and output response. As shown in Figure 29, an example is given for error and error dot triangular membership functions. The error is the difference between current/present value and the desired value. The error dot is the rate of change of this error with respect to time.

Mamdani fuzzy inference method is the most commonly seen fuzzy methodology. Mamdani method was among the first control systems built using fuzzy set theory. It was proposed in 1975 by Ebrahim Mamdani as an attempt to control a steam engine and boiler combination by synthesizing a set of linguistic control rules obtained from experienced human operators. Mamdani effort was based on Lotfi Zadeh's 1973 paper on fuzzy algorithms for complex systems and decision processes. Fuzzy control, which directly uses fuzzy rules, is the most important application in fuzzy theory.

The following are the basic steps in the implementation of a Mamdani fuzzy controller:

1. **Input:** number of input signals, number of derived states of each input signal, scaling
2. **Fuzzification:** type of membership functions, number of membership functions
3. **Rules:** number of antecedents, structure of rule base, type of membership functions in consequences.
4. **Rules evaluation:** aggregation operator in the antecedent
5. **Aggregation:** aggregation operator combining the results of individual rules
6. **Defuzzification:** defuzzification procedure
7. **Output:** number of output signals, scaling.

Mamdani fuzzy logic controller is used when the control problems require low accuracy and trivial minimal performance. The second widely used fuzzy controller is the Takagi-Sugeno fuzzy controller. It represents an effective representation of complex non linear systems in terms of fuzzy sets and fuzzy reasoning and is demonstrated in these research works [Ying, 1999, Garcia-Perez,1996, and Shih,1992]. Takagi-Sugeno fuzzy logic or Sugeno fuzzy logic was first introduced in 1985. It is the modification of Mamdani fuzzy logic. Fuzzifying the inputs and applying the fuzzy operation are exactly the same of Mamdani fuzzy logic. The different place between them is the output membership function. Sugeno-type's output membership functions are only linear or constant. When the output functions are constant, it can be called as zero-order Sugeno fuzzy model. For example, we can define a zero-order Sugeno fuzzy logic as:

If x is A and y is B , then $z = k$.

Where A and B are fuzzy set defined for the membership functions for x and y . k is a constant crisp value defined in the consequent. So the output of each rule is like a spike. The operator of implication and aggregation methods is simply multiplication and addition.

The first-order Sugeno fuzzy logic model has the rules like that:

If x is A and y is B , then $z = p * x + q * y + r$.

Where A and B are fuzzy sets in the antecedent, while p , q and r are all the constants.

A Sugeno fuzzy inference system is extremely well suited to the task of smoothly interpolating the linear gains that would be applied across the input space; it is a natural and efficient gain scheduler. Similarly, a Sugeno system is suited for modeling nonlinear systems by interpolating between multiple linear models. The advantages of Tagaki Sugeno Fuzzy logic controller are suitable to compute, can optimise the parameter to improve efficiency and uses linear techniques to control non linear environments. The disadvantage is that it is not an intuitive controller and becomes complex as the order increases [Seattle Robotics website, Mathworks website].

Because it is a more compact and computationally efficient representation than a Mamdani system, the Sugeno system lends itself to the use of adaptive techniques for

constructing fuzzy models. These adaptive techniques can be used to customize the membership functions so that the fuzzy system best models the data.

6.3 Implementation and Tests

The fuzzy logic control designed for the research is the Tagaki Sugeno fuzzy logic. The basic aim was to design a controller for dealing with complex environments. The robot force interaction with the environment is a complex multi input multi output (MIMO) system and the controller has to accommodate changes related to unpredictability of the environment, noise from the experimental setup, marginally stable processes and time varying process [Bhattachatya, 2003, Li 1998].

Precision deburring and polishing is mostly done by skilled human operators which are familiar with the process. When they grind a large burr they do not remove the large burr all at once but they usually move the tool back and forth so that the burr can be removed in an optimal manner. They may also accommodate the force applied to the tool in order to touch the burr gently without any damage to the tool or the work piece. Thus the operators monitor the state of the given task process and take control actions. The control behaviour of human experts can be represented in an IF-THEN relationship as used in fuzzy logic.

The expertise of an operator is difficult to describe in an analytical way. The task executed by the human operator has no detailed algorithms or methodology (Aertbelien et al, Asada

et al). The fuzzy control can be designed based on the human characteristics used in surface following operations. The stiffness of the electric actuator can be made programmable.

Therefore for following two dimensional surfaces with unknown geometry three input variables in the fuzzy logic scheme are used. They are explained as follows:

1. The first is the *error* (e), which is the difference between the desired and actual force acting on the surface. This is for ensuring the current of the motor remains in the required desired band.
2. The second is the *change of error* (Δe), which gives the rate of change of error as the contour is being followed. The change of error term is crucial in the controller structure as it depicts the contour being followed.
3. And the third is the *speed of traverse across the surface* (v), which is the tangential velocity of the tool across the surface. The speed of the traverse of the tool is important as it affects the finishing in the deburring process and affects the tracing of geometrical profiles in surface following operations.

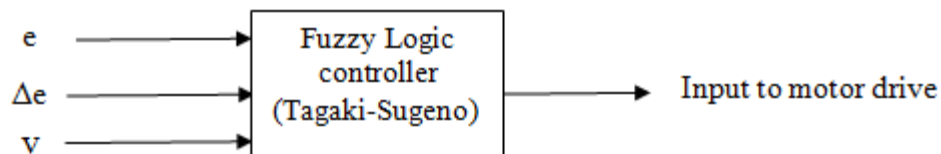


Figure 30: Design of Tagaki Sugeno fuzzy logic controller and specifying inputs and outputs

The fuzzy logic controller has been implemented in the software. The following Figures 31 and 32 show the resultant force profiles whilst following straight and inclined surfaces. In Figure 31, the surface is between the points A and B. It is seen that that the force is within the desired tolerance band. It has been seen that the force remains within the user desired force tolerance range.

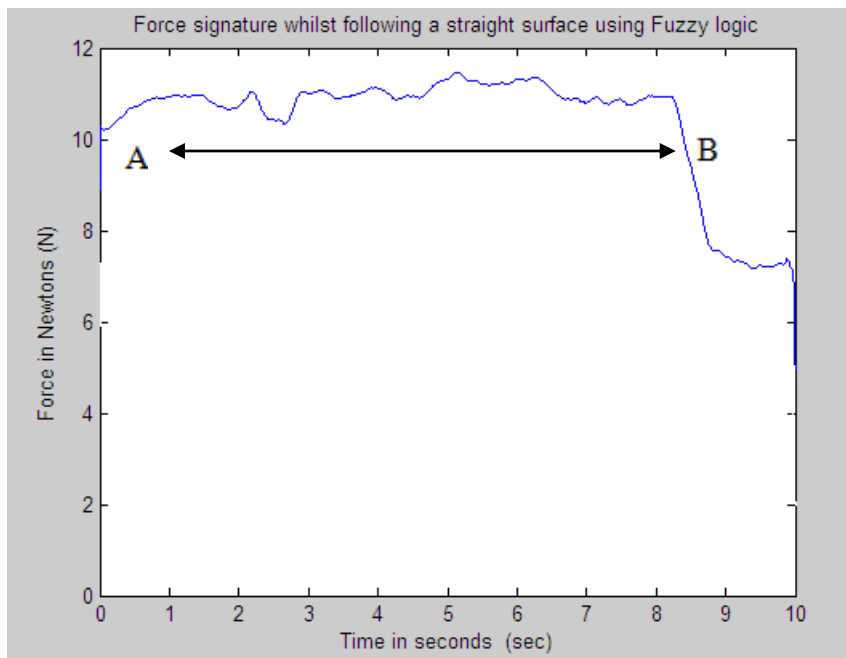


Figure 31: Force signature while following an inclined surface using fuzzy logic

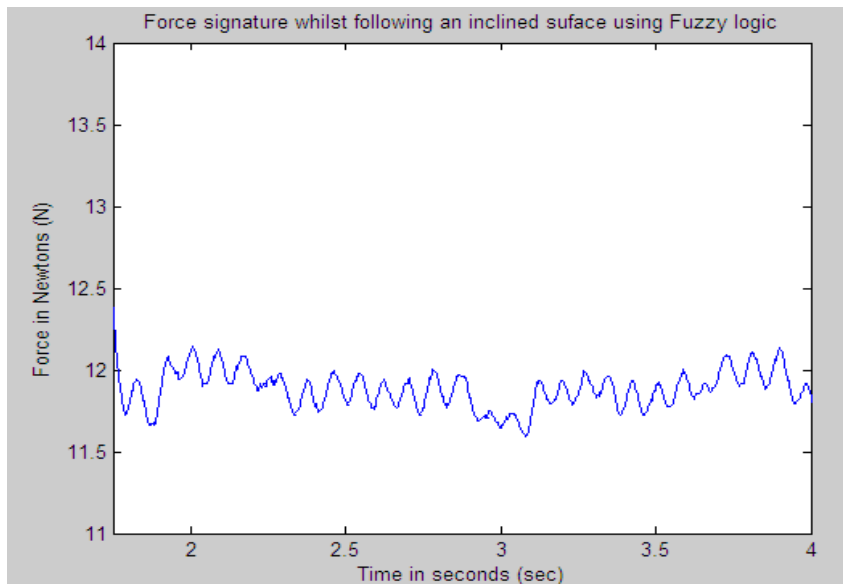


Figure 32: Force signature while following an inclined surface using fuzzy logic

6.4 Comparison between the performance of PID and fuzzy controllers

The following table depicts the comparison between the PID and the fuzzy control implemented on the experimental rig.

1. The comparison between the PID and fuzzy controller is based firstly on the speed of execution of the software. This factor decides the responsiveness of the system. The execution speed of the fuzzy control is large than that of PID controller. Therefore, the fuzzy control can be implemented in cases where it is needed only

and thus the computational time is saved and the responsiveness of the controller to any change can be improved.

2. The second comparison is based on the force deviation range whilst following contours with unknown geometries. While following simple geometrical shapes without any complexities, the force error band is $\pm 2\text{N}$ in case of PID controller while it is $\pm 1\text{N}$ in case of a fuzzy controller.

It is noted that the performance of these controllers is affected by the performance of the drive amplifier of the electric motor. The drive amplifier, in the present experimental setup, due to its lower speed reduces the system responsiveness and thereby the performance of the system. Secondly, the presented experimental work is carried out on a robot gantry manipulator with multiple degrees of freedom. The joints which are not used in the experiments are mechanically clamped. It is observed while performing the experiments that there is some introduction of a mechanical compliance and thereby it affects the performance.

The research work done with an aim to demonstrate a generic control philosophy of torque control in electric actuators. As stated earlier, this work is suitable to generalisation and this adaptive control structure can also be applied.

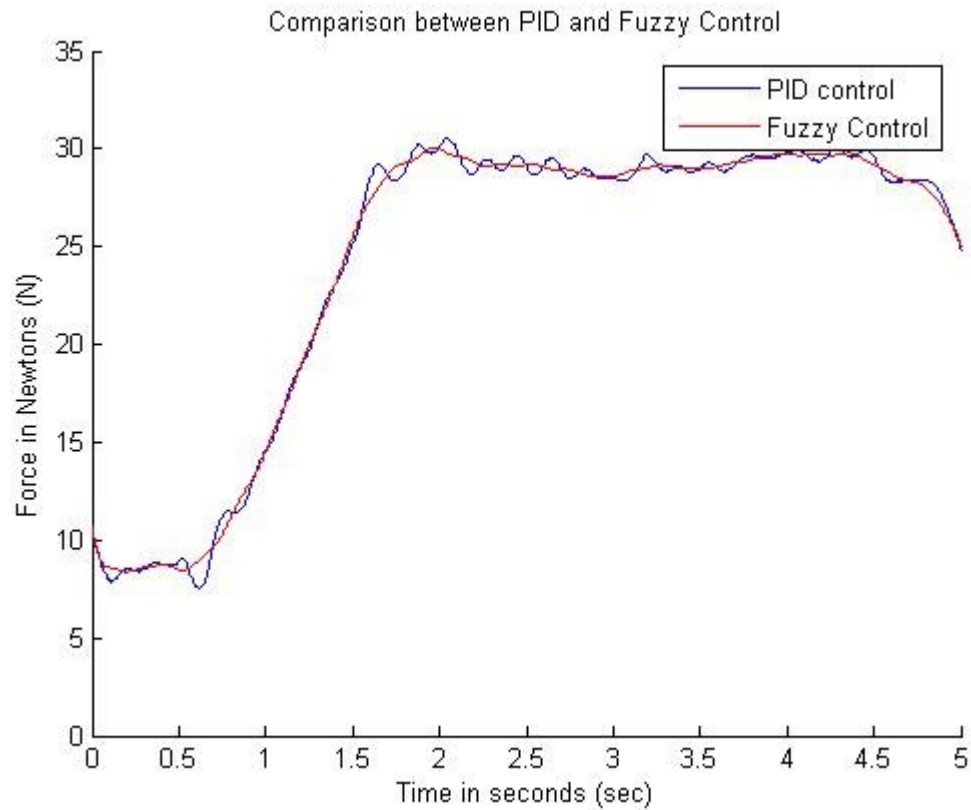


Figure 33: Comparison between the PID and Fuzzy Controller for geometrical profiles

3. While following simple geometrical shapes with some nonlinear complexities, the force error band is $\pm 2\text{N}$ in case of PID controller while it is $\pm 1\text{N}$ in case of a fuzzy controller. But it is observed that whilst reproducing the geometrical profile of the surface, the fuzzy controller is smoother rather than the jerky behaviour of the PID controller.

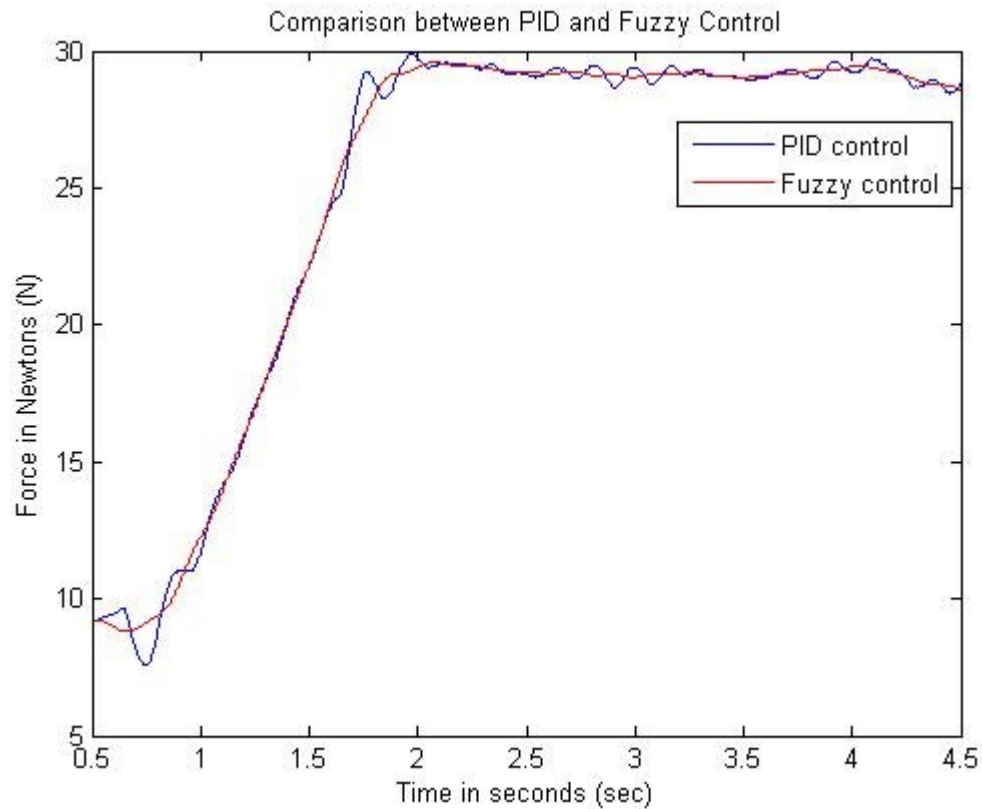


Figure 34: Comparison between the PID and Fuzzy Controller for geometrical profiles

4. The overshoot from the PID controller is 0.33% of the F.S.V. (Full Scale Value) and from the fuzzy controller is 0.2% of FSV.

	Execution speed (μ s) (Software based)	Force error (N) Simple shapes	Force error Complex shapes (N)	Overshoot
PID Controller	3.62 μ s	± 2 N	± 2 N	0.33% of FSV
Fuzzy Controller	12.8 μ s	± 1 N	± 1 N	0.2% of FSV

Table 35: Performance comparison between PID and Fuzzy Controller on the experimental rig

6.5 Proposed modified controller structure for PID+Fuzzy Controller

The torque control in electric actuator for the robot interaction with the environment has been demonstrated with the PID controller and the fuzzy controller. The PID controller due to its ease of implementation and good performance can be used for simple control tasks while the fuzzy controller can be incorporated whilst dealing with complex non linear environments. Therefore, in this section a modified control strategy has been proposed to include both the PID and the fuzzy controllers in a single control structure and to have a switching mechanism between the two controllers based on a selection criterion. As shown in the following block diagram, Figure 37, the decision for the controller is based on selection criterion and the decision is made in real time. The torque and position of the motor are monitored in real time and the force error and rate of change of force error information is used for the selection criterion. For example, in deburring or surface following operations, when the surface geometry is simple, PID controller is implemented when the error and change of force error are within the acceptable band. If the surface geometry changes, it is indicated in the error and rate of change of error, fuzzy logic is introduced to deal with complex non-linear environments. The transition from one controller to the other is done gradually so there is no jerky behaviour in the system which is important for surface finishing operations such as deburring.

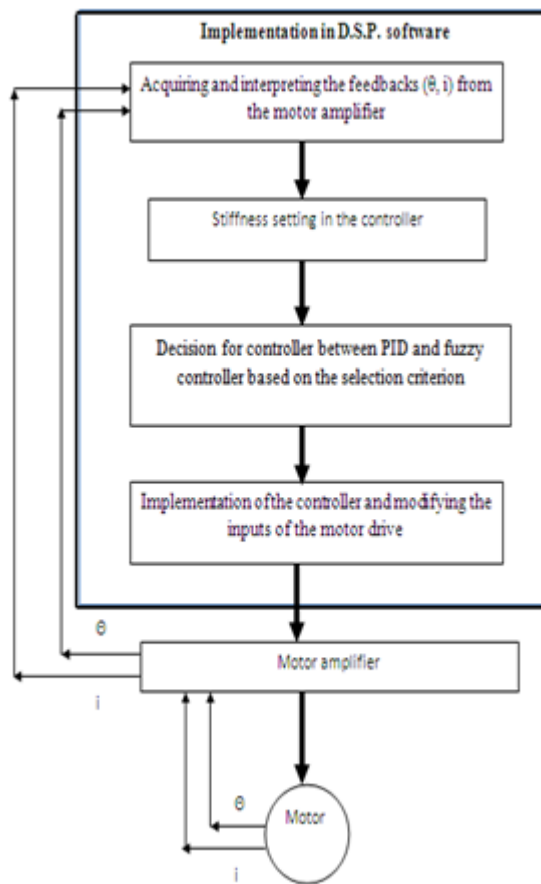


Figure 36: Modified Controller structure for PID+Fuzzy controllers

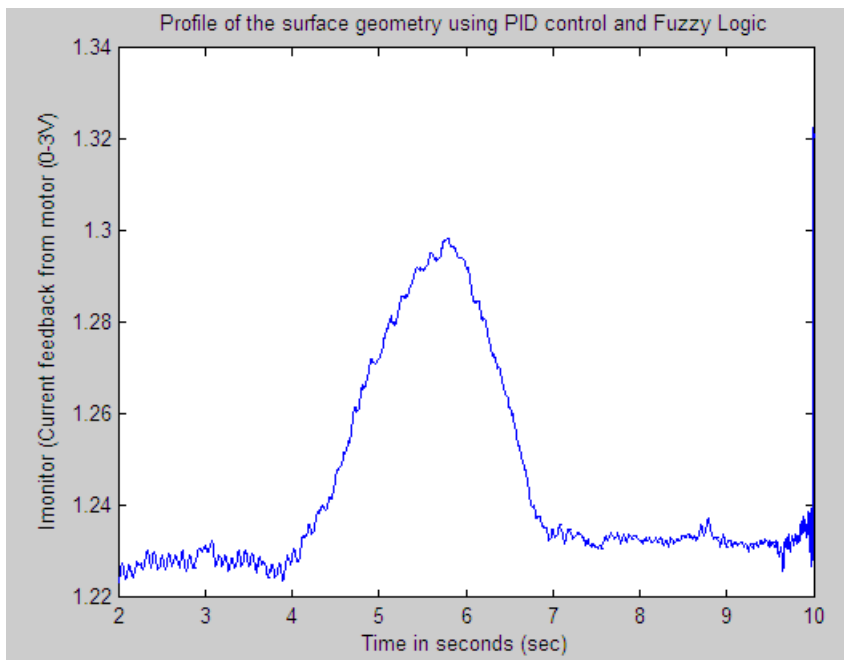


Figure 37: Profile of the surface following using the modified control strategy

Chapter 7

7. Main Contributions and Conclusions of the research

This work presents an approach for the control of robot electric actuators when the robot interacts with an external object or surface. The presented research work is primarily based on achieving accurate torque control in the robot electric actuators and introduction of software compliance in the system. The controlled interaction results in a stable and specified force contact with the surface. Therefore, robot force control is accomplished without the inclusion of any external sensors in the system. The subordinate advantages are cost, adaptable to different working conditions and increase in the responsiveness of the system. Due to these mentioned advantages, the control philosophy can be adapted to the traditionally manual manufacturing techniques such as deburring, composite layouts and also can be used in coordinate measuring machines.

The following are the main contributions of the presented work:

1. *Introduction of compliant behaviour in electric actuators*

A broad literature survey was carried out for robot force control. It was concluded that the current robot force control strategies employed for the interaction with the environment or object have inherent stiffness and rely on the sensory feedback to realise interaction forces. The research work has demonstrated the compliant behaviour, by varying the stiffness, in the joint robot electric actuators. The control philosophy, as opposite to stiff surfaces is applied in real time where the robot interacts with an external environment. This is achieved in real time torque control in the robot electric actuators. There are no external sensors connected to the robot and this was demonstrated on the experimental setup. The research has shown that the electric actuator stiffness can be altered and it can be compared to be a programmable spring.

2. *Mathematical representation of PMSM for torque control*

A mathematical representation of the electric actuator (PMSM), used in the research, is carried out. The operation of PMSM requires Vector control includes the decomposition of the three stator currents into imaginary two axes components for simplification of the operation. The derivation of torque to current and thereby relating it to the force exerted on the system. The operation of PMSM is difficult and the control philosophy has been demonstrated on the same platform and therefore, the presented research work presented is suitable for generalisation to other electric actuators such as dc motors.

3. Application for contour-following systems without geometrical knowledge

A two dimensional contour following system has been developed based on torque control of electric actuators. Software is designed and implemented for robot force control on external environments with no previous geometrical knowledge. It is shown the robot force control can be achieved for contour following applications. The two dimensional contour following was carried out on artefacts within the desired force tolerance range.

4. Study of control strategies –PID control and Fuzzy control

The inclusion of control strategies such as PID control and Fuzz logic control has been demonstrated and compared for following contours with unknown geometrical profiles. It was shown that the PID controller was within $\pm 2\text{N}$ and the fuzzy controller was within a $\pm 1\text{N}$. The results were based on the existing experimental setup. Then a modified controller structure (PID+Fuzzy) is proposed for processes with complexities and non-linearities during the contour following operations. The intention is to operate the system initially with PID control and then the selection criterion makes decision on whether to incorporate the fuzzy controller in the structure.

5. Survey of application areas for this novel control philosophy

The presented work is broadly based on the automation of manufacturing tasks like deburring and composite layouts but can be applied to other industrial applications. Therefore, a survey of the potential research and manufacturing areas of the research has been carried out where this control philosophy can be applied.

Chapter 8

8. Recommendations for future work

The main contributions of the research undertaken are presented in the last chapter. Several perspective research directions and modifications, based on the contributions of the presented research work, can be outlined as follows:

1. *Demonstration of the control philosophy on a three dimensional environment*

The presented experimental work is performed on a gantry robot manipulator interacting with a two dimensional environment. The control philosophy can be extended to three dimensional environments. Therefore, the philosophy can be easily applied to industrial manufacturing areas (like deburring, composite layouts) which deal with three dimensional environments.

2. *Inclusion of human behaviour in the automation of manufacturing tasks*

The primary aim of the research work was to automate the industrial applications which have been traditionally carried out by human skilled craftsmen. Therefore, it is vital to include the human expertise into the controller. The introduction of fuzzy logic in this work is the start of the inclusion of human behaviour in the

control structure. But, this needs further development in order to deal with work pieces with complex geometries.

3. *Comparison of the research work with other existing control philosophies*

The presented control philosophy is solely based upon the accurate and precise control of the robot electric actuators. The research work can be further extended to compare the results between this research work and robots with other existing methodologies such as -mounted force sensors; in industrial applications.

4. *Application of the research work to industrial six axes of freedom robot manipulator*

Industrial robot applications have robots with six axes of freedom. The control philosophy can be applied to each of the robot electric actuator but a supervisory controller has to be designed which will observe and calculate the forward kinematics of the robot.

5. *Development of the drive amplifier in the digital processor*

In the presented research, the performance of the electric actuator was limited by the drive amplifier. To overcome this problem, the vector controller of the motor can be developed in the digital processor. By achieving this capability, the electric actuator can be programmed in real time to behave as a programmable spring where the stiffness and the damping of the actuator can be controlled more

effectively. This will enhance the system responsiveness and also aid in accurate and compliant torque control.

6. *Applications in CAD directed robotic deburring*

The presented work can be used in applications with CAD directed robotic deburring. The work can be extended to get the present geometrical profile of the surface and then compared with the CAD model for the desired shape and the controller strategies can be modified or altered depending on the complexities of the surface or object.

References and Bibliography

Seattle Robotics, (2008), <http://www.seattlerobotics.org/encoder/Mar98/fuz/flindex.html>. (August, 2008)

Aertbelien E, Van Brussel H ,(1999), An observational model and segmentation algorithm for skill acquisition of a deburring task, , Proceedings of the 1999 IEEE/ASME, International Conference on Advanced Intelligent Mechatronics, U.S.A.

K.K. Ahn, D.Q. Truong, Force control for press machines using an online smart tuning fuzzy PID based on a robust extended Kalman filter, *Expert Systems with Applications* 38 (2011) 5879–5894

Airbus (2007), 'Composite Material usage', <http://www.airbus.com/en/corporate/innovation/> (July 2008)

Airbus (2007), 'Carbon Fibre Reinforced Plastic (CFRP)', <http://www.airbus.com/en/aircraftfamilies/a350/technology.html> (July 2008)

Anderson R and Spong MW , (1988)“Hybrid Impedance Control of Robotic Manipulators” *IEEE J. of Robotics and Automat.* **4** (5) , 549 – 556 .

Astrom KJ, Hagglund T, (1988), Automatic tuning of PID controllers. Instrument Society of America, New York.

Astrom KJ, Wittenmark B, (1989), Adaptive control. Addison-Wesley Publishing Company, Massachusetts.

Bhattacharya S, Chatterjee A, Munshi S,(2004), A new self-tuned PID-type fuzzy controller as a combination of two-term controllers *ISA Transactions*, 43.

Bigge B, Harvey I R, (2007), Programmable springs: developing actuators with programmable compliance for autonomous robots, *Robotics and Autonomous systems*, 55, pp 728-734

Blanchett TP , Kember GC , Dubay R, (2000) , PID gain scheduling using fuzzy logic, *ISA Transactions* 39 317±325

Bone GM, Elbestawi MA, (1991), Active end effector control of a low precision robot in deburring, *Robotics and Computer-Integrated Manufacturing*, Volume 8, Number 2, pages 87-96.

Borrel P , (1979)“Mode ` le de Comportement des Manipulators , Applications a ` leur Commande Automatique” *The ` ses* (Universite ´ des Sciences et Techniques du Languedoc ,Montpellier , France .

Borrison U, (1975), Self tuning regulators-Industrial application and multivariable theory, Lund Institute of Technology, Report 7513.

Bose BK, (1994), Expert System, Fuzzy Logic and Neural Network Applications in Power Electronics and Motion Control, Proceedings of the IEEE, vol.82, no.8, pp. 1303-1323.

Burn, K, Bicker, R, Short, M, (2003), Adaptive and non-linearly fuzzy force control techniques applied to robots operating in uncertain environments. *Journal of Robotics Systems*, Volume 20, Pages 391-400.

Changoon K, Chung Jae H., Daehie H, (2008), Coordination control of an active pneumatic deburring tool, *Robotics and Computer-Integrated Manufacturing* 24, pp 462-471.

Coelho Leandro dos Santos, Antonio Augusto Rodrigues Coelho ,(1999), Automatic tuning of PID and gain scheduling PID controllers by a derandomized evolution strategy Artificial Intelligence for Engineering Design, Analysis and Manufacturing, pp 341–349.

Coelho LS, Coelho AA, Chawdhry, PK, et al (1998), Genetic algorithms and evolution strategies applied in identification and control: Case study. In *Soft Computing in Engineering Design and Manufacturing*, pp. 430– 438. Springer-Verlag, London.

Colbaugh R ,Seraji H. and Glass K ,(1992) “Impedance Control for Dexterous Space Manipulators” *The 3 1 st Conf. on Decision and Control* , Tucson , Arizona (Dec . 1992) pp . 1881 – 1886

Dictionary Reference (2008), Automation - Definitions from Dictionary.com(April, 2008)
Dr M.J. Willis, (2008), Proportional-Integral-Derivative Control, Dept. of Chemical and Process Engineering, University of Newcastle. <http://lorien.ncl.ac.uk/ming/pid/PID.pdf> (August 2008)

Electric Drives - Motor Controllers and Control Systems (Description and Applications)
<http://www.mpoweruk.com/motorcontrols.htm> Accessed on 01/08/2008

Fitzgerald A.E., Kingsley Charles Jr., Umans Stephen D., (1983), *Electric Machinery*, McGraw-Hill Book Company.

Freescle Website (2008), Permanent magnet Synchronous motor<http://www.freescle.com/webapp/sps/site/overview.jsp?nodeId=02nQXGrrlPZL8l>

Gamez Garcia J., Robertsson, J. Gomez Ortega, R. Johansson, (2008), Self-calibrated robotic manipulator force observer, Robotics and Computer-Integrated Manufacturing,.

Glossas NI, Aspragathos NA,(2001), Fuzzy logic grasp control using tactile sensors, Mechatronics (11), 899-920

Hao Ying, Yongsheng Ding, Shakon Li, Shihuang Shao, (1999), Comparison of Necessary Conditions for Typical Tagaki-Sugeno and Mamdani Fuzzy Systems as Universal Approximators, IEEE Transactions on Systems, Man and Cybernetics, Volume 29, Number 5.

Hamit Erdem , Application of Neuro-Fuzzy Controller for Sumo Robot control, Expert Systems with Applications 38 (2011) 9752–9760

Hassan, B, (2002), The SOF-PID controller for the control of a MIMO robot arm
Kazemian, London Metropolitan University, IEEE Transactions on Fuzzy Systems, Volume 10, and Number 4.

Haugen F, (2004), PID Control, Tapir Academic Press, Trondheim, Norway.

Hogan N, (1985), Impedance control: an approach to manipulation. ASME Journal Dynamic Systems Measurement Control. 107:1-7.

Hsu Feng-Yi Fu Li-Chen,(2000) Intelligent robot deburring using adaptive fuzzy hybrid position/force control, IEEE Transactions on Robotics and automation, Volume 16, No. 4.
<http://www.mathworks.com/access/helpdesk/help/toolbox/fuzzy/index.html?/access/helpdesk/help/toolbox/fuzzy/fp351dup8.html&http://www.google.co.uk/search?hl=en&q=mamdani+fuzzy&meta=>

Huang Shiuh-Jer, Kuo-Ching Chiou, (1996), The application of neural networks in self tuning constant force control, International journal of machines tool manufacturing, volume 36, Number 1, pp 17-31.

Hyungbin Im a, HongHeeYoo b, JintaiChung, Dynamic analysis of a BLDC motor with mechanical and electromagnetic interaction due to air gap variation
Journal of Sound and Vibration 330 (2011) 1680–1691

Ilyas Eker, Yunis Torun, (2006), Fuzzy logic control to be conventional method Energy Conversion and Management 47 (2006) 377–394

Jih-Gau Juang, Ren-Wei Lin, Wen-Kai Liu , (2008), Comparison of classical control and intelligent control for a MIMO system, Applied Mathematics and Computation, Elsevier.

Kaewjinda W., Konghirum M., (2007), Vector Control of Permanent Magnet Synchronous Motor Using Resolver Sensor, ECTI Transactions on Electrical Engineering, Electronics, and Communications, Volume 5, No.1.

Kaitwanidvilai S, Parnichkun M, (2005), Force control in a pneumatic system using hybrid adaptive neuro-fuzzy model reference control, Elsevier, Mechatronics.

Kawasaki H, Ueki S, Ito S, (2006), Decentralized adaptive coordinated control of multiple robot arms without using a force sensor. ELSEVIER.

Kazemian H, (2001), Comparative study of a learning fuzzy PID controller and a self tuning controller, ISA Transactions, Elsevier Science.

Kazerooni H., (1987), Automated Robot Deburring Using Electronic Compliancy; Impedance Control, IEEE Transactions.

Kazerooni H., Kramer JJ, (1986), An approach to automated deburring by robot manipulators, J. Dynamics System Measurement and Control, Volume 108, No. 4, pp 354-359.

Khatib O , (1987),“A Unified Approach for Motion and Force Control of Robot Manipulators : The Operational Space Formulation” *IEEE J. of Robotics and Automat.* **RA-3** (1) ,43 – 53 (1987) .

Kiel E, Profumo F, Schumacher W, (1995), Microprocessor Control of AC Drives, Tutorial at EPE , Seville, Spain.

Li W., Chang X.G., Wahl F. M., Tso S.K.,(1999), Hybrid Fuzzy P+ID Control of manipulators under Uncertainty; Mechatronics, Pergamon Press, Elsevier science, Volume 9, Issue. 3.1.

Lia Garcia-Perez, Jose M. Canas, Maria C. Garcia-Alegre, Pablo Yanez, Domingo Guinea, (1996), Fuzzy control of a electropeumatic actuator, IEEE Transactions System, Man and Cybernetics.

Lia W, XG Chang F Wahl, SK Tso, (1999), Technical note, Hybrid fuzzy P_ID control of manipulators, under uncertainty, Pergamon, Mechatronics.

Liang L, Fengfeng X, Kefu L, (2008), Modelling and control of automated polishing/deburring process using a dual-purpose compliant toolhead, International Journal of Machine Tools & Manufacture.

Liao Liang, Xi Fengfeng (Jeff), Liu Kefu, (2008), Modelling and control of automated polishing/deburring process using a dual-purpose compliant toolhead, International Journal of Machine Tools and manufacture.

Llor A.M., Retif J.M., Lin-Shi, S. Arnalte, (2003), Direct stator flux linkage control technique for a permanent magnet synchronous machine, IEEE.

Lorenz R. D., Lipo T. A, Nowotny D. W., (1994), Motion Control with Induction Motors, Proceedings of the IEEE, vol.82, no.8, pp.1215-1240.

Lu S, and Asada H., (1992), Transferring manipulative skills to robots: Representation and acquisition of tool manipulative skills using a process dynamic control, J. Dynamics System Measurement and Control, Volume 114, pp. 220-228.

Lygouras JN, Botsaris PN, Vourvoulakis J, Kodogiannis V, (2007), Fuzzy logic controller implementation for a solar air-conditioning system., Applied Energy 84, pp1305–1318.

Lyshevski Sergey E., (1999), Electromechanical Systems, Electric machines, and Applied Mechatronics, CRC Press.

Malki Heidar A., Misir Dave, Feigenspan Denny, Chen Guanrong, (1997), Fuzzy PID Control of a flexible-Joint Robot Arm with Uncertainties from Time-Varying Loads, IEEE Transactions on Control Systems Technology, Volume 5, Number 3.

Marjan Golob, (2001), Decomposed fuzzy proportional–integral–derivative controllers, Applied Soft Computing .201–214

Mason M, (1981) “Compliance and Force Control for Computer Controlled Manipulators” *IEEE Trans. on Sys. Man. Cyber* **SMC-11** (6), 418 – 432.

Mathworks website, (2008), Tagaki Sugeno Fuzzy logic Controller,

Meystel AM, (1985) Intelligent Motion Control in Antropomorphic Machines, in Applications in Artificial Intelligence, (Edit. S.J. Andriole), pp. 317-351, Petrocelli Books Inc., Princeton.

M-H Liu, (1995), Force-controlled fuzzy-logic-based robotic deburring, Department of Control Engineering, Control system Theory and Robotics group, Germany, Pergamon, Control Engineering Practice, Volume 3, Number 2, pp 189-201.

Microchip Application notes, (2008), Sensorless Field Oriented Control of PMSM Motors, Number AN1078
<http://ww1.microchip.com/downloads/en/AppNotes/01078A.pdf> (June 2008)

Miller T. J. E., (1989), Brushless Permanent Magnet and Reluctance Motor Drives, Monographs in Electrical and Electronic Engineering No. 21, Oxford Science Publications.

Ming-Chang Shih and Nian-Liang Luor, (1992), Self tuning Neural fuzzy Control of a Pneumatic cylinder under Vertical Load, IEEE Transactions on IEEE , Volume 39, Number 6, pp 472-489.

Murphy M, Norcross RJ, Proctor FM, (1990), CAD directed robotic deburring, Third International Symposium on Robotics and Manufacturing, British Columbia, Canada.
NEC Corporation (2002), Application Note, An Introduction to Vector Control of AC Motors Using the V850, http://www.eu.necel.com/_pdf/U16483EE1V0AN00.PDF (June 2008)

Petriu E M, Whalen T E, (2008), Human Computer Interaction, University of Ottawa, Ottawa, ON, Canada. http://www.site.uottawa.ca/~petriu/ROSE2006%20-Symbiotic_HCI-v5-post.pdf

PID Control, (2008), http://en.wikipedia.org/wiki/PID_controller (August, 2008)

Pillay P, (1988), Modelling of Permanent Magnet Motor drives, IEEE Transactions on Industrial Electronics, Volume 35, and Number 4.

Pillay P., Freere P., (1989), Literature survey of Permanent magnet AC motors and drives, Department of Electrical Engineering, University of Newcastle upon Tyne, IEEE.

Raibert M H, Craig JJ, (1981), Hybrid position/force control of robot manipulators, ASME J Dynamic Systems Measurement Control. 102:126-133.

Raibert MH , and Craig JJ , “Hybrid Position / Force Control of Manipulators” *ASME J. of Dyn. Sys. Meas. Contr.* **102** , 126 – 133 (1981) .

Robotics Institute of America, (1979) , http://en.wikipedia.org/wiki/Robot#cite_note-0
Salisbury KJ , “Active Stiffness Control of a Manipulator in Cartesian Coordinates” *The 19th IEEE Conference . on Decision and Control* , Albuquerque (1980) pp . 95 – 100 .
Salisbury KJ and Craig JJ , “Articulated Hands : Force Control and Kinematic Issues” *International . Journal . of Robotics Res .* **1** (1) , 4 – 17 (1982) .

Schutter, J, Bruyninckx H, Zhu W, Sponge M, (1997), Force Control: a bird's eye view. IEEE CCS/RAS International Workshop on @Control Problems in Robotics and Automation Future Directions". San Diego, CA.

Schutter, J., Van Brussel, H. (sup.) (1986). Compliant robot motion: task formulation and control

Schutter, J., Torfs, D., Dutre, S., Bruyninckx, H. (1997). Invariant hybrid position/force control of a velocity controlled robot with compliant end effector using modal decoupling. *International Journal of Robotics Research*, 16(3), 340-356.

Schutter: Compliant Robot Motion: Task formulation and control, Katolieke Universiteit Leuven, Afdeling Mechanische Konstruktie En Productie, PhD Thesis 1986.

Sciavicco L , Siciliano B , (2000) Modelling and Control of Robot manipulators, Advanced Textbooks in Control and Signal Processing, Springer-Verlag London Ltd. Seattle Robotics website,

Seng-Chi Chen, Pi-Cheng Tung , (1999), Trajectory planning for automated robotic deburring on an unknown contour., *International Journal of Machine tools and manufacture, Design Research and Application*, 957-978.

Seng-Chi Chen, Pi-Cheng Tung, (2000), Application of a rule self-regulating fuzzy controller for robotic deburring on unknown contours, , *Fuzzy sets and systems*, 341-350.
Siciliano B, Villani L, (2001), Robot force control, Kluwer Academic publishers, Springer.

Silva G, Datta A, Bhattacharyya SP, Boston B, (2004), PID Controller for Time Delay systems, 1 edition .

Spong M, Vidyasagar M, (1989) Robot Dynamics and Control,, John Wiley and Sons.
Sung-Hyun Han, Man-Hyung Lee, (1999), Design of Real-Time Robust adaptive controller for an assembling robot based-on DSPs (TMS320C40), recent advances in Mechatronics, Springer link publications.

Texas Instruments Application Notes, (2008), Serial Peripheral Interface (SPI), SPRU059B. <http://focus.ti.com/lit/ug/spru059b/spru059b.pdf> (August 2008)

Texas Instruments, (2008), Using TMS320 Family DSPs in Motion Control Systems <http://focus.ti.com/lit/an/spra327/spra327.pdf> (August 2008)

Toliyat H, (2004), Campbell S., DSP-based electromechanical Motion Control, CRC Press.

Torgny Brogardh, (2007), Present and future robot control development-an industrial perspective, ELSEVIER, Annual reviews in Control.

Trusca M, Lazea G, (2003), An Adaptive PID learning controller for periodic robot motion, IEEE conference on Control Applications procedures. Volume 1, Pages 686-689.

VanDoren, VJ (1998), Advanced control software goes beyond PID. *Control Eng. Int.*, January, 57– 60.

Volpe R and Khosla P , “A Theoretical and Experimental Investigation of Explicit Force Control Strategies for Manipulators” *IEEE Trans . on Auto . Contr .* **38** (11) ,1634 – 1650 (1993)

Volpe R and Khosla P , “An Experimental Evaluation and Comparison of Explicit Force Control Strategies for Robotic Manipulators” *American Control Conference* ,Chicago IL (June , 1992) pp . 758 – 764 .

W Bolton, (1999), *Mechatronics- Electronic Control systems in mechanical and electrical Engineering*, 2nd edition. Longman Publications.

W. Lia; , X.G. Chang, F.M. Wahl, Jay Farrell, (2001), Tracking control of a manipulator under uncertainty by FUZZY P+ID controller , *Fuzzy Sets and Systems, Volume 122, Issue 1, 16, Pages 125-137*

Wang Qing-Guo, Chang-Cheih Hang, Qiang Bi, (1998), Continual Self tuning from load disturbances performances, *Institution of Chemical Engineers*, Volume 76, Part A.

Webster Dictionary(2008), <http://www.websters-online-dictionary.org/definition/robot>

Weera Kaewjinda1 and Mongkol Konghirun, (2007), Vector control of drive of Permanent magnet synchronous motor using resolver sensor, *ECTI transactions on Electrical Engineering, Electronics and Communications*, Volume 5, 2007.

Wescott T, (2008) <http://www.embedded.com/2000/0010/0010feat3.htm>

Whitney DE, “Force Feedback Control of Manipulator Fine Motions” *ASME J . of Dync . Sys . Meas . Contr .* **99** , 91 – 97 (1977) .

Whitney, DE , “Historical Perspective and State of the Art in Robot Force Control” *International. Journal. of Robotics Res .* **6** (1) , 3 – 14 (1987) .

Zadeh LA, (1996), Fuzzy logic=Computing with words, *IEEE transactions on Fuzzy systems* 4(2), pages 103-111.

Zeng G, Hemani A, (1997), An overview of robot force control, *Robotica*, Volume 15, pp 473-482

Zhijun Sun , Rentao Xing , Chunsheng Zhao , (2007), Weiqing Huang, Fuzzy auto-tuning PID control of multiple joint robot driven by ultrasonic motors, *Ultrasonics* 46 ,pp 303– 312.

Zhong L., Rahman M. F., Hu W. Y., Lim K.W., (1997), Analysis of Direct Torque control in Permanent magnet Synchronous motor drives, IEEE transactions on Power Electronics, Volume 12, Number 3.

Ziliani G., A. Visioli, G. Legnani, (2007), A mechatronic approach for robotic deburring, Elsevier, Mechatronics.

Appendices:

I. DSP TMS320F2812 Introduction-

- High-Performance Static CMOS Technology
 - 150 MHz (6.67-ns Cycle Time)
 - Low-Power (1.8-V Core @135 MHz, 1.9-V Core @150 MHz, 3.3-V I/O) Design
 - 3.3-V Flash Programming Voltage
- JTAG Boundary Scan Support
- High-Performance 32-Bit CPU (TMS320C28x)
 - 16 x 16 and 32 x 32 MAC Operations
 - 16 x 16 Dual MAC
 - Harvard Bus Architecture
 - Atomic Operations
 - Fast Interrupt Response and Processing
 - Unified Memory Programming Model
 - 4M Linear Program Address Reach
 - 4M Linear Data Address Reach
 - Code-Efficient (in C/C++ and Assembly)
 - TMS320F24x/LF240x Processor Source Code Compatible
- On-Chip Memory
 - Flash Devices: Up to 128K x 16 Flash
(Four 8K x 16 and Six 16K x 16 Sectors)
 - ROM Devices: Up to 128K x 16 ROM
 - 1K x 16 OTP ROM
 - L0 and L1: 2 Blocks of 4K x 16 Each Single-Access RAM (SARAM)
 - H0: 1 Block of 8K x 16 SARAM
 - M0 and M1: 2 Blocks of 1K x 16 Each SARAM
- Boot ROM (4K x 16)
 - With Software Boot Modes
 - Standard Math Tables
- External Interface (F2812)
 - Up to 1M Total Memory
 - Programmable Wait States
 - Programmable Read/Write Strobe Timing
 - Three Individual Chip Selects
- Clock and System Control
 - Dynamic PLL Ratio Changes Supported

- On-Chip Oscillator
 - Watchdog Timer Module
- Three External Interrupts
- Peripheral Interrupt Expansion (PIE) Block That Supports 45 Peripheral Interrupts
- 128-Bit Security Key/Lock
 - Protects Flash/ROM/OTP and L0/L1 SARAM
 - Prevents Firmware Reverse Engineering
- Three 32-Bit CPU-Timers
- Motor Control Peripherals
 - Two Event Managers (EVA, EVB)
 - Compatible to 240x Devices
- Serial Port Peripherals
 - Serial Peripheral Interface (SPI)
 - Two Serial Communications Interfaces (SCIs), Standard UART
 - Enhanced Controller Area Network (eCAN)
 - Multichannel Buffered Serial Port (McBSP) With SPI Mode
- 12-Bit ADC, 16 Channels
 - 2 x 8 Channel Input Multiplexer
 - Two Sample-and-Hold
 - Single/Simultaneous Conversions
 - Fast Conversion Rate: 80 ns/12.5 MSPS
- Up to 56 Individually Programmable, Multiplexed General-Purpose Input/Output (GPIO) Pins

TMS320F2812

	TMS320F2812
CPU	1 C28x
Peak MMACS	150
Frequency(MHz)	150
RAM	36 KB
OTP ROM	2 KB
Flash	256 KB
EMIF	1 16-Bit
PWM	1 16-Ch
CAP/QEP	6/2
ADC	1 16-Ch12-Bit
ADC Conversion Time	80 ns
McBSP	1
UART	2 SCI
SPI	1
CAN	1
Timers	416-BitGP,1 WD
GPIO	56

Core Supply (Volts)	1.9 V
IO Supply (Volts)	3.3 V
Operating Temperature Range (&deg;C)	-40 to 85,-40 to 125

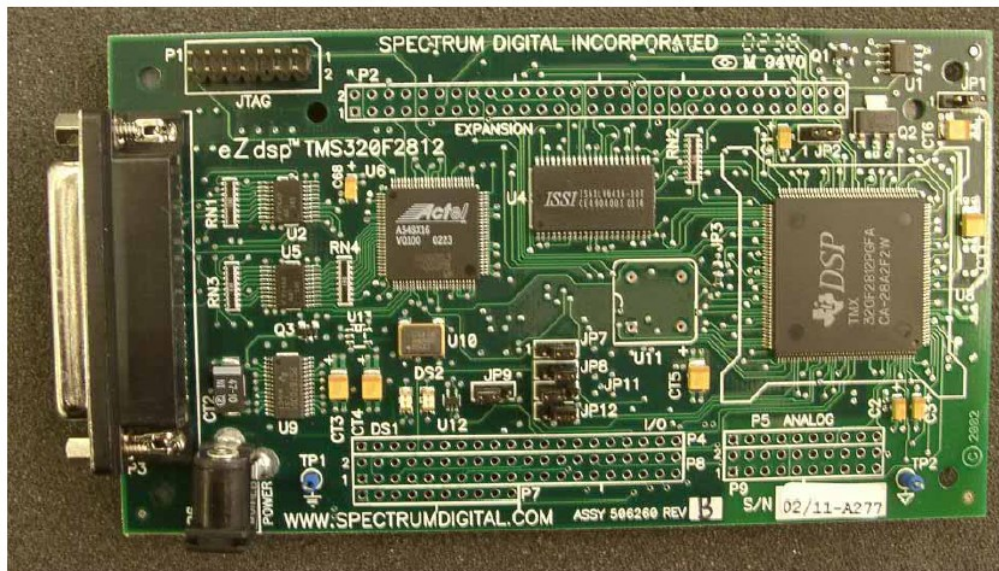


Figure 38: Top View of the ezdsp F2812 Board

Appendix C

http://www.mavilor.es/pdf_products/ma_series.pdf

III. Introduction and operation of PWM in the amplifier of the motor

A triangular wave signal is produced by an oscillator circuit and fed to a summing point. The output from the summing point is connected to the input of two threshold level circuits, one detecting positive level and the other negative level. The outputs of these threshold circuits provide the switching signals for the power circuits.

Also fed to the summing point is the i_{dc} error signal which, when added to the triangular waveform will trigger either the positive or negative level circuits.

Referring to fig. 1. With no i_{dc} signal, neither threshold circuit is triggered and so there is no output to the power circuits.

Referring to fig. 2. A small positive i_{dc} signal will have the effect of raising the triangular waveform so that the positive threshold circuit will be triggered for short periods of time every cycle. The resulting switching of the power circuits will result in a low level of average voltage (and hence current) fed to the motor.

Referring to figs. 3 to 5. As the triangular wave is raised higher by increasing values of i_{dc} , the time that the threshold circuit is conducting every cycle increases, causing the average voltage of the output to increase proportionately. In some versions of PWM circuits the triangular wave is raised above the threshold level, causing 100% modulation.

Referring to figs. 6 to 9. These diagrams show, that for negative values of i_{dc} , the other (negative) threshold circuit is triggered for increasing amounts of time, as the i_{dc} value gets larger. This switches the power circuits so that the current through the motor windings is in the reverse direction to that in figs. 2 to 5.

In a drive for a three phase brushless motor, three PWM circuits are used to control the currents in each of the phases individually. By combining the i_{dc} signal with signals derived from a resolver fitted to the motor shaft, commutation of the motor can be achieved. The outputs from the PWM circuits will be pseudo sine waves whose phase relationship will cause the motor to rotate in the correct direction.

At any instant the average voltage output to the motor combined with the back emf generated by the motor, if it is rotating, will determine the current flow through the motor windings. This in turn determines the torque produced by the motor. If the torque is higher than that to maintain the load on the motor at its present speed, the motor will accelerate, conversely if it is lower the motor will decelerate or stay at the same speed if the torque balances the load.

The frequency of the output is controlled automatically by the signal from the resolver being directly related to the motor instantaneous speed.

IV. PID Control Appendix

Part A:

The following section describes the mathematical/software implementation of the PID controller.

Proportional

Proportional control is the easiest feedback control to implement and it is just the error

signal multiplied by a constant and fed out to the motor drive. The proportional term gets calculated with the following code:

```
double pTerm;  
pTerm = pid->pGain * error;
```

Integral

Integral control is used to add long-term precision to a control loop which is almost always used in conjunction with proportional control. The code to implement an integrator is shown below. The integrator state, iState is the sum of all the preceding inputs. The parameters iMin and iMax are the minimum and maximum allowable integrator state values.

```
double iTerm;  
// calculate the integral state with appropriate limiting  
pid->iState += error;  
if (pid->iState > pid->iMax)  
    pid->iState = pid->iMax;  
else if (pid->iState < pid->iMin)  
    pid->iState = pid->iMin;  
iTerm = pid->iGain * iState;
```

Differential

Differential term is based on the rate of change of error. The code below shows the differential term of a PID controller.

```
double dTerm;  
dTerm = error - olderror;
```

Part B:

Future Work: Deburring application

The section describes a method to perform CAD directed robot deburring. The robot is allowed to trace the entire surface before deburring. The geometrical profile of the surface is obtained as shown in Figure 39 by monitoring the normal force component to the surface. The surface under consideration has got undulations. This can be then compared the desired CAD model of the surface. Thus, the deburring strategy can be developed and the controller structure can be modified or altered.

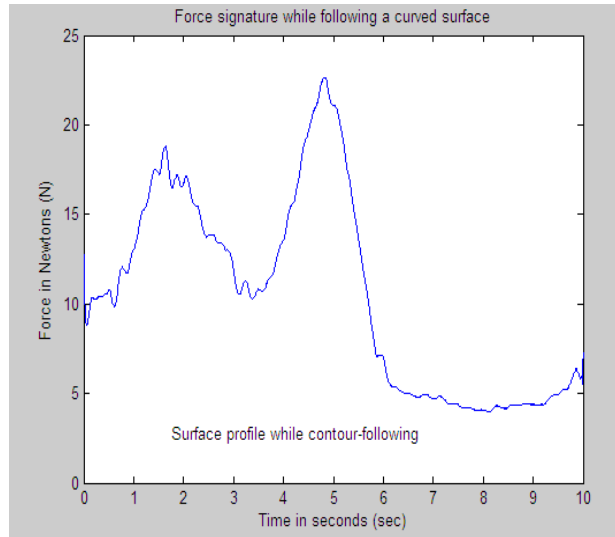


Figure 39: Force profile following a curved surface

V. Vector Control Summary

1. The 3-phase stator currents are measured. These measurements provide values i_u and i_v . i_w is calculated because i_u , i_v and i_w have this relationship: $i_u + i_v + i_w = 0$.

2. The 3-phase currents are converted to a two axis system. This conversion provides the variables id_s and iq_s from the measured i_u and i_v and the calculated values i_w . id_s and iq_s are time-varying quadrature current values as viewed from the perspective of the stator.

3. The two axis coordinate system is rotated to align with the rotor flux using a transformation angle calculated at the last iteration of the control loop. This conversion provides the id_s^r and iq_s^r variables from id_s and iq_s . id_s^r and iq_s^r are the quadrature currents transformed to the rotating coordinate system.

4. Error signals are formed using id_s^r , iq_s^r and reference values for each.

- The id_s^r reference controls rotor magnetizing flux.
- The iq_s^r reference controls the torque output of the motor.
- The error signals are input to PI controllers.
- The output of the controllers provides id_s^{r*} and iq_s^{r*} , which is a voltage vector that will be sent to the motor.

5. A new transformation angle is estimated id_s^* , iq_s^* and id_s^{r*} and iq_s^{r*} are the inputs. The new angle guides the vector control algorithm as to where to place the next voltage vector.

6. The id_s^{r*} and iq_s^{r*} output values from the PI controllers are rotated back to the stationary reference frame using the new angle. This calculation provides the next quadrature voltage values id_s^* and iq_s^* .

7. The id_s^* and iq_s^* values are transformed back to 3-phase values. The 3-phase voltage values are used to calculate new PWM duty cycle values that generate the desired voltage vector.

VI. Description of coordinate transforms

The first coordinate transform, called the Clarke Transform, as shown in Figure 45, moves a three axis two dimensional coordinate system, referenced to the stator, onto a two axis system, keeping the same reference.

Figure 45: Clarke transform

At this point, you have the stator current represented on a two axis orthogonal system with the axis called α - β . The next step is to transform into another two axis system that is rotating with the rotor flux. This transformation uses the Park Transform. This two axis rotating coordinate system is called the d-q axis. θ represents the rotor angle.

After the PI iteration you have two voltage component vectors in the rotating d-q axis. You will need to go through complementary inverse transforms to get back to the 3-phase motor voltage. First you transform from the two axis rotating d-q frame to the two axis stationary frame α - β . This transformation uses the Inverse Park Transform.

The next step is to transform from the stationary two axis α - β frame to the stationary three axes, 3-phase reference frame of the stator. Mathematically, this transformation is accomplished with the Inverse Clark Transform.

Inverse Park Transform

The following section [shows the Inverse Parke Transformation. i_{ds}^{r*} , i_{qs}^{r*} and θ_r are the inputs. The two rotating currents are transformed into a two phase orthogonal stationary frame. The equations are as follows:

$$i_{ds}^* = i_{ds}^{r*} \cos \theta_r - i_{qs}^{r*} \sin \theta_r \quad \dots\dots\dots(12)$$

$$i_{qs}^* = i_{ds}^{r*} \sin \theta_r + i_{qs}^{r*} \cos \theta_r \quad \dots\dots\dots(13)$$

Inverse Clarke Transform

The Inverse Clarke Transformation converts balanced two-phase quadrature quantities into balanced three-phase quantities. The equations are as follows:

$$i_u^* = i_{ds}^* \quad \dots\dots\dots(14)$$

$$i_v^* = \sqrt{3}/2(i_{qs}^*) - (i_{ds}^*)/2 \quad \dots\dots\dots(15)$$

$$i_w^* = -i_u^* - i_v^* \quad \dots\dots\dots(16)$$

Park Transform

The Park Transform is a well known three phase to two phase transformation in synchronous machines analysis. The mathematical equations are as follows:

$$i_{ds}^r = i_{qs} * \sin \theta_r + i_{ds} * \cos \theta_r \quad \dots\dots\dots(17)$$

$$i_{qs}^r = i_{qs} * \cos \theta_r - i_{ds} * \sin \theta_r \quad \dots\dots\dots(18)$$

Clarke Transform

In the implementation of the Clarke Transformation, three phase stationary parameters are converted into a two-phase stationary reference frame. The Clarke Transformation mathematical equations are as follows:

$$i_{ds} = i_u \quad \dots\dots\dots(19)$$

$$i_{qs} = 1/\sqrt{3} (i_u) + 2/\sqrt{3} (i_v) \quad \dots\dots\dots(20)$$

VII. Mathematical derivations for torque control in PMSM

The following section derives, with the aid of mathematical motor equations, the direct relationship between torque of the PMSM and the q axis component of the stator current, the torque increases with the increase in the angle between the stator flux linkage and the rotor flux linkage. Maximum torque is achieved at 90 degrees.

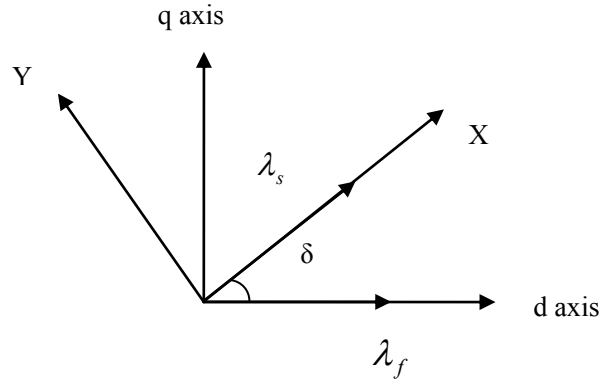


Figure 40: Stator and rotor flux linkages in different reference frames

In the equations (1), (2), (3) and (4), F represents voltage current flux linkages

$$\begin{bmatrix} F_x \\ F_y \end{bmatrix} = \begin{bmatrix} \cos \delta & \sin \delta \\ -\sin \delta & \cos \delta \end{bmatrix} \begin{bmatrix} F_d \\ F_q \end{bmatrix} \dots\dots\dots (1)$$

The inverse transformation is as follows,

$$\begin{bmatrix} F_d \\ F_q \end{bmatrix} = \begin{bmatrix} \cos \delta & -\sin \delta \\ \sin \delta & \cos \delta \end{bmatrix} \begin{bmatrix} F_x \\ F_y \end{bmatrix} \dots\dots\dots (2)$$

$$F_d = \cos \delta * F_x - \sin \delta * F_y \dots\dots\dots (3)$$

$$F_q = \sin \delta * F_x + \cos \delta * F_y \dots\dots\dots (4)$$

$$\cos \delta = \lambda_d / \lambda_s \dots\dots\dots (5)$$

$$\sin \delta = \lambda_q / \lambda_s \dots\dots\dots (6)$$

Substituting equations (14) and (15) in equation (5) we obtain,

$$T_e = \left(\frac{3}{2} \right) \left(\frac{P}{2} \right) \left(\lambda_d (i_x * \sin \delta + i_y * \cos \delta) \right) - \left(\lambda_q (i_x * \cos \delta - i_y * \sin \delta) \right) \dots\dots\dots (7)$$

Substituting equations (16) and (17) in equation (18) we have,

$$T_e = \left(\frac{3}{2}\right)\left(\frac{P}{2}\right)\left(\lambda_d \left(i_x * \frac{\lambda_q}{\lambda_s} + i_y * \frac{\lambda_d}{\lambda_s}\right) - \left(\lambda_q \left(i_x * \frac{\lambda_d}{\lambda_s} - i_y * \frac{\lambda_q}{\lambda_s}\right)\right)\right) \dots\dots\dots (8)$$

In the above equation, after expansion of brackets we obtain the following equation where it is shown that the torque is directly proportional to the y axis (q axis), as shown in Figure 49, component of the stator current if the amplitude of the stator flux linkage is kept constant.

$$T_e = \left(\frac{3}{2}\right)\left(\frac{P}{2}\right)\lambda_s i_y \dots\dots\dots (9)$$

$$T_e \propto i_y \dots\dots\dots (10)$$

Equations (3) and (4) from the previous section can be written as follows

$$\begin{bmatrix} \lambda_d \\ \lambda_q \end{bmatrix} = \begin{bmatrix} L_d & 0 \\ 0 & L_q \end{bmatrix} \begin{bmatrix} I_d \\ I_q \end{bmatrix} + \begin{bmatrix} \lambda_f \\ 0 \end{bmatrix} \dots\dots\dots (11)$$

$$\begin{bmatrix} \cos \delta & -\sin \delta \\ \sin \delta & \cos \delta \end{bmatrix} \begin{bmatrix} \lambda_x \\ \lambda_y \end{bmatrix} = \begin{bmatrix} L_d & 0 \\ 0 & L_q \end{bmatrix} \begin{bmatrix} \cos \delta & -\sin \delta \\ \sin \delta & \cos \delta \end{bmatrix} \begin{bmatrix} i_x \\ i_y \end{bmatrix} + \begin{bmatrix} \lambda_f \\ 0 \end{bmatrix}$$

$$\begin{bmatrix} \lambda_x \\ \lambda_y \end{bmatrix} = \begin{bmatrix} L_s & 0 \\ 0 & L_s \end{bmatrix} \begin{bmatrix} i_x \\ i_y \end{bmatrix} + \lambda_f \begin{bmatrix} \cos \delta \\ -\sin \delta \end{bmatrix}$$

As λ_y is zero, since the x-axis is fixed at the stator flux linkage, the equation of current i_y can be obtained from the above equation, which is as follows

$$i_y = (1/L_s) * \lambda_f * \sin \delta \dots\dots\dots (12)$$

From Equation (21) and (23), we obtain,

$$T_e \propto \delta \dots\dots\dots (13)$$

Therefore, from equations (12) and (13), it is proven that the torque increases with increase in δ and it is maximum at $\Pi/2$, if the amplitude of the stator flux linkage is kept constant.

VIII. DSP Software code-

The following sections include the software codes written in C language for the TMS320F2812 DSP using the code composer environment.

Program for the X axis controller for conventional PID controller

```

/*****
// Program created for Contour following applications on InFACT, UWE, Bristol.
// X-axis control program.
*****/
#include "DSP28_Device.h"
#include "math.h" // preprocessor commands
#include "string.h" // preprocessor commands
// Prototype statement for functions found within this file.
// The following three commands are used when the program needs to be downloaded on the onboard DSP
SD memory
//extern unsigned int secureRamFuncs_loadstart;
//extern unsigned int secureRamFuncs_loadend;
//extern unsigned int secureRamFuncs_runstart;

void InitECan(void); // subroutine for the initialization of the CAN bus
void spi_fifo_init(void); // subroutine for the initialization of the SPI (serial peripheral interface)
module
void spi_xmit(Uint16 a); // subroutine for the transmission of the SPI
void InitAdc1(void); // subroutine for the initialization of the A to D converter
void CurrentCal(void); // subroutine for the Current feedback from the motor
void PIDloop(void); // PID loop subroutine
void positionloop(void); // subroutine number 1 for position feedback from the motor
void positionloop1(void); // subroutine number 2 for position feedback from the motor
extern void DSP28x_usDelay(unsigned long Count);

// Global variables for this program are as follows
int j;
Uint16 dataread;
int x;//=0; //position counter variable
Uint16 average;
Uint16 y;//=0;
int a,i;
int avg;
Uint16 speed,speed1; //speed output from the DSP processor
Uint16 X,Y,Z;//=0;
int d;//=0; //Initial current (torque) setup variable
int level,actual,forcex,forcey,ftotal;
int e;//=0;
int p;//=0;
Uint16 final;
double force;
int can;//=0;
int can1;//=0;
Uint16 max_current;//=2048;
int check;//=0;
//short buffer[1000];
int trial;
Uint16 error,errordot,sumerror,olderror;//=0;

```



```
int control;  
int inc;//=0;  
int u;//=0;  
int t;
```

//Main Program is as follows

```
void main(void)  
{
```

```
//memcpy(&secureRamFuncs_runstart,&secureRamFuncs_loadstart,&secureRamFuncs_loadend-  
&secureRamFuncs_loadstart);
```

// This function is used when the program has to be downloaded in the Flash memory of the DSP

//InitFlash (); // Flash subroutine for the DSP

//All the variables are initialised to zero at the start of the program

```
x=0;  
y=0;  
X=0;  
Y=0;  
Z=0;  
d=0;  
e=0;  
p=0;  
can =0;  
can1=0;  
max_current =2048;  
check =0;  
olderror =0;  
inc =0;  
u=0;  
t=0;
```

InitSysCtrl(); // Initialise the system control registers, watchdog ,clocks to default state

```
EALLOW; // EALLOW and EDIS are the commands needed to access special purpose registers  
SysCtrlRegs.HISPCP.all = 0x3; // HSPCLK = SYSCLKOUT/6 clock speed is reduced  
EDIS;
```

```
EALLOW;  
  GpioMuxRegs.GPAMUX.all =0X0000; // Pins used for GPIO routines  
  GpioMuxRegs.GPADIR.all =0XF000; // Pins used for input/output operations  
  GpioMuxRegs.GPBMUX.all =0X0000; // Pins used for GPIO routines  
  GpioMuxRegs.GPBDIR.all =0X003F; // Pins used for input/output operations  
EDIS;
```

```
EALLOW;
```

```

    GpioDataRegs.GPBDAT.all = 0X0000; //Pins used for GPIO routines
    GpioDataRegs.GPADAT.all = 0X0000; // Pins used for input or output routines
EDIS;

EALLOW;
    GpioMuxRegs.GPFMUX.all = 0x00CF; // Pins used for SPI and CAN facility
    GpioMuxRegs.GPFDIR.all = 0X004F; // Pins used for input or output operations
EDIS;
    // Select GPIOs to be SPI pins and CAN pins

InitECan ();    // Initialise the A to D subroutine

EALLOW;
ECanaRegs.CANMC.bit.SUSP=1;
EDIS;

EALLOW;
SysCtrlRegs.PCLKCR.bit.ADCENCLK=1; // ADC clock enable
EDIS;

InitAdc (); // ADC routine
InitAdc1 (); // ADC routine

EALLOW;
SysCtrlRegs.PCLKCR.bit.SPIENCLK=1; //SPI clock enable
EDIS;

// the following registers are used for initialization of the CAN registers
//Write to the MSGID field of TRANSMIT mailbox MBOX0
    ECanaMboxes.MBOX0.MID.all = 0x9555AAA0;
    ECanaMboxes.MBOX1.MID.all = 0x9555AAA1;
    ECanaMboxes.MBOX2.MID.all = 0x9555AAA2;

    ECanaRegs.CANMD.all = 0xFFFFFFFF2;

    // Specify that 8 bits will be sent/received
    ECanaMboxes.MBOX0.MCF.bit.DLC = 8;

    ECanaMboxes.MBOX0.MDRL.all = 0x9555AAA0;
    ECanaMboxes.MBOX0.MDRH.all = 0x89999999;

    ECanaMboxes.MBOX1.MDRL.all = 0;
    ECanaMboxes.MBOX1.MDRH.all = 0;

    //ECanaMboxes.MBOX2.MDRL.all = 0;
    //ECanaMboxes.MBOX2.MDRH.all = 0;

    ECanaMboxes.MBOX2.MCF.bit.DLC = 8;

    ECanaMboxes.MBOX2.MDRL.all = 0x9555AAA2;
    ECanaMboxes.MBOX2.MDRH.all = 0x11111111;

    spi_fifo_init(); // Initialise the SPI of the processor

```

```

    //spi_xmit(0x7FF0);
    speed=0x7F00; //0x7E00;//0x7C00;//0x7A00;//less overshoot//changed from 0x7A00 for deburring
applications
    spi_xmit(speed);//Transmit the SPI speed

    // The speed command issues the signal to amplifier to move the motor until it interacts with an
environment
    //speed1=speed;
    can=0;
    control=1;

    while(x<3) // This while loop was used to overcome a tight spot in the travel. This part is solely
used for that purpose
    {
        positionloop1();
    }
/*
checkpoint:if(GpioDataRegs.GPADAT.bit.GPIOA1==1) //Position feedback
    {
        DELAY_US(2); // Delay of 2 micro seconds

        if(GpioDataRegs.GPADAT.bit.GPIOA1==1)
        {
            x++;
        }
        else
        {
            goto checkpoint;
        }
    }
    else
    {
        goto checkpoint;
    }

    if(x>3)*/
    //
    d=2048;
checkpoint1: CurrentCal(); //Current calculation subroutine

    if(d>1725) //changed the value from 1700 for deburring application
    {
        positionloop1();
        goto checkpoint1;
    }
    else
    {

        while(d<2060)//changed the value from 1700 for deburring application

```

```

        {
            //Reverse the motor to reduce overshoot
            // This part detects the interaction with the environment
            //speed=speed-100;
            speed=0x8600;
            spi_xmit(speed);
            CurrentCal();
        }
        goto begin;
    }
//
/*
    else
    {
Zero: if(GpioDataRegs.GPADAT.bit.GPIOA1==0)
    {
        goto checkpoint;
    }
    else
    {
        goto Zero;
    }
    }
*/

begin:  if(can==0) // The loop through the CAN bus instruct the Y controller to start the travel across the
work piece
    {

        ECanaRegs.CANME.all = 0xFFFFFFFF; //enables the CAN transmission
        ECanaRegs.CANTA.all = 0xFFFFFFFF;
        ECanaRegs.CANTRS.all = 0x00000001; // Set TRS for all transmit mailboxes

        while(ECanaRegs.CANTA.all != 0x00000001) {}
        ECanaRegs.CANTA.all = 0xFFFFFFFF;

    }

    Can =1;
//*****
    While (ECanaMboxes.MBOX1.MDRH.all!=0x12121212) //This loop is for an end of travel signal from
the Y controller after the axes has finished its travel
    {

//*****

        While (ECanaMboxes.MBOX1.MDRH.all==0x89999998) //This loop is for a
signal for X to get back into speed control

        {
            speed=speed+1;

```

```

        if(speed>0x8100)
        {
            speed=0x8100;
        }
        spi_xmit(speed); // Transmit the speed
        DELAY_US(300); // Delay of 300 micro seconds
        CurrentCal(); // Call the current subroutine

    }

//*****

// The following are the upper and lower current limits for the controller which are calibrated to force
values to be exerted on the environment

    if(d>2100 | d<2080)
    {

        while(d>2100) //& ECanaMboxes.MBOX2.MDRH.all!=0x12121212)
        {
            error=d-1700; // Calculate the error between the desired and actual current values
            //PIDloop(); // Call for the PID subroutine
            speed=speed-control; // The value for control variable is obtained from the PIDloop subroutine
            spi_xmit(speed);
            DELAY_US(200); // Delay of 200 microseconds
            CurrentCal(); // Call the current feedback subroutine

        }

        while(d<2080)// & ECanaMboxes.MBOX2.MDRH.all!=0x12121212)
        {
            error=1700-d; // Calculate the error between the desired and actual current values
            //PIDloop();// Call for the PID subroutine
            speed=speed+control; // The value for control variable is obtained from the PIDloop subroutine

            spi_xmit(speed);
            DELAY_US(200); // Delay of 200 microseconds
            CurrentCal();// Call the current feedback subroutine

        }

    }

    else
    {
        spi_xmit (speed); // If the current is within the desired upper and lower limits transmit the same speed
values through the SPI
    }

```

```

    CurrentCal (); // Get the updated current value

}

// the program control remains in the above while loop only till the Y axis is traversing the workpiece. As
// soon as it reaches the end it issues a command and the X control comes out of the loop. Then the X
// controller goes back to its home position. It counts up the number of position counts it went to reach the
// surface and comes back the same number and reaches the HOME position.

t=0;

speed =0x8100;
spi_xmit (speed); // speed in negative X to go to READY position
check =0;
while (t<x) // x is the number of counts required to move towards the surface and
           // t is the number of counts coming back from the surface
{

    Positionloop ();
    DELAY_US (300); // Delay of 300 micro seconds
}

spi_xmit (0x8000); //zero speed of X to retain ie to stop


ECanaRegs.CANME.all = 0xFFFFFFFF; //enables the CAN Xmission
ECanaRegs.CANTA.all = 0xFFFFFFFF;
ECanaRegs.CANTRS.all = 0x00000004; // Set TRS for all transmit mailboxes
While (ECanaRegs.CANTA.all != 0x00000004) {}
    ECanaRegs.CANTA.all = 0xFFFFFFFF;

end:    goto end;

}

// The following are the various initialization subroutines declared at the beginning of the software. They
// include Serial peripheral interface (SPI) , analog to Digital Conversion (ADC), PID control loop, Position
// feedback loop,
void spi_fifo_init()
{
    // Initialize SPI FIFO registers
    SpiaRegs.SPICCR.bit.SPISWRESET=0; // Reset SpI

    SpiaRegs.SPICCR.all=0x000F;    //16-bit character
    SpiaRegs.SPICTL.all=0x0006;
    // SpiaRegs.SPISTS.all=0x0000;
    SpiaRegs.SPIBRR=0x001E;    // Baud rate
    //SpiaRegs.SPIFFTX.all=0xC028;    // Enable FIFO's, set TX FIFO level to 8

```

```

//SpiaRegs.SPIFFCT.all=0x00;
SpiaRegs.SPIPRI.all=0x0010;

SpiaRegs.SPICCR.bit.SPISWRESET=1; // Enable SpI

//SpiaRegs.SPIFFTX.bit.TXFIFO=1;

}

void spi_xmit(Uint16 a)
{
    GpioDataRegs.GPBDAT.bit.GPIOB5= 0;

    SpiaRegs.SPITXBUF=a;

star: if(SpiaRegs.SPISTS.bit.INT_FLAG==1)
    {
        dataread = SpiaRegs.SPIRXBUF;
        GpioDataRegs.GPBDAT.bit.GPIOB5 =1;

    }
    else
    {
        goto star;
    }
}

void InitAdc1()

{
    AdcRegs.ADCMAXCONV.all = 0x0000;    // Setup 2 conv's on SEQ1
    AdcRegs.ADCCHSELSEQ1.bit.CONV00 = 0x0; // Setup ADCINA3 as 1st SEQ1 conv.
    //AdcRegs.ADCCHSELSEQ1.bit.CONV01 = 0; // Setup ADCINA2 as 2nd SEQ1 conv.
    //AdcRegs.ADCTRL1.bit.CONT_RUN= 1;    // set continuous conversion
    AdcRegs.ADCTRL1.all= 0x2040;
    AdcRegs.ADCTRL2.bit.SOC_SEQ1 = 1;
    AdcRegs.ADCTRL2.bit.EVA_SOC_SEQ1 = 1; // Enable EVASOC to start SEQ1
    // AdcRegs.ADCTRL2.bit.INT_ENA_SEQ1 = 1; // Enable SEQ1 interrupt (every
/*    AdcRegs.ADCTRL1.all= 0x0040;
    AdcRegs.ADCTRL2.all= 0x2000;
    AdcRegs.ADCTRL3.all= 0x00E1;
    AdcRegs.ADCMAXCONV.all= 0x0000;
    //AdcRegs.ADCASEQSR.all= 0x0000;
    //AdcRegs.ADCST.all= 0x0000;
    AdcRegs.ADCCHSELSEQ1.all= 0x0000;
    AdcRegs.ADCCHSELSEQ2.all= 0x0000;
    AdcRegs.ADCCHSELSEQ3.all= 0x0000;
    AdcRegs.ADCCHSELSEQ4.all= 0x0000;

    */

```

```
//AdcRegs.ADCTRL2.bit.RST_SEQ1 = 1;    // Reset SEQ1

}

void CurrentCal()

{

    e=0;

check_current:

    Y=(AdcRegs.ADCRESULT0);
    X=(Y >> 4);

    if(X>(d+200) | X<(d-200))
    {

        if(e==3)
        {
            goto check_current1;
        }

        DELAY_US(25);
        e=e+1;
        goto check_current;

    }

    else
    {
        goto check_current1;
    }

}

check_current1: d=X;

                if(d<max_current)
                {
                    max_current=d;
                }

                /*level=2048;
                actual=level-d;
                forcex=(actual/10);
                forcey=ECanaMboxes.MBOX2.MDRH.all;
                force=(forcey*forcey)+(forcex*forcex);
                ftotal=sqrt(force);
                if(inc>50 & u<1000)
                {
                    u++;
                    buffer[u]=ftotal;
                    inc=0;
```



```
        }
        else
        {
            inc++;
        }*/

    }

void PIDloop()
{

    errordot=error-olderror;
    sumerror=sumerror+error;
    olderror=error;
    control=(0.001*error)+(0.01*errordot)+(0.001*sumerror);// PID Control Kp, Ki and Kd
    /*if(control>3)
    {
        control=2;
    }
    else
    {
        control=1;
    }*/
    control=1;
}

void positionloop()
{
    if(GpioDataRegs.GPADAT.bit.GPIOA1==1)//Position feedback
    {
        if(check==0)
        {
            DELAY_US(40);

            if(GpioDataRegs.GPADAT.bit.GPIOA1==1)
            {
                t++;
                check=1;
            }
        }
    }

    else
    {
        check=0;
    }
}
```

```

void positionloop1()
{
    if(GpioDataRegs.GPADAT.bit.GPIOA1==1)//Position feedback
    {
        if(check==0)
        {
            DELAY_US(40);

            if(GpioDataRegs.GPADAT.bit.GPIOA1==1)
            {
                x++;
                check=1;
            }
        }
    }
    else
    {
        check=0;
    }
}

```

```
//=====
```

b Program for the Y axis controller for conventional PID controller

```

//*****
//Software for contour following applications on InFACT, UWE, Bristol for Y axis control
//*****

// preprocessor commands
#include "DSP28_Device.h"
#include "DSP28_Examples.h"

// Prototype statements for functions found within this file.

```

```
extern unsigned int secureRamFuncs_loadstart;
extern unsigned int secureRamFuncs_loadend;
extern unsigned int secureRamFuncs_runstart;
```

```
void InitECan(void); //initialization for CAN in the DSP
void spi_fifo_init(void); // initialization for the serial peripheral interface (SPI)
void spi_xmit(Uint16 a);
void InitAdc1(void); // initialization for the analog to digital converter (ADC)
void CurrentCal(void); //Current feedback calculation
void Currentloop(void);
void positionloop(void); //position feedback calculation
extern void DSP28x_usDelay(unsigned long Count); // subroutine for delay loop.
```

```
// Global variable for this example
```

```
Uint32 ErrorCount;
Uint32 MessageReceivedCount;
```

```
//Uint32 TestMbox1 = 0;
//Uint32 TestMbox2 = 0;
//Uint32 TestMbox3 = 0;
int j;
Uint16 dataread;
int x;//=0;
Uint16 X,Y,Z;//=0;
Uint16 d;//=0;
int e;//=0;
int a;
int can;
Uint16 speed,speed1;
int flag,level,actual,forcey;
int check;//=0;
int test;
int repeat;
int repeat1;
```

```
void main(void)
{
```

```
memcpy(&secureRamFuncs_runstart,&secureRamFuncs_loadstart,&secureRamFuncs_loadend-
&secureRamFuncs_loadstart);
```

```
InitFlash(); // Flash memory initialization
```

```
    x=0;
    X=0;
    Y=0;
    Z=0;
    e=0;
    check =0;
    d=0;
    repeat =0;
    repeat1 =0;
```

```

EALLOW;
GpioMuxRegs.GPAMUX.all=0X0000;
GpioMuxRegs.GPADIR.all=0XF000;
GpioMuxRegs.GPBMUX.all=0X0000;
GpioMuxRegs.GPBDIR.all=0X003F;
EDIS;

EALLOW;
GpioDataRegs.GPBDAT.all= 0X0000;
GpioDataRegs.GPADAT.all=0X0000;
EDIS;

EALLOW;
GpioMuxRegs.GPFMUX.all=0x00CF;
GpioMuxRegs.GPFDIR.all=0X004F;
EDIS;
    // Select GPIOs to be SPI pins
    // Port F MUX - x000 0000 0000 1111

InitSysCtrl (); // Initialize system control registers, watchdog, clocks to default state
EALLOW;
    SysCtrlRegs.HISPCP.all = 0x3; // HSPCLK = SYSCLKOUT/6
EDIS;

EALLOW;
SysCtrlRegs.PCLKCR.bit.SPIENCLK=1;
EDIS;
spi_fifo_init ();
spi_xmit (0x8050); //zero speed-8050
//d=2048;
Check =0;

InitECan (); // Initializing the CAN interface

EALLOW;
ECanaRegs.CANMC.bit.SUSP=1;
EDIS;

EALLOW;
SysCtrlRegs.PCLKCR.bit.SPIENCLK=1;
EDIS;

EALLOW;
SysCtrlRegs.PCLKCR.bit.ADCENCLK=1;
EDIS;

InitAdc (); // initializing the analog to digital converter
InitAdc1 (); // initializing the analog to digital converter

ECanaMboxes.MBOX0.MID.all = 0x9555AAA0;

```

```

ECanaMboxes.MBOX1.MID.all = 0x9555AAA1;
ECanaMboxes.MBOX2.MID.all = 0x9555AAA2;

ECanaMboxes.MBOX0.MDRL.all=0;
ECanaMboxes.MBOX0.MDRH.all=0;

ECanaMboxes.MBOX1.MCF.bit.DLC=8;
//ECanaMboxes.MBOX2.MCF.bit.DLC=8;

ECanaRegs.CANMD.all = 0xFFFFFFFF5;

ECanaMboxes.MBOX1.MDRL.all=0x9555AAA1;
ECanaMboxes.MBOX1.MDRH.all=0x00000000;

ECanaMboxes.MBOX2.MDRL.all=0;
ECanaMboxes.MBOX2.MDRH.all=0;

ECanaRegs.CANME.all = 0xFFFFFFFF;

    d=2048;
//    test=1;

// The Y controller waits to receive a start signal from the X controller indicating it is in contact with an
// environment. As soon as the Y controller receives the signal it starts to traverse the component or work
// piece initially in speed control but if the Y controller encounters an obstacle it sends a signal through the
// CAN bus indicating to X to switch to speed loop. Thus there is a constant real time switching in between the
// speed and the current loops depending on the situation.

zerospeed: if(ECanaMboxes.MBOX0.MDRH.all==0x89999999)
{
    //speed=0x8060;
    DELAY_US(500000); //no time delay- taken out for deburring application
    speed=0x8100;
    spi_xmit(0x8100);
    //speed1=speed;
}

else
{
    goto zerospeed;
}

while(x<10) //span of traverse of the Y controller
{
    CurrentCal();
    positionloop();

    if(d>2150) // & repeat1==0)

```

```

    {
        ECanaMboxes.MBOX1.MDRL.all=0x9555AAA1;
        ECanaMboxes.MBOX1.MDRH.all=0x89999998;
        ECanaRegs.CANME.all = 0xFFFFFFFF;//enables the CAN Xmission
        ECanaRegs.CANTA.all = 0xFFFFFFFF;
        ECanaRegs.CANTRS.all = 0x00000002;// Set TRS for all transmit

        //while(ECanaRegs.CANTA.all != 0x00000002) {}
        ECanaRegs.CANTA.all = 0xFFFFFFFF;
        repeat1=1;
        repeat=0;
    }

    CurrentCal();

    if(d<2150) // & repeat==0)
    {

        ECanaMboxes.MBOX1.MDRL.all=0x9555AAA1;
        ECanaMboxes.MBOX1.MDRH.all=0x89999997;
        ECanaRegs.CANME.all = 0xFFFFFFFF;//enables the CAN
        ECanaRegs.CANTA.all = 0xFFFFFFFF;
        ECanaRegs.CANTRS.all = 0x00000002;// Set TRS for all transmit

        //while(ECanaRegs.CANTA.all != 0x00000002) {}
        ECanaRegs.CANTA.all = 0xFFFFFFFF;
        repeat=1;
        repeat1=0;
    }

}

    spi_xmit(0x8050);

    DELAY_US(300);

    x=0;
    check=0;
    //spi_xmit(0x8050);

    //DELAY_US(300);

    ECanaMboxes.MBOX1.MDRL.all=0x9555AAA1;
    ECanaMboxes.MBOX1.MDRH.all=0x12121212;
    ECanaRegs.CANME.all = 0xFFFFFFFF;//enables the CAN Xmission

```

```

    ECanaRegs.CANTA.all = 0xFFFFFFFF;
    ECanaRegs.CANTRS.all = 0x00000002; // Set TRS for all transmit mailboxes

    //while(ECanaRegs.CANTA.all != 0x00000004) {}
    ECanaRegs.CANTA.all = 0xFFFFFFFF;

    //DELAY_US(1000);

    while(ECanaMboxes.MBOX2.MDRH.all!=0x11111111);

    spi_xmit(0x7EA0);

    while(x<11) // the span of the Y controller
    {
        positionloop();
    }

end: spi_xmit(0x8050);
    goto end;

}

// The following sections are the subroutines for the SPI, ADC , current feedback and position feedback
// loops which are called from the main program.

void spi_fifo_init()
{
    // Initialize SPI FIFO registers
    SpiaRegs.SPICCR.bit.SPISWRESET=0; // Reset SpI

    SpiaRegs.SPICCR.all=0x000F;    //16-bit character
    SpiaRegs.SPICTL.all=0x0006;
    // SpiaRegs.SPISTS.all=0x0000;
    SpiaRegs.SPIBRR=0x001E;        // Baud rate
    //SpiaRegs.SPIFFTX.all=0xC028;    // Enable FIFO's, set TX FIFO level to 8

    //SpiaRegs.SPIFFCT.all=0x00;
    SpiaRegs.SPIPRI.all=0x0010;

    SpiaRegs.SPICCR.bit.SPISWRESET=1; // Enable SpI

    //SpiaRegs.SPIFFTX.bit.TXFIFO=1;

}

void spi_xmit(Uint16 a)
{
    GpioDataRegs.GPBDAT.bit.GPIOB5= 0;

```

```

    SpiaRegs.SPITXBUF=a;

star: if(SpiaRegs.SPISTS.bit.INT_FLAG==1)
    {
        dataread = SpiaRegs.SPIRXBUF;
        GpioDataRegs.GPBDAT.bit.GPIOB5 =1;

    }
    else
    {
        goto star;
    }

}

void InitAdc1()
{
    AdcRegs.ADCMAXCONV.all = 0x0000;    // Setup 2 conv's on SEQ1
    AdcRegs.ADCCHSELSEQ1.bit.CONV00 = 0x0; // Setup ADCINA3 as 1st SEQ1 conv.
    //AdcRegs.ADCCHSELSEQ1.bit.CONV01 = 0; // Setup ADCINA2 as 2nd SEQ1 conv.
    //AdcRegs.ADCTRL1.bit.CONT_RUN= 1;    // set continuous conversion
    AdcRegs.ADCTRL1.all= 0x2040;
    AdcRegs.ADCTRL2.bit.SOC_SEQ1 = 1;
    AdcRegs.ADCTRL2.bit.EVA_SOC_SEQ1 = 1; // Enable EVASOC to start SEQ1
    // AdcRegs.ADCTRL2.bit.INT_ENA_SEQ1 = 1; // Enable SEQ1 interrupt (every
/*    AdcRegs.ADCTRL1.all= 0x0040;
    AdcRegs.ADCTRL2.all= 0x2000;
    AdcRegs.ADCTRL3.all= 0x00E1;
    AdcRegs.ADCMAXCONV.all= 0x0000;
    //AdcRegs.ADCASEQSR.all= 0x0000;
    //AdcRegs.ADCST.all= 0x0000;
    AdcRegs.ADCCHSELSEQ1.all= 0x0000;
    AdcRegs.ADCCHSELSEQ2.all= 0x0000;
    AdcRegs.ADCCHSELSEQ3.all= 0x0000;
    AdcRegs.ADCCHSELSEQ4.all= 0x0000;

    */

    //AdcRegs.ADCTRL2.bit.RST_SEQ1 = 1;    // Reset SEQ1

}

void CurrentCal()
{
    e=0;

check_current:
    Y=(AdcRegs.ADCRESULT0);
    X=(Y >> 4);

```



```

        if(X>(d+200) | X<(d-200))
        {

            if(e==3)
            {
                goto check_current1;
            }

            DELAY_US(25);
            e=e+1;
            goto check_current;

        }

        /*else
        {
            goto check_current1;
        }
        */

check_current1: d=X;

                                /*level=2048;
                                actual=d-2048;
                                forcey=(actual/10);

ECanaMboxes.MBOX2.MDRL.all=0x9555AAA1;
ECanaMboxes.MBOX2.MDRH.all=forcey;
                                ECanaRegs.CANME.all = 0xFFFFFFFF;//enables the CAN Xmission
                                ECanaRegs.CANTA.all = 0xFFFFFFFF;
                                ECanaRegs.CANTRS.all = 0x00000004;// Set TRS for all transmit
mailboxes

                                while(ECanaRegs.CANTA.all != 0x00000004) {}
                                ECanaRegs.CANTA.all = 0xFFFFFFFF; */
}

void positionloop()
{
    if(GpioDataRegs.GPADAT.bit.GPIOA0==1)//Position feedback
    {

        if(check==0)
        {

            DELAY_US(40);

            if(GpioDataRegs.GPADAT.bit.GPIOA0==1)
            {

```

```

                                x++;
                                check=1;
                                }
                                }
                                }
else
{
check=0;
}
}

//=====
// No more.
//=====

```

c. Program for the X axis controller for fuzzy controller

```

//*****
// Program created for Contour following applications on InFACT, UWE, Bristol.
// X-axis control program.
//*****
#include "DSP28_Device.h"
#include "math.h" // preprocessor commands
#include "string.h" // preprocessor commands
// Prototype statement for functions found within this file.
//extern unsigned int secureRamFuncs_loadstart;
//extern unsigned int secureRamFuncs_loadend;
//extern unsigned int secureRamFuncs_runstart;

```

```

void InitECan(void); // subroutine for the initialization of the CAN bus
void spi_fifo_init(void); // subroutine for the initialization of the SPI (serial peripheral interface)
module
void spi_xmit(Uint16 a); // subroutine for the transmission of the SPI
void InitAdc1(void); // subroutine for the initialization of the A to D converter
void CurrentCal(void); // subroutine for the Current feedback from the motor
void PIDloop(void); // PID loop subroutine
void positionloop(void); // subroutine number 1 for position feedback from the motor
void positionloop1(void); // subroutine number 2 for position feedback from the motor
extern void DSP28x_usDelay(unsigned long Count);

```

```

#define NORULES 3
#define NUMINPUTS 2

```

```

typedef struct
{
    int centre;
    int width;
    float activation;
}MFNin;

```

```

typedef struct
{
    float control;
}MFNout;

```

```

typedef struct
{
    MFNin lhs[NUMINPUTS];
    MFNout rhs;
    float strength;
}FRULE;

```

```

void init_rules(void);
void fuzzy(void);
void eval_strengths(void);
float Membership(MFNin,int);
void eval_output(void);

```

```

FRULE r[NORULES];
int input[NUMINPUTS];
float control=0;

```

// Global variables for this program are as follows

```

int j;
Uint16 dataread;
int x;//=0;
Uint16 average;
Uint16 y;//=0;
int a,i;

```

```

int avg;
Uint16 speed,speed1;
Uint16 X,Y,Z;//=0;
int d;//=0;
int level,actual,forcex,forcey,ftotal;
int e;//=0;
int p;//=0;
Uint16 final;
double force;
int can;//=0;
int can1;//=0;
Uint16 max_current;//=2048;
int check;//=0;
//short buffer[1000];
int trial;
Uint16 error,errordot,sumerror,olderror;//=0;
int control;
int inc;//=0;
int u;//=0;
int t;

```

//Main Program is as follows

```

void main(void)
{
    //memcpy(&secureRamFuncs_runstart,&secureRamFuncs_loadstart,&secureRamFuncs_loadend-
    &secureRamFuncs_loadstart);

```

// This function is used when the program has to be downloaded in the Flash memory of the DSP

//InitFlash (); // Flash subroutine for the DSP

```

x=0;
y=0;
X=0;
Y=0;
Z=0;
d=0;
e=0;
p=0;
can =0;
can1=0;
max_current =2048;
check =0;
olderror =0;
inc =0;
u=0;
t=0;

```

InitSysCtrl(); // Initialise the system control registers, watchdog ,clocks to default state

```
EALLOW; // EALLOW and EDIS are the commands needed to access special purpose registers
SysCtrlRegs.HISPCP.all = 0x3; // HSPCLK = SYSCLKOUT/6 clock speed is reduced
EDIS;
```

```
EALLOW;
  GpioMuxRegs.GPAMUX.all = 0X0000; // Pins used for GPIO routines
  GpioMuxRegs.GPADIR.all = 0XF000; // Pins used for input/output operations
  GpioMuxRegs.GPBMUX.all = 0X0000; // Pins used for GPIO routines
  GpioMuxRegs.GPBDIR.all = 0X003F; // Pins used for input/output operations
EDIS;
```

```
EALLOW;
  GpioDataRegs.GPBDAT.all = 0X0000; //Pins used for GPIO routines
  GpioDataRegs.GPADAT.all = 0X0000; // Pins used for input or output routines
EDIS;
```

```
EALLOW;
  GpioMuxRegs.GPFMUX.all = 0x00CF; // Pins used for SPI and CAN facility
  GpioMuxRegs.GPFDIR.all = 0X004F; // Pins used for input or output operations
EDIS;
  // Select GPIOs to be SPI pins and CAN pins
```

```
InitECan (); // Initialise the A to D subroutine
```

```
EALLOW;
ECanaRegs.CANMC.bit.SUSP=1;
EDIS;
```

```
EALLOW;
SysCtrlRegs.PCLKCR.bit.ADCENCLK=1; // ADC clock enable
EDIS;
```

```
InitAdc (); // ADC routine
InitAdc1 (); // ADC routine
```

```
Initrules ();
Fuzzy();
```

```
EALLOW;
SysCtrlRegs.PCLKCR.bit.SPIENCLK=1; //SPI clock enable
EDIS;
```

```
// the following registers are used for initialization of the CAN registers
//Write to the MSGID field of TRANSMIT mailbox MBOX0
```

```
ECanaMboxes.MBOX0.MID.all = 0x9555AAA0;
ECanaMboxes.MBOX1.MID.all = 0x9555AAA1;
ECanaMboxes.MBOX2.MID.all = 0x9555AAA2;
```

```
ECanaRegs.CANMD.all = 0xFFFFFFFF2;
```

```
// Specify that 8 bits will be sent/received
```

```

ECanaMboxes.MBOX0.MCF.bit.DLC = 8;

ECanaMboxes.MBOX0.MDRL.all = 0x9555AAA0;
ECanaMboxes.MBOX0.MDRH.all = 0x89999999;

ECanaMboxes.MBOX1.MDRL.all = 0;
ECanaMboxes.MBOX1.MDRH.all = 0;

//ECanaMboxes.MBOX2.MDRL.all = 0;
//ECanaMboxes.MBOX2.MDRH.all = 0;

ECanaMboxes.MBOX2.MCF.bit.DLC = 8;

ECanaMboxes.MBOX2.MDRL.all = 0x9555AAA2;
ECanaMboxes.MBOX2.MDRH.all = 0x11111111;

spi_fifo_init(); // Initialise the SPI of the processor
//spi_xmit(0x7FF0);
speed=0x7F00; //0x7E00;//0x7C00;//0x7A00;//less overshoot//changed from 0x7A00 fo deburring
appl. spi_xmit(speed);

// The speed command issues the signal to amplifier to move the motor until it interacts with an
environment
//speed1=speed;
can=0;
control=1;

while(x<3) // This while loop was used to overcome a tight spot in the travel. This part is solely
used for that purpose
{
    positionloop1();
}
/*
checkpoint:if(GpioDataRegs.GPADAT.bit.GPIOA1==1) //Position feedback
{
    DELAY_US(2); // Delay of 2 micro seconds

    if(GpioDataRegs.GPADAT.bit.GPIOA1==1)
    {
        x++;
    }
    else
    {
        goto checkpoint;
    }
}
else
{
    goto checkpoint;
}

```

```

        if(x>3)*/
        //
        {
            d=2048;
            checkpoint1: CurrentCal(); //Current calculation subroutine

            if(d>1725) //changed the value from 1700 for deburring application

            {
                positionloop1();
                goto checkpoint1;
            }
            else
            {
                while(d<2060) //changed the value from 1700 for deburring application
                {
                    //Reverse the motor to reduce overshoot
                    // This part detects the interaction with the environment
                    //speed=speed-100;
                    speed=0x8600;
                    spi_xmit(speed);
                    CurrentCal();
                }
                goto begin;
            }
        }
        //
        /*
        else
        {
Zero: if(GpioDataRegs.GPADAT.bit.GPIOA1==0)
        {
            goto checkpoint;
        }
        else
        {
            goto Zero;
        }
        }
        */

begin:  if(can==0) // The loop through the CAN bus instruct the Y controller to start the travel across the
work piece
        {

            ECanaRegs.CANME.all = 0xFFFFFFFF; //enables the CAN transmission
            ECanaRegs.CANTA.all = 0xFFFFFFFF;
            ECanaRegs.CANTRS.all = 0x00000001; // Set TRS for all transmit mailboxes

            while(ECanaRegs.CANTA.all != 0x00000001) {}
            ECanaRegs.CANTA.all = 0xFFFFFFFF;

```

```

    }

    Can=1;
    /*******
    While (ECanaMboxes.MBOX1.MDRH.all!=0x12121212) //This loop is for an end of travel signal from
    the Y controller after the axes has finished its travel
    {

    /*******

        While (ECanaMboxes.MBOX1.MDRH.all==0x89999998) //This loop is for a
        signal for X to get back into speed control

        {
            speed=speed+1;
            if(speed>0x8100)
        {
            speed=0x8100;
        }
        spi_xmit(speed); // Transmit the speed
        DELAY_US(300); // Delay of 300 micro seconds
        CurrentCal(); // Call the current subroutine

        }

    /*******

    // The following are the upper and lower current limits for the controller which are calibrated to force
    values to be exerted on the environment

    if(d>2100 | d<2080)
    {

    while(d>2100) //& ECanaMboxes.MBOX2.MDRH.all!=0x12121212)
    {
        error=d-1700; // Calculate the error between the desired and actual current values
        fuzzy (); // Call for the fuzzy subroutine
        speed=speed-control; // The value for control variable is obtained from the fuzzy loop subroutine
        spi_xmit(speed);
        DELAY_US(200); // Delay of 200 microseconds
        CurrentCal(); // Call the current feedback subroutine

    }

    while(d<2080)// & ECanaMboxes.MBOX2.MDRH.all!=0x12121212)
    {
        error=1700-d; // Calculate the error between the desired and actual current values

```



```

    fuzzy (); // Call for the fuzzy subroutine
    speed=speed+control; // The value for control variable is obtained from the fuzzyloop subroutine
    spi_xmit(speed);
    DELAY_US(200); // Delay of 200 microseconds
    CurrentCal(); // Call the current feedback subroutine

}
}

else
{
    spi_xmit (speed); // If the current is within the desired upper and lower limits transmit the same speed
    values through the SPI
}

```

```

    CurrentCal (); // Get the updated current value

```

```

}

```

// the program control remains in the above while loop only till the Y axis is traversing the workpiece. As soon as it reaches the end it issues a command and the X control comes out of the loop. Then the X controller goes back to its home position. It counts up the number of position counts it went to reach the surface and comes back the same number and reaches the HOME position.

```

t=0;

```

```

speed =0x8100;
spi_xmit (speed); // speed in negative X to go to READY position
check =0;
while (t<x) // x is the number of counts required to move towards the surface and
            t is the number of counts coming back from the surface

```

```

{

```

```

    Positionloop ();
    //DELAY_US (300); // Delay of 300 micro seconds
}

```

```

spi_xmit (0x8000); //zero speed of X to retain ie to stop

```

```

ECanaRegs.CANME.all = 0xFFFFFFFF; //enables the CAN Xmission
ECanaRegs.CANTA.all = 0xFFFFFFFF;
ECanaRegs.CANTRS.all = 0x00000004; // Set TRS for all transmit mailboxes
While (ECanaRegs.CANTA.all != 0x00000004) {}
    ECanaRegs.CANTA.all = 0xFFFFFFFF;

```

```

end:    goto end;

```

```

}

```

// The following are the various initialization subroutines declared at the beginning of the software. They include Serial peripheral interface (SPI) , analog to Digital Conversion (ADC), Fuzzy loop, Position feedback loop,

//*****FUZZY LOGIC SOFTWARE BEGIN*****

void init_rules()

{

```

r[0].lhs[0].centre=0;
r[0].lhs[0].width=100;
r[0].lhs[1].centre=0;
r[0].lhs[1].width=100;
r[0].rhs.control=2;

```

```

r[1].lhs[0].centre=100;
r[1].lhs[0].width=100;
r[1].lhs[1].centre=100;
r[1].lhs[1].width=100;
r[1].rhs.control=4;

```

```

r[2].lhs[0].centre=200;
r[2].lhs[0].width=100;
r[2].lhs[1].centre=200;
r[2].lhs[1].width=100;
r[2].rhs.control=6;

```

}

void fuzzy()

{

```

    input[0]=d;
    input[1]=derivative;
    eval_strengths();
    eval_output();

```

}

void eval_strengths()

{

```

    int i,j;
    for(i=0;i<NORULES;i++)
    {
        r[i].strength=1.0;
        for(j=0;j<NUMINPUTS;j++)
        {
            r[i].strength *=Membership(r[i].lhs[j],input[j]);
        }
    }

```

}

}

```
float Membership(MFNin mf, int xin)
```

```
{
    float temp;
    temp=mf.centre-xin;
    if(temp<0.0)
    {
        temp= -temp;
    }

    if(temp>mf.width)
    {
        return 0.0;
    }
    else
    {
        return(1.0-temp/mf.width);
    }
}
```

```
void eval_output()
```

```
{
    int i;
    float strength;
    control=0;
    strength=0.0;

    for(i=0;i<NORULES;i++)
    {
        if(r[i].strength>0.0)
        {
            control +=r[i].strength*r[i].rhs.control;
            strength +=r[i].strength;
        }
    }

    if(strength>0.0)
    {
        control /=strength;
    }
}
```

```
/******FUZZY LOGIC SOFTWARE END*****
```

```
void spi_fifo_init()
```

```
{
    // Initialize SPI FIFO registers
    SpiaRegs.SPICCR.bit.SPISWRESET=0; // Reset Spi
```

```

    SpiaRegs.SPICCR.all=0x000F;    //16-bit character
    SpiaRegs.SPICTL.all=0x0006;
// SpiaRegs.SPISTS.all=0x0000;
    SpiaRegs.SPIBRR=0x001E;    // Baud rate
    //SpiaRegs.SPIFFTX.all=0xC028;    // Enable FIFO's, set TX FIFO level to 8

    //SpiaRegs.SPIFFCT.all=0x00;
    SpiaRegs.SPIPRI.all=0x0010;

    SpiaRegs.SPICCR.bit.SPISWRESET=1; // Enable SpI

    //SpiaRegs.SPIFFTX.bit.TXFIFO=1;

}

void spi_xmit(Uint16 a)
{
    GpioDataRegs.GPBDAT.bit.GPIOB5= 0;

    SpiaRegs.SPITXBUF=a;

star:  if(SpiaRegs.SPISTS.bit.INT_FLAG==1)
    {
        dataread = SpiaRegs.SPIRXBUF;
        GpioDataRegs.GPBDAT.bit.GPIOB5 =1;

    }
    else
    {
        goto star;
    }

}

void InitAdc1()
{
    AdcRegs.ADCMAXCONV.all = 0x0000;    // Setup 2 conv's on SEQ1
    AdcRegs.ADCCHSELSEQ1.bit.CONV00 = 0x0; // Setup ADCINA3 as 1st SEQ1 conv.
    //AdcRegs.ADCCHSELSEQ1.bit.CONV01 = 0; // Setup ADCINA2 as 2nd SEQ1 conv.
    //AdcRegs.ADCTRL1.bit.CONT_RUN= 1;    // set continuous conversion
    AdcRegs.ADCTRL1.all= 0x2040;
    AdcRegs.ADCTRL2.bit.SOC_SEQ1 = 1;
    AdcRegs.ADCTRL2.bit.EVA_SOC_SEQ1 = 1; // Enable EVASOC to start SEQ1
    // AdcRegs.ADCTRL2.bit.INT_ENA_SEQ1 = 1; // Enable SEQ1 interrupt (every
/*    AdcRegs.ADCTRL1.all= 0x0040;
    AdcRegs.ADCTRL2.all= 0x2000;
    AdcRegs.ADCTRL3.all= 0x00E1;
    AdcRegs.ADCMAXCONV.all= 0x0000;
    //AdcRegs.ADCASEQSR.all= 0x0000;
    //AdcRegs.ADCST.all= 0x0000;

```

```
    AdcRegs.ADCCHSELSEQ1.all= 0x0000;
    AdcRegs.ADCCHSELSEQ2.all= 0x0000;
    AdcRegs.ADCCHSELSEQ3.all= 0x0000;
    AdcRegs.ADCCHSELSEQ4.all= 0x0000;

    */

    //AdcRegs.ADCTRL2.bit.RST_SEQ1 = 1;    // Reset SEQ1
}

void CurrentCal()
{
    e=0;
check_current:
    Y=(AdcRegs.ADCRESULT0);
    X=(Y >> 4);

    if(X>(d+200) | X<(d-200))
    {

        if(e==3)
        {
            goto check_current1;
        }

        DELAY_US(25);
        e=e+1;
        goto check_current;
    }

    else
    {
        goto check_current1;
    }
}

check_current1: d=X;

        if(d<max_current)
        {
            max_current=d;
        }

        /*level=2048;
        actual=level-d;
        forcex=(actual/10);
        forcey=ECanaMboxes.MBOX2.MDRH.all;
        force=(forcey*forcey)+(forcex*forcex);
```

```

        ftotal=sqrt(force);
        if(inc>50 & u<1000)
        {
            u++;
            buffer[u]=ftotal;
            inc=0;
        }
        else
        {
            inc++;
        }*/
    }

void PIDloop()
{

    errordot=error-olderror;
    sumerror=sumerror+error;
    olderror=error;
    control=(0.001*error)+(0.01*errordot)+(0.001*sumerror);// PID Control Kp, Ki and Kd
    /*if(control>3)
    {
        control=2;
    }
    else
    {
        control=1;
    }*/
    control=1;
}

void positionloop()
{
    if(GpioDataRegs.GPADAT.bit.GPIOA1==1)//Position feedback
    {
        if(check==0)
        {
            DELAY_US(40);

            if(GpioDataRegs.GPADAT.bit.GPIOA1==1)
            {
                t++;
                check=1;
            }
        }
    }
    else

```

```
        {
            check=0;
        }
    }

void positionloop1()
{
    if(GpioDataRegs.GPADAT.bit.GPIOA1==1)//Position feedback
    {

        if(check==0)
        {

            DELAY_US(40);

            if(GpioDataRegs.GPADAT.bit.GPIOA1==1)
            {

                x++;
                check=1;
            }
        }
    }

    else
    {
        check=0;
    }
}

//=====
// No more.
//=====
```